NBTE

Netherlands society for Biomaterials and Tissue Engineering

Program 29th Annual Meeting, 26 & 27 November 2020

at

ONLINE

Thursday, 26 November

12.30	***Opening***
12.35 – 13.15	***Opening Keynote Lecture:*** ***Organ on Chips as Models of Human Physiology with Focus on Neurovascular Models*** *Prof. Dr. Anna Herland (KTH Royal Institute of Technology Sweden)*

13.15 – 13.30	***Coffee break***

13.30 – 13.35	**Optics11 pitch**
13.35 – 14.35 (10+2 min)	**Oral Presentations**
01	**High-throughput screening to elucidate biomaterial-induced fibrosis** T van der Boon, W.J. Kolff Institute, University of Groningen
02	**Steering keratocyte phenotype and collagen production using micro-patterned cell culture substrates** C van der Putten, Department of Biomedical Engineering, Eindhoven University of Technology
03	**Testing Bone Adhesive Barrier Membranes Based on Alendronate and N-hydroxysuccinimide-functionalized Poly(2-oxazoline)s for Guided Bone Regeneration on a New Ex Vivo Perfusion-Based Mandibular Model** M van Erk, Department of Surgery, Radboud University Medical Centre
04	**Directing lineage commitment in kidney organoids using supramolecular materials** J van Sprang, Department of Biomedical Engineering, Eindhoven University of Technology
05	**Cardiac fibroblast mechanoresponse guides anisotropic organization of hIPSC-derived cardiomyocytes** D Mostert, Department of Biomedical Engineering, Eindhoven University of Technology

14.35 – 15.00	***Coffee break and break-out room Optics11***

15.00 – 16.00 (10+2 min)	**Oral Presentations**
06	**Influence of microcapsule parameters and initiator concentration on the self-healing capacity of resin-based dental composites** K Ning, Department of Dentistry, Radboud University Medical Center
07	**Human Platelet Lysate Defeats Fetal Bovine Serum for Human Osteoclast Formation and Resorption** B de Wildt, Department of Biomedical Engineering, Eindhoven University of Technology
08	**Copper-Containing Mesoporous Bioactive Glass nanoparticles for Therapeutic Application in Bone Regeneration** N Besheli, Department of Dentistry, Radboud University Medical Center
09	**Cartilage Tissue Engineering using Bioinspired Growth Factor Immobilization on Microfiber Scaffolds** MJ Ainsworth, Department of Orthopedics, University Medical Center Utrecht
10	**Bone-Adhesive Barrier Membranes Based on Alendronate-Functionalized Poly(2-oxazoline)s** MJ Sánchez-Fernández, Department of Dentistry-Regenerative Biomaterials, Radboud University Medical Center

16.00 – 16.30	***Coffee break and break-out room Optics11***

16.30 – 16.40	***Scientific Photo Competition award***
16.40 – 17.30	***General Assembly***

NBTE Focus session

19.30 – 21.00	**Battle of the Matrix: natural or synthetic matrices** *Prof. Dr. Janette Burgess* *University Medical Center Groningen* *Dr. Matthew Baker* *Maastricht University* Plenary Discussion

Friday, 27 November

09.00 – 9.45	***Belgian Society for Tissue Engineering Keynote:*** ***From brewing beer to building bone*** *Prof. Dr. Liesbet Geris (KU Leuven)*

9.45 – 10.15	***Coffee break and break-out room Optics11***

10.15 – 11.15 (10+2 min)	**Oral Presentations**
11	**Hydrogel-based bioinks for cell electrowriting of well-organized living structures with micrometer-scale resolution** P.N. Bernal, Department of Orthopedics, University Medical Center Utrecht
12	**Zonal-cell density 3D bioprinting for biomimetic cartilage tissue engineering** PJ Díaz-Payno, Department of Biomechanical Engineering, Delft University of Technology
13	**Melt Electrowriting of a Meniscus Scaffold seeded with MSCs and Meniscus Cells** JV Korpershoek, Department of Orthopaedics, Regenerative Medicine, University of Utrecht
14	**Bioengineering Clinically-Sized Microporous Annealed Scaffolds via In-Air Production of Dual-Crosslinking Microgels** M Schot, Department of Developmental BioEngineering, University of Twente
15	**Silk-based Materials to Create High Resolution Three-dimensional Structures Using Electrohydrodynamic Printing** M. Viola, Department of Orthopedics, University Medical Center Utrecht

11.15 – 11.30	***Coffee break and break-out room Optics11***

11.30 – 12.30 (10+2 min)	**Oral Presentations**
16	**Patterning Self-Organizing Microvascular Networks within Engineered Matrices** D. Rana, Department of Biomedical Engineering, University of Twente
17	**A new non-invasive technique for measuring the 3D-oxygen gradient in wells during mammalian cell culture** CJ Peniche Silva, MERLN Institute for Technology-Inspired Regenerative Medicine, Maastricht University
18	**Generation of Immunoprotective and Enzymatically Crosslinked Polyethylene Glycol-Tyramine Microcapsules for Beta-cell Delivery using Microfluidics** N Araújo-Gomes, Department of Developmental BioEngineering, University of Twente
19	**Assessment of the Neutrophil Response to a Panel of Synthetic and Natural derived Biomaterials; a Novel Comprehensive in vitro Approach** M Wesdorp, Erasmus MC, University Medical Center Rotterdam
20	**Synovial membrane on chip: studying immune response over inflammation in a multi-cellular system** CA Paggi, Department of Developmental BioEngineering, University of Twente
12.30	***Closure of the meeting***

Thursday, 26th November

12.35-13.15	**Keynote lecture**

Title: Organ on Chips as Models of Human Physiology with Focus on Neurovascular Models

Prof. Dr. Anna Herland

KTH Royal Institute of Technology
Sweden

Engineered human Organ-on-Chip models have emerged as a new promising pre-clinical technology. While this field has progressed significantly, today, no human engineered system recapitulates drug absorption and physiological vascular coupling to combine multiple organ models. Moreover, the reported Organ-on-Chip models do not enable accurate *in vitro-to-in vivo* extrapolation (IVIVE) of pharmacokinetics and pharmacodynamics (PK/PD). We have developed a 10 Organ Chip automated platform to recapitulate a full human Body-on-Chip. This Body-on-Chip system allowed studies of intestinal (oral) uptake, or intravenous (IV) injection, first-pass metabolism and excretion, and organ-specific responses.
Our specific focus is the neurovascular unit (NVU), the restrictive barrier that lines the capillaries that course through the brain and spinal cord. We are using micro-engineering to create vascular-mimicking, fluidic Organ-on-Chip models of NVU. These models are populated with human primary or pluripotent stem cell-derived vascular and neural cells. We have tailored the design and material of the NVU-on-Chip to study barrier penetration small drugs and biopharmaceuticals and studies of cellular interactions and inflammatory responses.

High-throughput Screening to Elucidate Biomaterial-induced Fibrosis

Torben (T.A.B.) van der Boon, Liangliang Yang, Lu Ge, dr. Qihui Zhou, and dr. Patrick van Rijn

W.J. Kolff Institute for Biomedical Engineering and Materials Science, University of Groningen/ University Medical Center Groningen (UMCG), Ant. Deusinglaan 1, Groningen, The Netherlands

Introduction: Nowadays, it is becoming common knowledge that the human body, its tissues and cells react to biophysical and biochemical cues located on biomaterial surfaces.[1,2] Identifying how these parameters influence cellular behavior is of crucial importance and will aid us in the further development of medical implant technology. Unfortunately, in many studies attempting to identify these physicochemical properties' influence on cell behavior, investigation of individual properties is the conventional method, leaving out a significant number of other variables which are encountered *in vivo*, which is where cells always interact with multiple cues simultaneously.[3,4] We are developing an orthogonal double gradient platform which allows us to investigate just such complex situations in a high-throughput screening (HTS) fashion. The platform grants us the power to screen the cell response towards thousands of these combined parameters in single cell experiments, which will result in the optimization of material properties to enhance biomaterial and implant function. Currently, we are in the final platform optimization stage, after which we will screen silicone rubber's susceptibility to fibrosis and scar tissue formation.

Method: PDMS orthogonal double gradients are prepared by sequential imprinting – and shielded air plasma oxidation treatments in accordance with previously published methodology.[4–7]

Results and Discussion: Every imaginable position on the orthogonal double gradient surfaces has a unique combination of three surface parameters, possessing 'real', clinically relevant values. Wavy topography gradients range from λ = 1,5 µm – 12 µm and A = 50nm – 2,5 µm, the smallest wavelengths corresponding with the smallest amplitudes going from small to big, in a coupled fashion. Stiffness gradients range in Young's Modulus from ~30 – 300 MPa, and 'wettability' gradients from 5 – 90 ° in water contact angle (WCA). As a 'proof of concept', we cultured hBM-MSCs on the platforms for 24 h, imaged the cells via automated fluorescence microscopy and identified the cell response with respect to cell density, cell spreading, nucleus area, and vinculin expression. We have found that the synergistic effect of abovementioned parameter combinations all influence cell behavior in a different manner with regard to these relatively 'simple' assessable characteristics. Our next steps involve the translation of regions of interest (ROI) to homogeneous parameter substrates, as a last verification step in the optimization process.

Conclusion: The highly efficient cell screening tool we have created with our DOG platform allows us to screen cell response to combined physical parameter influence in a high-throughput fashion, investigating thousands of different parameter combinations in single cell experiments. It will serve its purpose to facilitate enhanced biomaterial development.

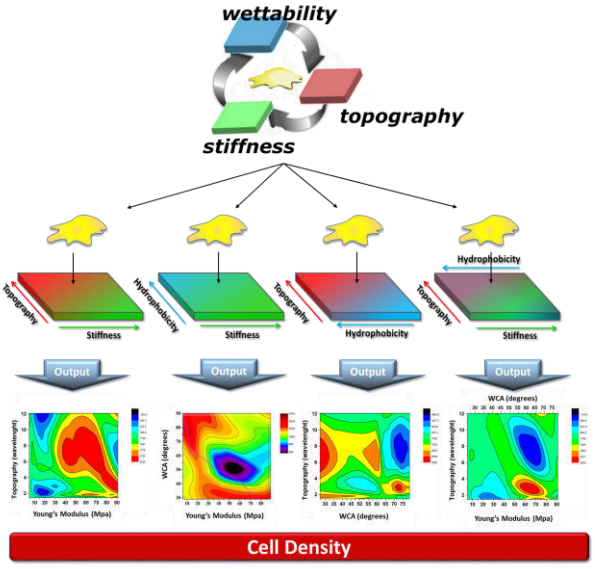

Figure 1. HTS approach. Different physicochemical biomaterial properties influence cell behavior in a complex manner. The screening platforms enables all parameter combinations to be present within a gradient-like range. The influence on, in this example 'Cell density', is identified via fluorescence immune-staining and semi-automated imaging and analysis.

References:

[1] G. Huang, F. Li, X. Zhao, Y. Ma, Y. Li, M. Lin, G. Jin, T. J. Lu, G. M. Genin, F. Xu, *Chem. Rev.* **2017**, Oct 25; 117(20):12764-12850.

[2] W. L. Murphy, T. C. McDevitt, A. J. Engler, *Nat. Mater.* **2014**, Jun; 13(6):547-57.

[3] A. M. Schaap-Oziemlak, P. T. Kühn, T. G. van Kooten, P. van Rijn, *RSC Adv.* **2014**, *4*, 53307.

[4] P. T. Kühn, Q. Zhou, T. A. B. van Der Boon, A. M. Schaap-Oziemlak, T. G. van Kooten, P. van Rijn, *ChemNanoMat* **2016**, 2, 407 - 413

[5] Q. Zhou, P. T. Kühn, T. Huisman, E. Nieboer, C. van Zwol, T. G. van Kooten, P. van Rijn, *Sci. Rep.* **2015**, *5*, 16240.

[6] Q. Zhou, L. Ge, C. F. Guimarães, P. T. Kühn, L. Yang, P. van Rijn, *Adv. Mater. Interfaces* **2018**, 5(18)

[7] L. Yang, L. Ge, and P. Van Rijn, *ACS Appl. Mater. Interfaces* **2020**, 12, 25591-25603

[8] T.A.B. van der Boon, L. Yang, L. Li, D. E. Córdova Galván, Q. Zhou, J. de Boer, P. van Rijn, *Adv. Biosyst*. 2020, 4, 1900218.

Steering Keratocyte Phenotype and Collagen Production using Micro-Patterned Cell Culture Substrates

C. van der Putten[1,2], N. Formisano[3], G. Sahin[3], S. Giselbrecht[3], C.V.C. Bouten[1,2] & N.A. Kurniawan[1,2]
1. Soft Tissue Engineering and Mechanobiology, Department of Biomedical Engineering, Eindhoven University of Technology, PO Box 513, 5600 MB Eindhoven, The Netherlands
2. ICMS, Eindhoven University of Technology, 5600 MB Eindhoven, The Netherlands
3. Instructive Biomaterial Engineering, MERLN Institute for Technology-Inspired Regenerative Medicine, 6229 ER Maastricht, The Netherlands

Introduction | Loss of vision due to opacity in the corneal stroma affects more than 23 million people worldwide, from which 4.6 million people are also suffering from bilateral corneal blindness[1]. The most successful treatment is keratoplasty or corneal transplantation. This surgical procedure is the most commonly performed transplantation worldwide with 65,000 operations each year, however, the demand for suitable donor tissue is still higher than the availability[2,3]. Hence, alternatives for allogenic transplants need to be developed, possibly by a tissue engineering approach. One way to realize this is by mimicking the native corneal environment in tissue engineering constructs by implementing the structure and organization of the native corneal tissue. The corneal stroma, representing approximately 90% of the total corneal thickness, mainly consists of highly organized collagen lamellae, maintained by keratocytes[4]. Therefore, this study aims to produce an aligned collagen network formed by keratocytes. In order to obtain this collagen organization, we first stimulate the production of collagen networks by keratocytes *in vitro*, followed by guiding the alignment of keratocytes using micropatterned cell culture substrates. Eventually, this approach may aid in the development of tissue engineered solutions for corneal defects.

Methods | A Human Corneal Keratocyte cell line is seeded with and without Fetal Bovine Serum (FBS) on plastic cell culture substrates and collagen deposition is visualized over time using the CNA35-OG488 probe. In order to induce alignment of cells *in vitro*, PDMS cell culture substrates are passivated using poly-l-lysine and mPEG-SVA and subsequently patterned (parallel lines or concentric circles) using an optics-based projection system (PRIMO, Alvéole). Afterwards, an FNC coating mix is applied to the surface of the substrates in order to induce a contact guidance response. Primary keratocytes, isolated from donor material, are used to investigate the cell alignment response.

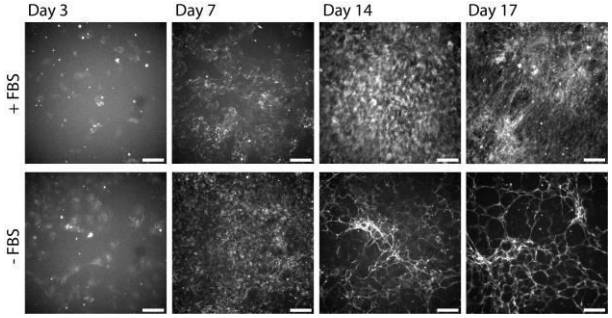

Figure 1: Collagen deposition by keratocytes cultured with and without FBS over time. Grey: collagens (CNA35-OG488). Scale bar: 100 µm

Results and Discussion | Keratocytes produced a dense, fibrous collagen network in approximately 14 days (see Figure 1). Upon activation of the cells with FBS, more collagen is deposited. A downside of the addition of FBS however, is that keratocytes may undergo an unwanted phenotypic change towards corneal fibroblasts. Primary keratocytes on FNC micropatterns show a contact guidance response by aligning in the direction of the provided patterns (see Figure 2). The FNC patterns on PDMS substrates induced cell alignment not only during the initial 2 days of culture, but also over a period of 14 days.

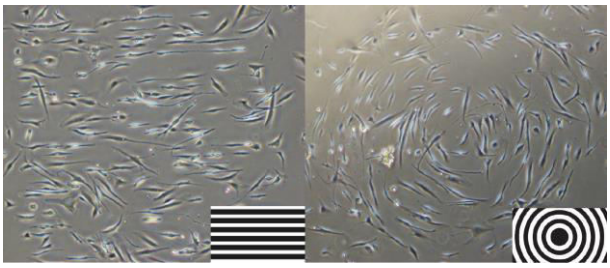

Figure 2: Primary keratocytes cultured 2 days on micropatterned substrates. Left pattern: FNC lines, 20 µm wide (white) and 30µm gaps (black). Right pattern: FNC circles, 30 µm wide (white) and 30 µm gaps (black).

Conclusion and Outlook | The results indicate that keratocyte activation stimulates the production of collagen. Besides, a culture period of approximately 14 days is sufficient to produce a dense, fibrous network. Secondly, the patterning approach enables the guidance of the keratocyte alignment response *in vitro.* Future experiments will combine the presented results with the overall aim to produce an aligned collagen matrix *in vitro*. Besides gaining fundamental understanding about collagen formation by keratocytes, this study also aids in the development of aligned sheets of collagen that may offer a solution to restore diseased corneas in patients suffering from corneal disease.

[1] Hertsenberg A.J. et al., Stem Cells in the Cornea, Prog Mol Biol Transl Sci, 134, 25-41, 2015
[2] Tan D.T. et al., Corneal transplantation, The Lancet, 379(9827), 1749-1761, 2012
[3] Williams K.A. et al., Prospects for genetic modulation of corneal graft survival, Eye, 23(10), 1904-1909, 2009
[4] Reinstein D.Z. et al., Stromal Thickness in the Normal Cornea: Three-dimensional Display With Artemis Very High-frequency Digital Ultrasound, J Refract Surg., 25(9), 776-786, 2009

This work was performed under the framework of Chemelot InSciTe.

Cell Viability of Fibroblasts and Osteoblasts in Response to Bone Adhesive Alendronate-functionalized Poly(2-oxazoline)

M. van Erk[1], N. Calon[1], R. Lomme[1], H. van Goor[1]
[1]*Department of Surgery, Radboud University Medical Centre, Postbus 9101 (route 618), 6500 HB, Nijmegen, The Netherlands.*

Introduction

Osteosynthesis materials are frequently used in the orthopedic clinic to stabilize fractures and support the bone regenerating process. However, fixation of these materials, often done with screws, creates new bone damage and therefore alternative materials are investigated including bone adhesive materials. One of the bone adhesive materials currently researched is the alendronate-functionalized poly(2-oxazoline) (POx-ale) polymer which has a strong affinity to the mineral content of bone tissue and is therefore adhesive to bone tissue. In this study, the cytotoxicity of the POx-ale polymer is investigated with murine fibroblasts (NIH3T3) and pre-osteoblasts (MC3T3).

Materials & Methods

POx-ale polymer (5, 2.5, 1,3, 0.6, 0.3 mg/mL) and control conditions P(EtOx) (5 mg/mL), sodium alendronate trihydrate (2.14 mg/mL) or ethanol (20% v/v) were mixed with culture medium for cytotoxicity tests. Cell viability after 24h and 48h and cell proliferation after 3 and 7 days in presence of experimental or control conditions was measured using cell counting kit-8 (CCK-8). Cell viability was expressed as a percentage of blank control condition. Supernatants of fibroblasts proliferation assays were collected to determine expression of matrix metalloproteinases (MMP) 2 and 9. Osteoblastic cell differentiation and function was characterized by determining the calcium content and by alizarin red S staining.

Results

First results of the study demonstrated a dose-dependent toxic effect of POx-ale on both murine fibroblasts and osteoblasts in the cytotoxicity tests. A concentration of 5 mg/mL led to a significant reduction of cell viability in both cell types and proliferation of osteoblasts, while a concentration of ≥2.5 mg/mL of POx-ale led to a reduction in fibroblast proliferation. The results of the gelatine zymography showed the presence and expression of MMP-2 and MMP-9 in the medium of the fibroblasts cultured in 1.3, 0.6, 0.3 mg/mL POx-ale, P(EtOx), as well as in medium only (blank).

Conclusion

Based on the preliminary data, we conclude that there is a dose-dependent toxic effect of POx-ale on both murine fibroblasts and osteoblasts. More experiments will be performed to effectively evaluate the effects of the bone adhesive POx-ale polymer on cell viability and function.

Directing lineage commitment in kidney organoids using supramolecular materials

Johnick F. van Sprang, Patricia Y.W. Dankers
[1] Laboratory for Cell and Tissue Engineering, Department of Biomedical Engineering, Eindhoven University of Technology, PO Box 513, 5600 MB Eindhoven, The Netherlands.
[2] Institute for Complex Molecular Systems, Eindhoven University of Technology, PO Box 513, 5600 MB Eindhoven, The Netherlands.
[3] Laboratory of Chemical Biology, Department of Biomedical Engineering, Eindhoven University of Technology, PO Box 513, 5600 MB Eindhoven, The Netherlands.

Introduction

Kidney organoids are three-dimensional aggregates of renal cells organized into functional microstructures that are also found in their native counterparts. As such, organoids hold great translational promise as a regenerative therapy for patients suffering from renal failure. These human-induced pluripotent stem cell (hiPSC)-derived tissues initially contain four different progenitor cell populations that organize and differentiate into nephrons (functional renal units), interstitium, and a vascular network. However, the lineage commitment of these progenitor cell populations is difficult to control, which leads to a distorted segmentation of nephrons. Incorrect segmentation of nephrons may greatly impede function of these organoids and thereby form a barrier for future translational applications.

Lineage commitment of nephron progenitor cells (NPCs) has previously been shown to be controllable using soluble small molecules. Differentiation towards distal tubular lineages is possible by extended exposure to the GSK-3α inhibitor CHIR99021. Furthermore, the differentiation towards more proximal phenotypes, such as podocytes, was possible using TGF-beta inhibitor SB-431542 and canonical Wnt signalling inhibitor IWR-1. Tuning NPC lineage commitment using soluble components is inherently limited in the fine-tuning of this delicate process. As such, directing this process via different means may allow for even more precise control over NPC lineage commitment.

Here, we encapsulate kidney organoids in hydrogels based on ureido-pyrimidinone (UPy) molecules. These supramolecular molecules are capable of reversibly self-assembling into fibrous aggregates using quadruple hydrogen bonding and π-π interactions. The reversible nature of these non-covalent interactions yields a dynamic material with an architecture resembling the natural extracellular matrix. The encapsulation of kidney organoids within this synthetic microenvironment greatly impacts the final phenotype of the organoids. We show that encapsulation leads to a strong bias of NPCs to differentiate to more proximal phenotypes (e.g. podocytes), which in turn impacts differentiation of other progenitor populations. These results indicate that biomaterials may be used as an additional tool to direct differentiation of progenitor populations within complex tissues.

Materials and Methods

hiPSCs were seeded on a vitronectin-coated polystyrene well-plate and differentiated towards renal progenitor cells using CHIR99021, FGF-9, and heparin over a 7-day culture period. On day 7, the renal progenitor cells were centrifuged into cell aggregates and cultured on an air-liquid interface for an 18-day period. On day 9 or 12, the kidney organoids were encapsulated in UPy-hydrogels consisting of a monofunctional UPy-glycinamide and bifunctional UPy_2-PEG_{10k}. Furthermore, UPy-hydrogels were supplemented with either 0 or 1 mM UPy-cRGDfK.

Results and Discussion

The multicomponent UPy-hydrogels were designed as a synthetic microenvironment with the ability to influence cell behaviour. The addition of the additive UPy-cRGDfK allows for integrin-binding and in turn mechanotransduction with cells at the organoid-hydrogel interface. Encapsulation of developing organoids did not affect cell viability based on live/dead microscopy. Organoids did become more compacted as opposed to non-encapsulated organoids. Furthermore, nephrons showed segmentation based on immunostainings, with glomerular structures ($Nephrin^+$, $WT1^+$) connected to a proximal tubule (LTL^+), and a distal tubule ($E\text{-}cadherin^+$). However, the segmentation did show a shift towards glomerular segments in organoids encapsulated in UPy-hydrogels supplemented with both 0 and 1 mM UPy-cRGDfK. Interestingly, this shift was accompanied by a change in the vascular network. Organoids encapsulated in UPy-hydrogels without UPy-cRGDfK demonstrated wider endothelial vessels. Encapsulation within UPy-hydrogels supplemented with 1 mM UPy-cRGDfK resulted in a more branched vascular network compared to non-encapsulated organoids. This association in change of nephron segmentation and vascular phenotype may be explained by the secretory profile of podocytes. As these are the cells responsible for secreting VEGF-A during renal organogenesis.

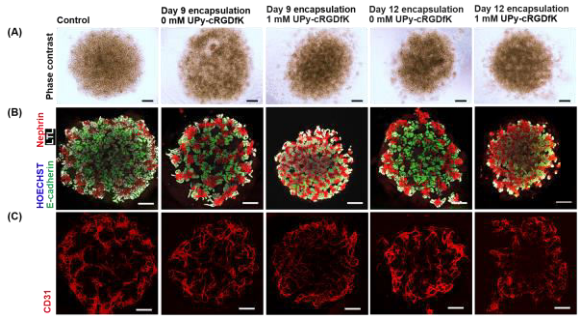

Figure 1. kidney organoids cultured in UPy-hydrogels on day 25. (A) Phase-contrast images of kidney organoids. Scale bar = 1 mm. **(B)** Immunofluorescent images of nephron segmentation in kidney organoids, and **(C)** the vascular network present in kidney organoids. Scale bar = 500 µm.

Conclusion and Outlook

We demonstrated that biomaterials may be used as an additional tool to direct lineage commitment of progenitor cells in organoid-like tissues. Encapsulation of kidney organoids shifted the differentiation of NPCs more towards glomerular phenotypes, which led to an accompanied change in the vascular network. Next, we intend to quantify this shift using flow cytometry.

Cardiac Fibroblast Mechanoresponse Guides Anisotropic Organization of hIPSC-derived Cardiomyocytes

Dylan Mostert[1,2], Leda Klouda[1], Nicholas A. Kurniawan[1,2], Carlijn V.C. Bouten[1,2]

1 Eindhoven University of Technology, Department of Biomedical Engineering, PO Box 513, 5600 MB Eindhoven, The Netherlands. Tel: +31 (0)402472279

2 Institute for Complex Molecular Systems (ICMS), PO Box 513, 5600 MB Eindhoven, The Netherlands. Tel: +31 (0)402473532

Corresponding email: d.mostert@tue.nl

Introduction: The human myocardium is a mechanically active tissue typified by its anisotropic organization of cells and extracellular matrix. In a healthy human myocardium, cardiomyocytes (CMs) and cardiac fibroblasts (cFBs) are linearly arranged as dense cell sheets in anisotropic collagen, enabling electrical coupling between CMs and aiding synchronous contraction [1]. Upon injury, such as myocardial infarction, the myocardium undergoes dramatic alterations, resulting in disruption of anisotropy and loss of coordinated contraction. Moreover, loss of anisotropic organization hampers the differentiation, matrix production, and mechanotransduction of resident and newly injected cardiac cells [2]. Therefore, understanding how anisotropic organization in the adult myocardium is shaped and disrupted by environmental cues is critical, not only for unravelling the processes taking place during disease progression, but also for developing therapeutic strategies to recover tissue function.

In this study, we investigated the effect of mechanical and structural cues, inspired by myocardial biology, on the organization of cardiac cells. Specifically, we used a two-dimensional *in vitro* approach to decouple the two major physical cues that are inherent in the myocardium: structural ECM and mechanical strain. This approach allowed controlled presentation of structural cues and mechanical strains independently and simultaneously, to study their effect on the organization of cardiomyocytes (hiPSC-CMs) and cardiac fibroblasts (cFBs). To further understand how changes in the cellular composition of the myocardium affected the sensitivity of tissue organization to structural and mechanical cues, we constructed co-cultures of hiPSC-CMs and cFBs with varying cell ratios.

Aim: We aim to investigate if structural and mechanical cues present in the myocardium can shape or disrupt the collective organization of cardiac cells.

Materials and Methods: cFBs (epicardial derived cells) and hiPSC-CMs were seeded on deformable membranes with anisotropic or disorganized fibronectin patterns made by micro-contact printing (Figure). By applying uniaxial cyclic strain (Flexcell inc.) we were able to study the influence of ECM anisotropy, uniaxial strain and their combined effects on the organization of individual cardiac cell types and co-cultures, representing the healthy contractile (70% hiPSC-CMs : 30% cFBs) or diseased fibrotic (70% cFBs : 30% hiPSC-CMs) cellular environment within the myocardium. Cell organization was visualized and quantified using Calcein AM live staining and the directionality plugin from Fiji, respectively. Moreover, we designed a novel quantification tool to assess the structure and quantity of focal adhesions (FAs) and actin stress fibers (SFs), both key players in contact-guided and strain-mediated responses, respectively.

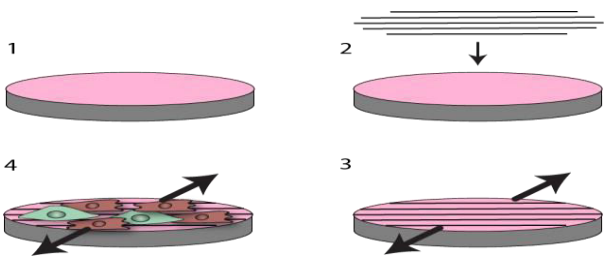

Results and Discussion: In this project, we studied the effect of mechanical and structural cues, inspired by myocardial biology, on the organization of cardiac cells. We showed that uniaxial cyclic strain, mimicking the local deformation of cardiac beating, led to anisotropic organization of cardiac fibroblasts (cFBs), but not of cardiomyocytes (hiPSC-CMs). Quantification of the key mechanosensing players revealed distinct, cell-type-dependent presentation of SFs, suggesting that the intracellular distribution of SFs impair hiPSC-CM mechanoresponse. Next, we reconstructed the cellular compositions of normal and pathological myocardium using co-cultures with varying cell ratios. Surprisingly, contrary to the response of the hiPSC-CM monoculture, the co-cultures adopted an anisotropic organization under uniaxial cyclic strain, regardless of the co-culture composition. These data suggest that the mechanoresponsiveness of cFBs may be critical in determining myocardial tissue structure and function.

Conclusion and Outlook: Our study shows that the mechanoresponsiveness of hiPSC-CMs and cFBs differs significantly. Upon co-culture with varying cell ratios of cFBs and hiPSC-CMs, anisotropic organization was found upon cyclic strain administration, whereas this was not observed in hiPSC-CM monoculture. Thus, our study proposes the importance of cFBs, a cell type often overlooked, in determining myocardial architecture and function. By exploiting the mechanoresponsiveness of cFBs to uniaxial cyclic strain, the formation of anisotropic structure in scaffolds and tissue engineering constructs can be promoted, aiding the design of strategies for structural organization of the myocardium.

Acknowledgements: This project is funded by the Materials Driven Regeneration (MDR) Gravitation Program.

References:

[1] LeGrice, I. J., Smaill, B. H., Chai, L. Z., Edgar, S. G., Gavin, J. B., & Hunter, P. J. (1995). *American Journal of Physiology - Heart and Circulatory Physiology*, *269*(2 38-2).

[2] Feinberg, A. W., Alford, P. W., Jin, H., Ripplinger, C. M., Werdich, A. A., Sheehy, S. P., … Parker, K. K. (2012). *Biomaterials*, *33*(23), 5732–5741.

Influence of microcapsule parameters and initiator concentration on the self-healing capacity of resin-based dental composites

K. Ning[1], C. Yeung[1], F. Yang[1], B. Loomans[2], S. Leeuwenburgh[1]

[1.] Radboud university medical center, Radboud Institute for Molecular Life Sciences, Department of Dentistry – Regenerative Biomaterials, Philips van Leydenlaan 25, Nijmegen, The Netherlands.
[2.] Radboud university medical center, Radboud Institute for Health Sciences, Department of Preventive and Restorative Dentistry, Philips van Leydenlaan 25, Nijmegen, The Netherlands.

Introduction

Resin-based dental composites composed of an acrylic matrix reinforced with glass filler microparticles are used on a routine basis in restorative dentistry to restore damaged teeth. Nevertheless, fracture is one of the main causes of failure of resin-based composite restorations. To overcome this drawback, self-healing resin-based composites have been designed by incorporation of microcapsules. So far, self-healing composites have been developed by incorporation of bio-incompatible poly(urea-formaldehyde) (PUF) microcapsules containing acrylic monomers as healing agent [1, 2]. However, the relationship between their self-healing capacity and microcapsule and resin parameters is still poorly understood. Therefore, the objective of this study was to systematically investigate the effect of initiator concentration (in the resin) and microcapsule size and concentration on the self-healing performance of commercially available flowable resin-based composites.

Materials and Methods

The PUF microcapsules containing triethylene glycol dimethacrylate (TEGDMA) and N, N-Dimethyl-p-toluidine (DHEPT) as the healing liquid were synthesized by *in situ* polymerization. Microcapsules in three distinct size ranges were achieved by adjusting the stirring speed during the microcapsule synthesis at either 400, 800 or 1200 rpm. PUF microcapsules (5 – 15 wt%) of different sizes and benzoyl peroxide (BPO) as the initiator (0.5 – 2.0 wt%) were added to a commercially available flowable resin-based composite (Clearfil Majesty™ ES flow). Fracture toughness K_{IC} of the resulting composites was measured via a single edge V-notched beam method. After fracture, the broken pieces were held together by a rubber band and healed for 48 h. Subsequently, fracture toughness of the healed composites ($K_{IC\text{-}healed}$) was tested. Healing efficiency was calculated as $K_{IC\text{-}healed}/K_{IC} \times 100\%$.

Results and Discussion

Poly(urea-formaldehyde) (PUF) microcapsules containing acrylic healing liquid were synthesized in small (33 ± 8 µm), medium (68 ± 21 µm) and large sizes (198 ± 43 µm) and characterized. The fracture toughness of healed dental composites significantly increased with increasing microcapsule size and concentration ($p<0.05$) at an initiator concentration of 2 wt% BPO. The initiator is a crucial component of extrinsic self-healing systems by triggering the rupture-induced polymerization. From our study, it can be concluded that a minimal initiator concentration (BPO) is required to achieve extrinsic self-healing. From the linear regression analysis, the fracture toughness after healing ($K_{IC\text{-}healed}$) increased evidently with increasing microcapsule size and concentration. Medium and small microcapsules showed a comparable self-healing performance, which was however inferior to the self-healing capacity of composites containing larger microcapsules. The highest self-healing efficiencies (up to 76%) were obtained for self-healing resin-based composites containing large microcapsules (198 ± 43 um).

Conclusions

Commercially available resin-based composites can be rendered self-healing most efficiently by incorporation of larger microcapsules (198 ± 43 µm). The self-healing capacity of commercially available flowable composites enriched with microcapsules containing healing liquid increases with increasing microcapsule size and concentration as well as initiator concentration. The composite has a positive influence on self-healing performance.

References

1. Wu J, Xie X, Zhou H, Tay FR, Weir MD, Melo MAS, et al. Development of a new class of self-healing and therapeutic dental resins. Polymer Degradation and Stability, 2019; 163: 87-99. http://dx.doi.org/10.1016/j.polymdegradstab.2019.02.024.

2. Wu J, Weir MD, Melo MA, Strassler HE, Xu HH. Effects of water-aging on self-healing dental composite containing microcapsules. J Dent, 2016; 47: 86-93. http://dx.doi.org/10.1016/j.jdent.2016.01.008

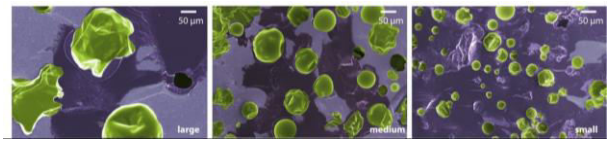

Fig. 1 SEM images at higher magnification of resin-based composites containing large, medium and small microcapsules. Green areas represent the microcapsules, purple areas correspond to the resin matrix, and dark purple shows the polymerized self-healing liquid. Colors were added to guide the eye.

Human Platelet Lysate Defeats Fetal Bovine Serum for Human Osteoclast Formation and Resorption

B.W.M de Wildt, K. Ito and S. Hofmann

Orthopedic Biomechanics, Department of Biomedical Engineering and Institute for Complex Molecular Systems (ICMS), Eindhoven University of Technology, PO Box 513, 5600 MB Eindhoven, The Netherlands

Introduction: Bone has multiple mechanical and metabolic functions that are maintained through lifelong remodeling by osteoclasts (bone-resorbing cells), osteoblasts (bone-forming cells), and osteocytes (regulating cells). To study this process while addressing the principle of replacement, reduction and refinement of animal experiments (3Rs), human *in vitro* bone remodeling models are being developed. Despite increasing safety, scientific, and ethical concerns [1], the nutritional medium supplement fetal bovine serum (FBS) is still routinely used in these models. To comply with the 3Rs and to improve reproducibility of such *in vitro* models, xenogeneic-free medium supplements should be investigated [1]. Human platelet lysate (hPL) might be a good xenogeneic-free alternative to FBS for *in vitro* human bone remodeling models as it may accelerate osteogenic differentiation of mesenchymal stromal cells (MSCs) and improve subsequent mineralization [2, 3]. However, for a human *in vitro* bone remodeling model, hPL should also be able to adequately induce osteoclastogenesis and stimulate subsequent resorption. This study investigates the potential of hPL in comparison with FBS as a medium supplement for osteoclast formation and resorption.

Materials and Methods: Mononuclear cells were extracted from a human peripheral blood buffy coat. Monocytes were subsequently isolated by magnetic-activated cell sorting and seeded on 96-wells plates to assess osteoclast formation (N=3), and 96-well Corning® osteo assay plates to assess osteoclast resorption (N=3). Monocytes were cultured in α-MEM supplemented with either 10% FBS or 10%, 5%, or 2.5% hPL (PL BioScience, Aachen), 1% Antibiotic-Antimycotic, 50 ng/ml M-CSF, and after 2 days culture 50 ng/ml RANKL. After 21 days, cells were fixed and assessed for their morphology and cells on the osteo assay plates were removed with 5% bleach to check for their resorptive activity. Images of the osteo assay wells were segmented to quantify the resorbed surface of the well.

Results: After 21 days culture, monocytes cultured in medium supplemented with FBS exhibited spindle shaped and round cells (Figure 1A), indicating a heterogeneous cell population. Monocytes cultured in medium supplemented with 10% hPL were much larger and showed a homogeneous morphology typical for osteoclasts (Figure 1B). These findings were confirmed by the resorbed surface of the osteo assay plates after 21 days, where osteoclasts cultured with FBS were almost unable to resorb (median resorbed surface of 2.6%, Figure 1C). Osteoclasts cultured with hPL resorbed in all used concentrations more, with a median resorbed surface of 92% for 10% hPL (Figure 1D), 90% for 5% hPL and 20.27% for 2.5% hPL (data not shown).

Discussion and Conclusion: For *in vitro* human bone remodeling models, xenogeneic-free alternatives to FBS are needed to comply with the 3Rs and to improve reproducibility of results. Osteogenic differentiation of MSCs, and mineralization have already been demonstrated to be accelerated by hPL [2, 3]. Here, we showed that the use of hPL in the culture medium can also improve the formation of osteoclasts and their subsequent resorptive activity. Therefore, we consider hPL as a good xenogeneic-free alternative to FBS for *in vitro* bone remodeling models.

References:

1. J van der Valk et al., ALTEX, 35(1): 99-118, 2018.
2. W Xia et al., Cell Biol. Int., 35:639-643, 2011.
3. M Karadjian et al., Cells, 9(918), 2020.

Acknowledgements:
This work is part of the research program TTW with project number TTW 016.Vidi.188.021, which is (partly) financed by the Netherlands Organization for Scientific Research (NWO).

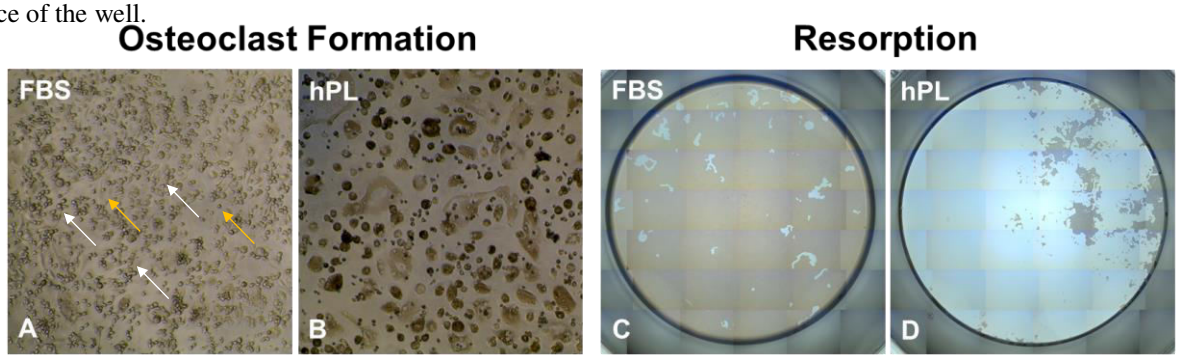

Figure 1. Phase-contrast micrographs of monocytes cultured with either 10% FBS (A) or 10% hPL (B) and the resorbed surface (C and D, respectively) after 21 days culture. Monocytes cultured with FBS exhibit a heterogeneous morphology including spindle shaped cells (orange arrows) and round cells (white arrows) (A), whereas monocytes cultured with hPL show a for osteoclasts typical morphology (B).

Copper-Containing Mesoporous Bioactive Glass nanoparticles for Therapeutic Application in Bone Regeneration

Negar Hassani Besheli, Maryam Hosseini Malekroudi, Fang Yang, Sander Leeuwenburgh

Radboud University Medical Center, Radboud Institute for Molecular Life Sciences, Department of Dentistry - Regenerative Biomaterials, Philips van Leydenlaan 25, Nijmegen, The Netherlands

Introduction: Reconstruction of infected bone defects is still a formidable clinical challenge. Surgical debridement combined with long-term systemic antibiotic therapy is still the common treatment modality. However, this strategy results in adverse side effects, major patient morbidity, and development of antibiotic-resistant bacteria. Therefore, antibiotic-free antibacterial bone graft substitutes are urgently required to simultaneously eradicate the infection while promoting bone regeneration, thereby avoiding delayed reconstruction and follow-up surgeries. Mesoporous bioactive glass (MBG) possesses high surface area, cell-penetrating properties, excellent cytocompatibility, and apatite mineralization [1]. When these glasses dissolve in biological fluids, ions (e.g. Ca and Si) are released which create an environment that promotes osteogenesis but inhibits bacterial proliferation. Moreover, their therapeutic efficacy can be further upgraded by doping with trace amounts of metallic ions like copper which has antibacterial and angiogenic properties [2]. In this research, we focus on the synthesis of a library of antibiotic-free antibacterial MBG nanoparticles with different chemical compositions (Si, Ca, and Cu contents) and investigate their surface properties along with cytocompatibility and antibacterial efficacy. We hypothesize that their calcium and copper content is positively correlated with their antibacterial capacity.

Methods: MBG nanoparticles were synthesized through the microemulsion assisted sol-gel method. The nanoparticle surface properties were characterized by different techniques, like energy-dispersive X-ray spectroscopy (EDX), Brunauer-Emmett-Teller (BET) and scanning electron microscopy (SEM). The surface reactivity of the particles was evaluated by quantifying their apatite-forming capability in Simulated Body Fluid (SBF). The dissolution of MBG nanoparticles and the release of Si, Ca and Cu ions were determined using ICP-MS. Moreover, the cytotoxicity and antibacterial efficacy of nanoparticles were investigated against pre-osteoblast cells (MC3T3-E1) and Methicillin-resistant Staphylococcus aureus (MRSA) bacteria, respectively.

Results: Results showed that spherical monodispersed MBG nanoparticles with a diameter in the range of 100-120 nm, 328 m^2/g surface area and different content of incorporated calcium and copper were successfully synthesized. The content of incorporated ions could be tailored by adjusting the amount of copper and calcium precursor, which did not significantly affect the morphological and structural characteristics of the nanoparticles. MBG nanoparticles exhibited apatite-forming ability, since apatite was formed on the MBG particles after immersion in SBF for 3 days (figure 1). In addition, both Si and Ca were released in cell culture medium and SBF in a sustained manner for at least 14 days confirming the degradability of particles, whereas Cu ions were released within 48 h. Moreover, all MBG nanoparticles showed dose-dependent cytocompatibility toward pre-osteoblast cells. Copper-containing nanoparticles containing 5% of Cu (MBG-5Cu) exhibited the most pronounced antibacterial performance against MRSA as evidenced by a complete eradication of MRSA bacteria at concentrations higher than 0.5 mg/ml (figure 2).

Conclusion: MBG nanoparticles combine meso/nanoscale morphological characteristics with a favorable apatite-forming ability, sustained release profiles of ions, and low cytotoxicity. These features render MBG nanoparticles attractive candidates for bone regeneration applications. Moreover, their antibacterial properties will open up new avenues for the design of antibiotic-free antimicrobial biomaterials for treatment of infected bone defects.

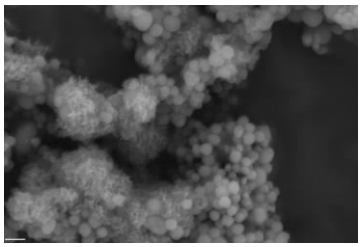

Figure 1- Representative SEM image of MBG-5Cu after immersion in SBF for 3 days (scale bar, 200 nm)

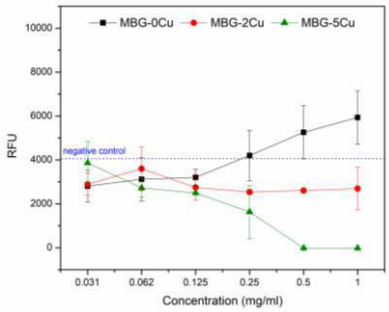

Figure 2- Antibacterial properties of MBG nanoparticles against MRSA bacteria after 24h incubation

References:

1. Wu, C. and J. Chang, *Mesoporous bioactive glasses: structure characteristics, drug/growth factor delivery and bone regeneration application.* Interface Focus, 2012. **2**(3): p. 292-306.
2. Li, J., et al., *Preparation of copper-containing bioactive glass/eggshell membrane nanocomposites for improving angiogenesis, antibacterial activity and wound healing.* Acta Biomater, 2016. **36**: p. 254-66.

Cartilage Tissue Engineering using Bioinspired Growth Factor Immobilization on Microfiber Scaffolds

M.J. Ainsworth[1,2], O. Lotz[3-5], D. McKenzie[5], M.M.M. Bilek[3-7], J. Malda[1,2,8], B. Akhavan[3-5], M. Castilho[1,2,9]
[1]Regenerative Medicine Centre Utrecht, University Medical Center Utrecht, Utrecht, the Netherlands
[2]Department of Orthopedics, University Medical Center Utrecht, Utrecht, the Netherlands
[3]School of Biomedical Engineering, University of Sydney, NSW, Australia
[4]School of Aerospace, Mechanical & Mechatronic Engineering, The University of Sydney, NSW, Australia.
[5]School of Physics, University of Sydney, NSW, Australia
[6]Charles Perkins Centre, University of Sydney, NSW, Australia
[7]Sydney Nano Institute, University of Sydney, NSW, Australia
[8]Department of Veterinary Sciences, Utrecht University, Utrecht, the Netherlands
[9]Department of Biomedical Engineering, Technical University of Eindhoven, Eindhoven, the Netherlands

Introduction: Osteoarthritis is one of the most common chronic diseases globally, with 10% and 13% of men and women affected, respectively [1]. Currently, there is no mechanically competent, biologically functional treatment for the end-stage cartilage degeneration it causes. In this study we hypothesize that the fabrication of well-organized microfiber reinforcing scaffolds [2] with locally, covalently immobilized growth factors could support and guide the formation of new cartilaginous tissue. The addition of such biomolecular cues, particularly transforming growth factor beta 1 (TGFβ1), are crucial for the differentiation and maintenance of cartilage tissue [3]. To create a complex mechanical structure with the necessary biomolecular cues, we combined melt electrowriting (MEW) and atmospheric-pressure plasma (APP) treatment to produce well-organized microfiber scaffolds with selectively, covalently-immobilized TGFβ1.

Methods: Poly-ε-caprolactone MEW scaffolds were fabricated using a 3DDiscovery printer (RegenHU), then functionalized using a computer-controlled APP device (4.5 kV discharge voltage, 1.9 L/min feed gas flow, 60 mm/s, 5 mm spacing zigzag trajectory), generating a controlled functionalization pattern. TGFβ1 was then immobilized onto the MEW scaffold using submersion in solution (0.01-2 µg/mL TGFβ1 in PBS, 24 hrs, 4°C). Detergent (Tween20/sodium dodecyl sulfate (SDS)) washing steps were undertaken to remove non-covalently bound protein. Characterization of protein immobilization was performed by Fourier-transform Infrared (FTIR) spectroscopy and immunofluorescence detection. *In vitro* experiments were performed by seeding equine mesenchymal stromal cells (MSCs) (~$16x10^6$ cells/mL) into the MEW scaffolds and were cultured for 28 days. The culture groups consisted of (i) plasma-treated-scaffolds w/ immobilized TGFβ1, (ii) plasma-treated-scaffolds w/o TGFβ1, (iii) untreated-scaffolds w/ TGFβ1 in the culture medium, and (iv) untreated-scaffolds in basal medium. Neo-cartilage formation was quantified with dimethyl methylene blue/picogreen assays for glycosaminoglycan (GAG) production and confirmed with histological analysis.

Results: Covalent immobilization of TGFβ1 was achieved using the APP-functionalization approach. FTIR confirmed a protein signature on the samples following intensive 5% SDS washing and immunofluorescently-labelled TGFβ1 was detected in microfiber scaffolds (following 0.1% Tween20 washing). *In vitro* analysis demonstrated that GAG production (DNA-normalized) was significantly enhanced in both the immobilized TGFβ1 (i) and TGFβ1 in medium groups (iii), compared to the control groups (ii & iv). This finding was further validated by the heightened production of GAGs and collagen type II, observed in histological sections (Figure 1). Additionally, this increase in matrix production was seen to become more pronounced as the concentration of immobilized TGFβ1 increased.

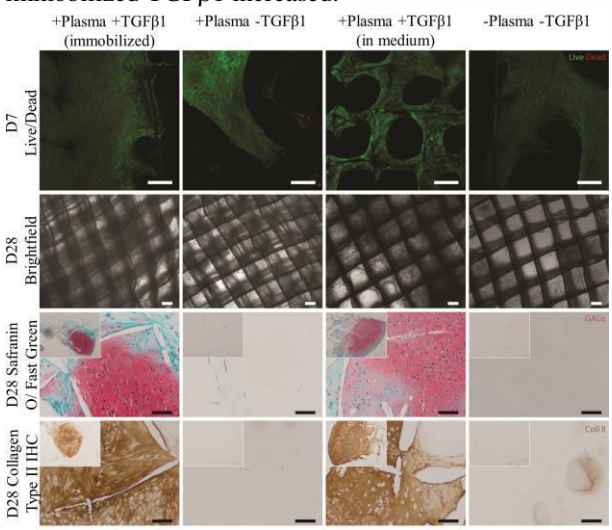

Figure 1: Images of D7 live/dead fluorescent cell imaging (first row), D28 brightfield (second row), D28 safranin O/fast green histology sections (third row) and D28 immunohistochemistry collagen type II sections (fourth row). Experimental groups are organized into four columns with the descriptions above. Scale bars = 200 µm.

Conclusions: We have demonstrated that APP-facilitated covalent immobilization of TGFβ1 retains the growth factor's bioactivity and allows for cellular interactions that stimulate the differentiation of MSCs into the chondrogenic lineage. Our results also demonstrate that the new constructs with locally-immobilized TGFβ1 are able to support neo-cartilage formation. Furthermore, we are currently integrating MEW and plasma functionalization within a single printing platform. This will allow for functionalization during the MEW of microfiber scaffolds for gradient and patterned protein guidance for neo-cartilage formation.

Acknowledgements: This research was funded by the Netherlands Organization for Scientific Research (024.003.013), the EU's H2020 Marie Skłodowska-Curie RESCUE co-fund (#801540), and an Office of Global Engagement Partnership Collaboration Award between the University of Sydney, Utrecht University, and the Australian Research Council.

Bone-Adhesive Barrier Membranes Based on Alendronate-Functionalized Poly(2-oxazoline)s

M. J. Sánchez-Fernández,[a] M. Peerlings,[a] R. P. Félix Lanao,[b] J. C. M. E. Bender, [b] J. C. M. van Hest,[c] and S. C. G. Leeuwenburgh.[a,*]

[a] Department of Dentistry–Regenerative Biomaterials, Radboud Institute for Molecular Life Sciences, Radboud University Medical Center, 6525 EX Nijmegen, the Netherlands.
[b] GATT Technologies BV, 6525 ED, Nijmegen, the Netherlands.
[c] Department of Bio-Organic Chemistry, Institute for Complex Molecular Systems, Eindhoven University of Technology, 5600 MB Eindhoven, the Netherlands.

Introduction:

Oral implants should be tightly fixated in alveolar bone, but this fixation is often hampered by a lack of supporting bone caused by a degenerative process, such as periodontitis, peri-implantitis, aging or trauma. To overcome this problem, barrier membranes are routinely used to isolate bone defects from surrounding fast-growing soft tissues and stimulate the natural healing process of bone. So far, various types of membranes have become commercially available. However, they are associated with several drawbacks, such as poor clinical manageability caused by their poor adhesion to bone.

We propose that the next generation of biodegradable barrier membranes should become adhesive to bone. To this end, a novel and effective bone-adhesive material, rationally designed based on the composition of bone, should be developed first. Biodegradable synthetic polymers could be specifically designed to attach tightly to bone tissue through functionalization with pendant chemical groups of high affinity with the components of bone tissue. Bisphosphonates (BP), such as alendronate (Ale), are known for their exceptionally strong binding affinity to hydroxyapatite, the mineral phase of bone. Organic compounds such as hydroxyl side groups can exhibit a strong affinity for Ca^{2+}. Conventional synthetic polymers as polyethylene glycol and PLGA, can only be functionalized at the end-groups. However, polyoxazolines (POxs) can be functionalized along the entire polymeric backbone. POxs are not only interesting because of their high functionalization possibilities, but also high versatility by copolymerization, narrow molecular weight distribution, tunable properties, good biocompatibility, stealth behavior, and low dispersity.

Materials and Methods:

Adhesive membranes were prepared by dry deposition of polymer particles (≤ 63 µm) into commercially available layered gelatin fibrous carriers (GELITA TUFT-IT®) using a high voltage electrostatic impregnation system (Fibroline SL-Preg) at 40 kV, 100 Hz for 20 seconds, in a weight ratio of polymer/carrier 65%:35, obtaining a homogenous distribution of the polymers through the gelatin carriers. Afterward, an occlusive polyester backing layer was adhered to the carriers by two cycles of heating while compressing at 150 °C, 30 N for 3 seconds, obtaining a final weight ratio of polymer/carrier/backing 42%:28%:30%, calculated by weighing the membranes before and after impregnation, and after adding the backing layer.

In total, five prototypes of membranes were prepared: 1) pure fibrous gelatin carrier, 2) gelatin carrier comprising a backing layer (blank), 3) blank impregnated with alendronate-functionalized POx ($P(EtOx_{70}\text{-}Ale_{30})$), 4) blank impregnated with hydroxyl ad alendronate-functionalized POx ($P(EtOx_{70}\text{-}OH_{10}\text{-}Ale_{20})$), and 5) blank impregnated with alendronate-free POx ($P(EtOx)$). These membranes were characterized in terms of their wettability and mechanical properties. Moreover, adhesion of these membranes to apatite-coated model surfaces as well as bone was assessed in vitro. Finally, the degradation of these membranes was evaluated in vitro in PBS with and without collagenase.

Results and Discussion:

Both the maximum tensile strength and tensile modulus of the membranes were 3-fold higher for membranes comprising a backing layer, compared to membranes consisting of pure fibrous gelatin carriers, proving that the backing layer reinforces the membranes. Membranes comprising POx polymers showed good adhesive properties to both apatite-coated substrates and bone. Their lap-shear adhesion strength to apatite-coated substrates and bone was considerably higher (4 to 8-fold and 8 to 15-fold, respectively, compared to blank membranes, whereas the adhesion strength of the POx-impregnated membranes to both apatite-free coated control substrates and demineralized bone specimens was significantly lower (1 to 16-fold and 11 to 41-fold lower, respectively) than to their corresponding mineralized control substrates.

Afterwards, the adhesion of the membranes was evaluated underwater. As expected, only the membranes comprising POx-Ale polymers remained adhesive to bone after 24 h immersion in water. Moreover, these membranes showed reduced degrees of swelling.

The in vitro degradation of the membranes was calculated as the weight loss of the membranes after immersion in PBS solutions with and without collagenase at different time points. The results showed that the weight loss of the membranes, and therefore, their degradation occurred in a sustained manner, between 58–72% in PBS and 81–88% in PBS with collagenase after 14 days of immersion.

Conclusions:

A new generation of barrier membranes adhesive to bone was developed using a high voltage electrostatic impregnation system. Membranes comprising POx-Ale reacted strongly and specifically with calcium-containing substrates, and they remained adhesive to bone after 24 h immersed in water. The gelatin membranes can be degraded enzymatically. Furthermore, the degradation rate of the backing layer can be controlled over time periods from weeks to months by easily tuning its composition, rendering these

16.30-16.40	**NBTE Scientific Photo Competition Award**

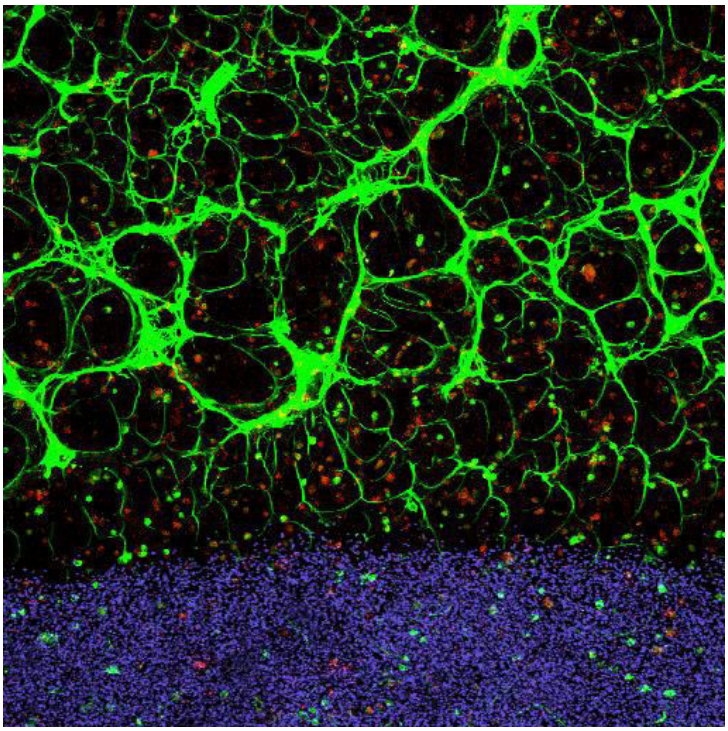

“**A Stormy Night: Green light thunderstorms over the blue horizon” by Deepti Rana (University of Twente)**

This image shows patterning of self-organizing microvascular networks within 3D microenvironment, looking similar to a thunderstorm at night over the blue ocean. For patterning, the VEGF specific aptamer functionalized GelMA bio-inks with MSCs & HUVECs were bioprinted in lines next to plain GelMA bio-ink (with blue fluorescent micro-particles). Subsequently, the samples were loaded with VEGF, expecting aptamer lines would sequester VEGF but not GelMA lines. After 10 days of culture, we observed microvascular network formation confined within the aptamer lines only. This behaviour confirmed that the VEGF loaded aptamer lines were able to guide the network formation within 3D microenvironment.

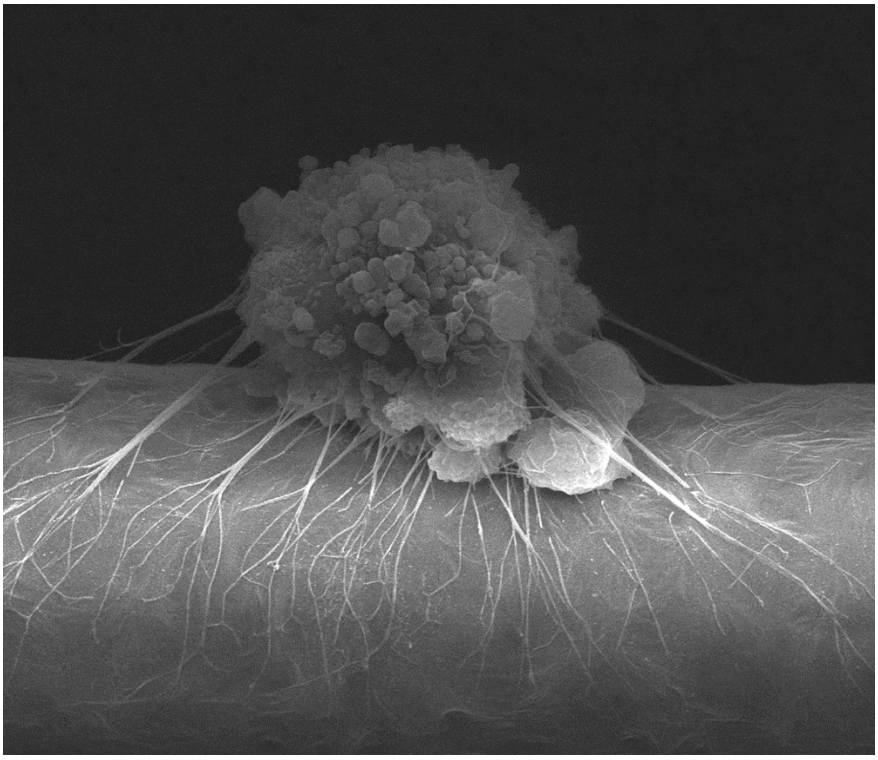

“ Human Trabecular Meshwork cell attached to the printed Polycaprolactone fiber” by Malgorzata Wlodarczyk-Biegun (University of Groningen)

The image shows the Human Trabecular Meshwork (HTM) cell growing on the scaffold prepared by Melt Electrowriting (MEW) of Polycaprolactone. HTM is a fine, intricate network located in the eye and is responsible for maintaining proper pressure in the ocular chamber. HTM dysfunctions lead to glaucoma, one of the leading causes of blindness worldwide. By employing the advanced biofabrication technique of MEW, which utilizes high voltage to deposit well-organized fibers of the polymer melt, we aim at the reconstruction of the complexity of the native HTM tissue.

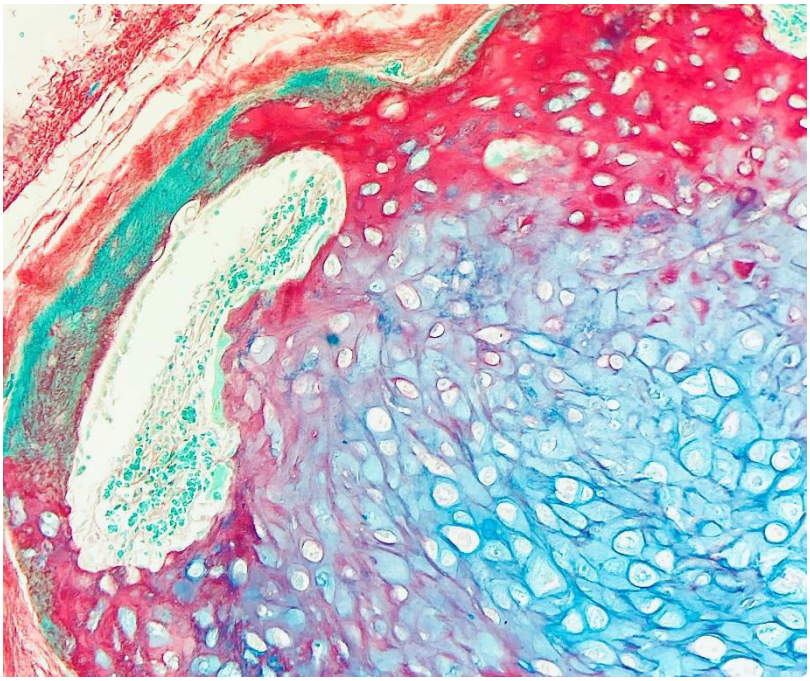

“A wonderful Red-Green-Blue staining on MSC pellets in vivo” by Nicole Kops (ErasmusMC)

We recently were notified about a novel RGB staining comprising Sirius Red, Fast Green and Alcian Blue and we were immediately enthusiastic about it since it can also stain osteoid in paraffin sections which before was, to our knowledge, only possible in MMA (plastic) sections. Besides this mayor benefit this staining is also very well capable of showing the different grades of bone formation through cartilage modulation by a large range of colours going from bright blue to red to green and mixtures of these as shown in this chondrogenic MSC pellet that has been implanted in a mouse.

19.30 – 21.00	**Battle of the Matrix** ***Natural or Synthetic? The path forward for biomaterials.*** **Prof. Dr. Janette Burgess** **University Medical Center Groningen**   **Dr. Matthew Baker** **Maastricht University** **Plenary Discussion**

In the design of biomaterials, the use of natural or synthetic materials and systems has long been argued; in venues ranging from the lab-bench to international conferences. Most researchers strongly support one side over the other, but what is the right answer? Is there a right answer? How do we treat this argument academically? With a good old-fashioned debate, of course! In this session, we will bring this debate to the fore front with a proponent for each side of the argument. During the debate the representatives will logically defend their viewpoint on key issues, and facilitate the audience reaching their own conclusions. Each side has some strengths and weaknesses—can we determine the best way forward as a community?

Friday, 27th November

9.00-9.45	**Belgian Society for Tissue Engineering Keynote** ***Title: From brewing beer to building bone*** **Prof. Dr. Liesbet Geris** **Dep. Biomechanics-Prometheus** **KULeuven-ULiège** 

With the proof of concept now delivered for various approaches to successful bone tissue engineering, the next challenge is to translate these laboratory-scale practices into manufacturing processes able to deliver clinically relevant living implants. This translation encompasses upscaling of the biological processes, identification of critical quality attributes and preparation of regulatory filing, amongst others. A number of key principles of this translation are not unique to biological processes, though they are more challenging. In this lecture I will draw the parallel between another process, a typically Belgian one, namely that of brewing beer, and the process of building biological bone implants. The use of enabling technologies will be discussed as a critical tool in successfully realizing the translation from bench to bedside. Specific examples will be given, ranging from biomaterial optimization over cell culture to organoid-based tissue engineering.

Hydrogel-based bioinks for cell electrowriting of well-organized living structures with micrometer-scale resolution

M. Castilho[1,2], R. Levato[1,3], P.N. Bernal[1], M. de Ruijter[1], C.Y. Sheng[1], J. van Duijn[1], S. Piluso[1,4], K. Ito[1,2], J. Malda[1,3]

[1] Department of Orthopaedics, University Medical Center Utrecht, Heidelberglaan 100, 3584 CX, Utrecht, The Netherlands

[2] Department of Biomedical Engineering, Eindhoven University of Technology,P. O. Box 513, 5600 MB Eindhoven, The Netherlands

[3] Department of Clinical Sciences, Faculty of Veterinary Science, Utrecht University, Yalelaan 1, 3584 CL, Utrecht, The Netherlands

[4] Department of Developmental BioEngineering, Technical Medical Centre, University of Twente, Enschede, The Netherlands

Introduction: Biofabrication has come to the forefront of biomedical research because of its design versatility and potential for guiding cellular organization and behavior. While a wide range of *in vitro* models and pre-clinical implants have been developed with existing techniques, the resolution exhibited so far is within the order of hundreds of micrometers, leading to challenges in mimicking the structure and composition of the extracellular matrix (ECM). Development of bioprinting processes that can achieve higher resolutions and mimic the microstructure of the fibrillar components surrounding cells can potentially enhance essential behavioral and morphological processes. Electrohydrodynamic (EHD) approaches have been widely used for tissue engineering applications due to their ability to fabricate fibers in the tens of micro- and nano-meter ranges. However, most EHD processes incorporate factors that are not compatible with cells such as the use of toxic solvents and/or thermoplastic materials that employ harmful processing temperatures. Herein, the process of cell electrowriting (CEW) is introduced. Through the development of rapidly crosslinkable, biocompatible and EHD-friendly bioinks, controlled deposition of highly organized fibers within the tens of micrometers capable of encapsulating single cells was achieved, more closely mimicking the high-resolution, hierarchical nature of native tissues.

Materials and methods: Two types of protein-based bioinks that exhibit ECM-like properties were developed for CEW (gelatin norbornene (gelNOR) and silk fibroin). The bioinks were optimized to meet key requirements of EHD processes: 1) low electrical conductivity, 2) enhanced viscosity generate stable jets and fibers, 3) rapid photocrosslinking system to allow for immediate fiber stabilization upon deposition. Once the optimized bioink composition was developed, electrowriting parameters were optimized to fabricate stable, high resolution fibers that could be stacked to create complex 3D constructs: applied voltage, collector speed and air pressure. Upon cell incorporation, the mechanical properties and biocompatibility of the process was assessed and compared to conventional extrusion bioprinting methods. Finally, development of multi-cellular and/or multi-material processing was assessed to replicate more complex fiber architectures.

Results and discussion: GelNOR and silk fibroin-based bioinks were developed for CEW. Low conductivity gels were crosslinked within seconds using thiol-ene click and di-tyrosine oxidation photochemistries, respectively and viscosity was tailored with polyethylene oxide. When introduced in an electrowriting set up, both materials exhibited similar printing behavior as previously investigated thermoplastics, exhibiting straight, homogenous fibers at a critical translation speed, and becoming smaller in diameter at higher voltages and collector speeds, as well as lower air pressures and vice versa. Straight, homogenous fibers exhibited diameters of 3-6 and 40-45µm for gelNOR and silk fibroin respectively, a much higher resolution range than conventional extrusion bioprinting (EB; >300µm). Both bioink fibers exhibited stacking capabilities and silk fibroin CEW fibers exhibited enhanced mechanical properties compared to extrusion printed filaments. Both bioinks maintained a cell viability of >70% throughout 7-day culture, comparable to extrusion printed and cast samples (Figure 1). Moreover, it was shown that cell-laden fiber deposition could be controlled to produce complex architectures (curved, hexagonal, squared) and multi-material and multi-cellular constructs.

Conclusions: Through the use of two biocompatible bioinks, CEW was able to achieve previously unreported contextual fiber deposition control and resolution in the presence of viable cells. The potential to introduce cells and multiple materials, in a controlled spatial manner and in an array of complex architectures opens exciting possibilities for high resolution biofabrication of hierarchical structures that can guide cell morphology and behavior.

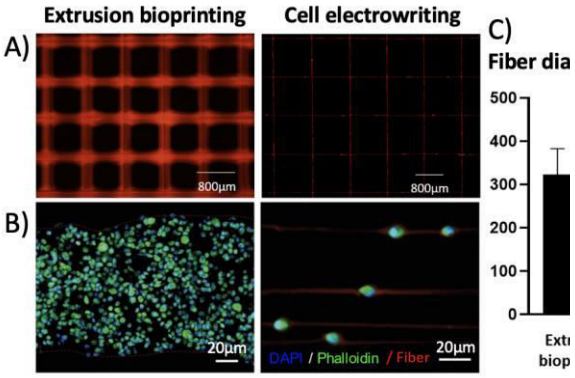

Zonal-cell density 3D bioprinting for biomimetic cartilage tissue engineering

P.J. Díaz-Payno[1,2], A. Dimaraki[1], M. Minneboo[1], M.J. Mirzaali[1], M. Nouri-Goushki[1], N. Kops[2], R. Narcisi[2], G.J.V.M. van Osch[1,2,3], L.E. Fratila-Apachitei[1], A.A. Zadpoor[1]

1 Department of Biomechanical Engineering, Faculty of Mechanical, Maritime and Materials Engineering, Delft University of Technology, Delft, The Netherlands

2 Department of Orthopaedics, Erasmus MC University Medical Center, Rotterdam, The Netherlands

3 Department of Otorhinolaryngology, Erasmus MC University Medical Center, Rotterdam, The Netherlands

p.j.diazpayno@tudelft.nl

INTRODUCTION: Articular cartilage (AC) is a graded tissue characterized by the presence of three layers exhibiting differences in cell density: the superficial zone having the highest cell density and the deep zone, the lowest cell density [1]. Only a few studies have introduced a cell gradient into 3D printed scaffolds [2] and, as far as we are aware, none have optimized the scaffold mechanical properties, hence failing to recapitulate a more biomimetic environment. In this study, we aimed to bioprint scaffolds with different zonal cell densities, assess the scaffold stiffness and the influence of the cell density on the cell viability and tissue deposition.

METHODS: The scaffolds were bioprinted using an alginate-based bioink (Cellink) containing human articular chondrocytes and a polycaprolactone (PCL) support structure. The design of the scaffolds included three cell densities: 20E6 (high), 10E6 (mid) and 5E6 cells/ml (low). Different PCL designs were assessed by compressive tests. The scaffolds were cultured in chondrogenic medium for 25 days and analysed by live-dead and histological staining (Alcian blue, Hematoxilin-Eosin, and Picrosirius-red).

RESULTS: The PCL design showing the closest stiffness to the native AC (8.35 ± 0.35 MPa) was used for bioprinting of the zonal scaffolds. The results of the live-dead at day 14 revealed the ability to generate a defined zonal cell density keeping a high cells viability in the two zones of the scaffolds. The images of the sagittal plane showed a smooth transition between the zones with low and high cell density. Ongoing histological analyses will evaluate the effect of cell density on matrix deposition

DISCUSSION & CONCLUSIONS: This qualitative data demonstrate the generation of different zonal cell densities within bioprinted scaffolds recapitulating the tri-phasic organization of AC. Follow-up studies should look at the addition of a stiffness gradient along the cell gradient.

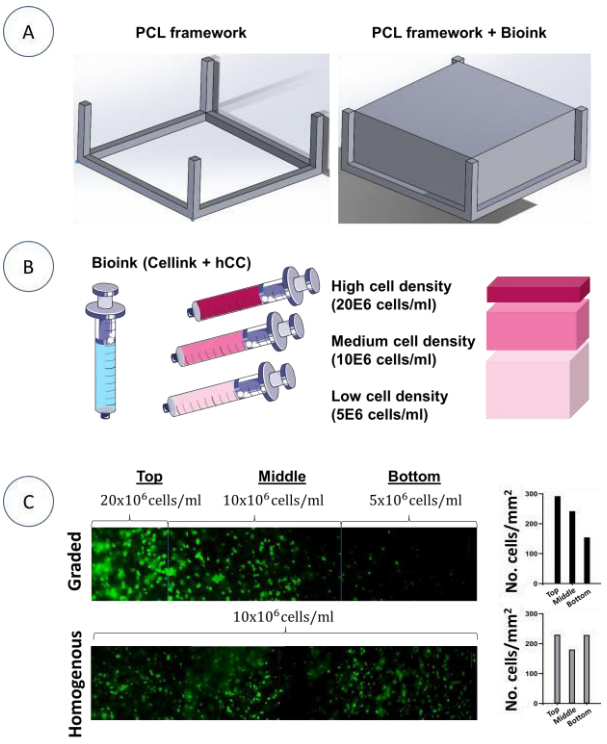

Fig1. A) Schematic of the printed structure PCL framework or PCL+Bioink. B) Schematic of the human articular chondrocyte (hCC) cell density distribution within the bioprinted construct. C) Live/dead images (right) and quantification (right) of bioprinted constructs at day 14, demonstrating high cell viability and zonal distribution in the graded scaffold.

ACKNOWLEDGEMENTS:

Performed as part of Dutch Medical Delta project: RegMed4D.

REFERENCES:

[1] Huber M. et al., Invest. Radiol. 2000; 35(10):573-580.

[2] Ren X. et al., BMC Musculoskeletal Disorders. 2016;17(1):301.

Melt Electrowriting of a Meniscus Scaffold seeded with MSCs and Meniscus Cells

JV Korpershoek[1], M de Ruijter[1], BF Terhaard[1], MH Hagmeijer[1], M Castilho[1,2], J Malda[1,3], LA Vonk[1,#]
[1] Department of Orthopaedics, Regenerative Medicine Utrecht, UMC Utrecht, University of Utrecht, The Netherlands.
[2] Department of Biomedical Engineering, Eindhoven University of Technology, The Netherlands
[3] Department of Clinical Sciences, Faculty of Veterinary Medicine, Utrecht University, The Netherlands
[#] Current Adress: CO.DON AG, Warthestraße 21, D-14513 Teltow, Germany

INTRODUCTION: The human meniscus is composed of an organized network of radial and circumferential collagen fibres and plays a crucial role in load transmission in the knee. Because of the limited regenerative potential of the meniscus, treatment of meniscus injury often involves meniscectomy, which is associated with a high risk of developing osteoarthritis. Therefore there is a need for functional meniscus replacements. Using melt electrowriting (MEW), medical grade materials can be deposited in radial and circumferential micro-fibres to achieve a scaffold architecture that approximates the collagen organization in the native meniscus.

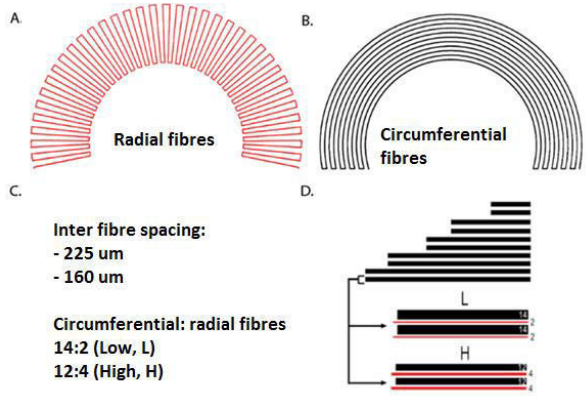

Fig. 1. Scaffold design inspired by native fiber architecture. A) Printhead trajectory of MEW circumferential fibres. B) Printhead trajectory of MEW radial fibres. C) Variables in design include variety in inter fibre spacing and in the ratio between the circumferential and radial fibres. D) Illustration of low (L) and high (H) circumferential:radial fibres ratio.

METHODS: Scaffolds were made using MEW using medical grade polycaprolactone (Corbion). Two different architectures were deposited (Fig. 1A,B) with a programmed inter fibre spacing of 225 µm or 160 µm. The ratio of circumferential : radial fibres was 14:2 or 12:4 (Fig. 1C,D). Printability was assessed using scanning electron microscopy (SEM). The scaffolds were seeded with co-cultures of human primary osteoarthritic meniscus cells and human bone marrow mesenchymal stromal cells (MSC) in fibrin glue. The constructs were compared to a CMI that was reduced to the same form and size using cutting guides. Compressive Young's Modulus was assessed under uniaxial confined compression. After 4 weeks of culture, proteoglycan content was assessed using the Dimethylmethylene Blue (DMMB) assay to quantify sulfated glycosaminoglycans. DNA content was quantified using the Quant-iT PicoGreen kit. Cell distribution throughout the scaffold was assessed at 3 locations and 2 orientations using Hematoxylin and Eosin (H&E) staining.

RESULTS: MEW scaffolds showed a clear distinction between radial and circumferential fibres with an average fibre diameter of 15.92 µm ± 1.37 µm. After 28 days of culture, proteoglycan production of co-cultured meniscus cells and MSCs was comparable in the different MEW constructs, the CMI® and fibrin glue cultured without a scaffold. The group with low inter fibre spacing (160 µm) and low ratio of radial fibres (14:2) was mechanically superior to the CMI after 28 days of co-culture. After 28 days culture without cells, the groups with high and low inter fibre spacing and high ratios (12:4) of radial fibres were both mechanically superior to the CMI®.

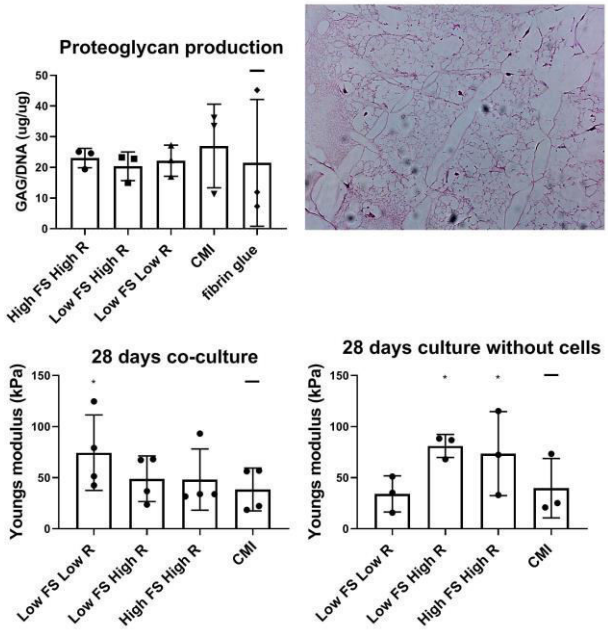

Fig. 2. Proteoglycan (glycosaminoglycan; GAG) production normalized for DNA, HE-stained section showing cell distribution along fibres, Compressive Young's Modulus after 28 days of co-culture with meniscus cells and MSCs (20:80) or without cells.

CONCLUSIONS: This study shows proof-of-concept of a wedge-shaped meniscus construct made with MEW composed of medical-grade materials. Here, the feasibility of seeding the constructs with a clinically feasible cell-source and number for one-stage treatment of meniscal injury is shown. The co-cultured construct with low (160 µm) programmed inter fibre spacing and low (14:2) ratio of circumferential:radial fibers shows mechanical superiority compared to a clinically available implant and therefore shows potential for clinical translation.

Bioengineering Clinically-Sized Microporous Annealed Scaffolds via In-Air Production of Dual-Crosslinking Microgels

M.R. Schot[1], M.L. Becker[1], J.C.H. Leijten[1]

[1] *Department of Developmental BioEngineering, TechMed Centre, University of Twente, The Netherlands*

Introduction: Microfluidic technologies have facilitated the creation of microporous tissue scaffolds in recent years. The microporous nature of MAPs associates with improved perfusability, cell migration, implant survival, and tissue integration.[1,2] However, the low throughput of current microfluidic strategies has prevented the translation of this technology into a clinical setting. We hypothesized that in-air microfluidics (IAMF) would allow for the ultra-high throughput production of monodisperse microgels, which would enable the fabrication of clinically sized MAPs.[3] To allow for the generated microgels to form inter-particle bonds, we developed and synthesized a dual-crosslinking biomaterial: Alginate-Tyramine (ATA). We here combine this material with IAMF to, for the first time, enable ultra-high throughput production of MAPs.

Materials and Methods:
Alginate (80-120cP) was modified with tyramine moieties using standard DMTMM-based coupling. The degree of substitution was quantified using UV-Vis spectroscopy. Vial-tilting was used to verify the sol-gel phase transition of the material following ionic and/or covalent crosslinking. Calcium chloride was used for in-air ionic crosslinking of microgels, while Ruthenium/Sodium Persulfate (Ru/SPS) was used for covalent crosslinking of the microgels to form MAPs. To generate microgels, ATA (0.5% w/v) and $CaCl_2$ (0.1mM in 10% w/v ethanol) were used as two in-air colliding jets. Upon impact, calcium chloride wraps around the alginate drops via Marangoni flow, and microgels are formed via outside-in diffusion of calcium ions. MAPs were created by packing particles using suction-assisted filtration and spiking the packed constructs with Ru/SPS solutions before applying visible light for 30 seconds. Construct stability was validated via agitation analysis. Constructs porosity was characterized by quantitating fluorophore diffusion using fluorescent confocal imaging. Cells were encapsulated in microgels by generating microgels in air with $1x10^6$ cells/mL in 0.5% ATA. Viability was analyzed using standard live/dead assays.

Results and Discussion:
Successful functionalization of ATA was achieved using DMTMM chemistry, with degrees of substitution ranging from 2.5% to 6.6% as determined with UV-Vis spectroscopy. ATA samples were able to form crosslinks using ionic as well as light-based covalent chemistries. Using IAMF, microparticles of controlled sizes ranging from 50 µm to 350 µm with a CV below 5% could be produced with flow rates ranging from 0.9 mL/min to 3.5 mL/min depending on nozzle size (Figure 1A). Several cell types were successfully encapsulated with cell viabilities of ≥88% (Figure 1B). After particle packing, MAP formation was achieved using injection molding followed by crosslinking with visible light in the presence of Ru/SPS. Upon exposure to hydrodynamic stress, the construct without Ru/SPS crosslink (blue) dissolved rapidly, whereas the dual-crosslinked MAPs (orange) remained fully intact (Figure 2A). Confocal microscopy was used to visualize the MAPs' internal structure, which demonstrated an interconnected network of pores between packed microgels with pore diameters ranging from 5 to 200 micron depending on microgel size.

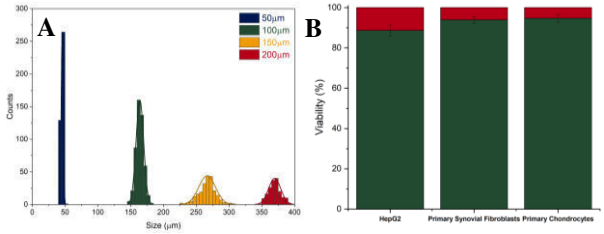

Figure 1 **A)** *Size distribution of microgels created with IAMF.* **B)** *Viability plots (day 1) of several cell types encapsulated in 100µm microgels.*

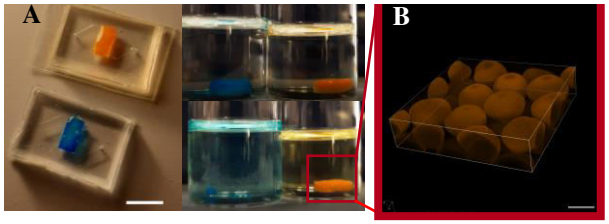

Figure 2 A) Left: *Microgels injected into a PDMS mold with Ru/SPS (orange) or food coloring (blue). (scalebar: 1cm).* ***Right:*** *Upon agitation, MAPs stay intact (orange) whereas single crosslinked packed microgels dissolve into individual particles.* ***B)*** *Internal structure of MAP as imaged with confocal fluorescence microscopy. (scalebar: 100 µm)*

Conclusions:
By combining IAMF and ATA, we were able to produce microgels of controlled sizes in ultra-high throughput, which allowed for the production of voluminous MAPs using a second, visible light based crosslinking system. All MAPs contained interconnected porous networks, and associated with high viability of encapsulated cells. Currently, we are creating liver MAPs and analyzing their functionality in vitro.

Acknowledgements:
Financial support was received from the European Research Council (ERC, Starting Grant, #759425).

Bibliography:
1 Griffin, D. R. *et al. Nat. Mater.* 14, 737–744 (2015)
2 Annamalai, R. T. *et al. Ann. Biomed. Eng.* 47, 1223–1236 (2019)
3 Visser, C. W. *et al. Sci. Adv.* 4, 1–9 (2018)

Contact
M.R. Schot; +31-534-898-152; m.r.schot@utwente.nl

Silk-based Materials to Create High Resolution Three-dimensional Structures Using Electrohydrodynamic Printing

Martina Viola [1,2], Susanna Piluso [1], Marko Mihajlovic [2], Jos Malda [1], Miguel Castilho [1], Tina Vermonden [2]

[1.] Department of Orthopedics, University Medical Center Utrecht (UMCU); Heidelberglaan 100, 3584 CX Utrecht, The Netherlands.

[2.] Department of Pharmaceutics, Utrecht Institute for Pharmaceutical Sciences (UIPS), Faculty of Science, Utrecht University, P.O. Box 80082, 3508 TB Utrecht, The Netherlands

Email m.viola@uu.nl

Mimicking the complex hierarchical structure of the extracellular matrix (ECM) has always been a major goal in tissue engineering (TE) approaches [1] [2]. Despite the great advances in biomaterial processing technologies, one of the main limitations concern the processing of protein-based natural-derived materials at micron and sub-micrometer scale.

Here, we combine silk fibroin (SF) [5], a highly potent biopolymer that intrinsically has the ability to form fibrous structures, with electrohydrodynamic printing, a 3D printing technique that allows fibre patterning at micro and sub micrometer scale. To fabricate complex structures, electrohydrodynamic printing applies a voltage between the needle and the collector screen to charge the polymer solution, with a consequent thinning of the fibers, making it possible to reach optimal resolution for recreating the hierarchical and fibrillar structure of ECM [3] [4]. By slightly modifying the processing of raw silk, we obtained different molecular weight of SF (SF5, SF10 and SF20, where the number indicates the minutes of boiling time). The solutions of SF were mixed with a small amount of Polyethylene Oxide (MW = 600 – 1000 kDa) to increase the viscosity. The rheological characterization showed shear thinning behavior and we could demonstrate that, by tuning the concentrations (SF 10 w/v% and PEO from 1 %w/v to 2 %w/v), we were able to obtain well-defined straight fibers with diameters ranging between 10-20 μm (Fig 1). After the printing, we observed that a water solution of Na_3PO_4 (1M) induced SF physical crosslinking via the formation of β-sheet structures. These structures were stable in aqueous environments for more than one week. We compared the mechanical properties of the gels with SF crosslinked with methanol, observing that with Na_3PO_4 (1M) the gel has an elastic behavior while with MeOH was stiffer.

In summary, electrohydrodynamic writing processed SF fibres are a versatile material that can be of great interest for soft tissue engineering.

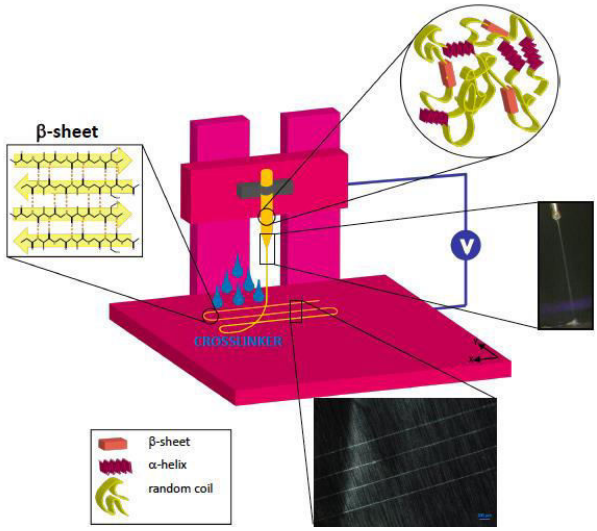

Fig 1: ***Schematic representation of electrohydrodynamic printing of SF. Before printing SF appears as a viscous solution and most of the chains are in random coil conformation. The after-printing crosslinking induces the formation of β-sheet structures, making the fibers insoluble in water.***

References

[1] R. O. Hynes, "The Extracellular Matrix: Not Just Pretty Fibrils," Science, vol. 326, no. 5957, pp. 1216-1219, 2009.

[2] M. P. Lutolf and J. A. Hubbell, "Synthetic biomaterials as instructive extracellular microenvironments for morphogenesis in tissue engineering," Nature Biotechnology, vol. 23, pp. 47-55, 2005.

[3] M. Castilho, A. van Mil, M. Maher, C. H. G. Metz, G. Hochleitner, J. Groll, P. A. Doevendans, K. Ito, J. P.G. Sluijter and J. Malda, "Melt Electrowriting Allows Tailored Microstructural and Mechanical Design of Scaffolds to Advance Functional Human Myocardial Tissue Formation," Advaned Functional Material, vol. 28, 2018.

[4] T. M. Robinson, D. W. Hutmacher and P. Dalton, "The Next Frontier in Melt Electrospinning: Taming the Jet," Advanced Functional Material, no. 1904664, 2019.

[5] L. Koh, Y. Cheng, C. Teng, Y. Khin, X. Loh, S. Tee, M. Low, E.Ye, H. Yu,Y. Zhang, M. Han, "Structures, mechanical properties and applications of silkfibroin materials," Progress in Polymer Science, vol. 46, pp. 86-110, 2015.

Patterning Self-Organizing Microvascular Networks within Engineered Matrices

D. Rana, V. Trikalitis, V.R. Rangel, A. Kandar, J. Rouwkema

Department of Biomechanical Engineering, Technical Medical Centre,
University of Twente, 7522NB Enschede, The Netherlands
Presenting Author's Email: d.rana@utwente.nl

Introduction

Hierarchically arranged self-organizing vasculature is a long-sought goal of tissue engineering. In native tissues, various factors such as fluid flow, biomechanical cues and biochemical cues (growth factors & cytokines) work in synergy to achieve high precision over vasculature. To this end, by employing spatiotemporally controlled growth factor's availability within engineered tissues could help in guiding the developing vasculature. However, the conventional approaches for growth factor delivery often focuses on their immobilization or coupling within the engineered matrices (hydrogel), via various linker proteins or peptides. Even though it provides stable release rates, but imparts limitations upon upscaling with high specificity of multiple growth factors delivery. To overcome this limitation, the present study employed oligonucleotides based aptamers, that are affinity ligands designed to recognize proteins with high affinity and specificity.[1] The developed aptamer-functionalized biomaterials were systematically studied for achieving patterned self-organizing microvascular networks in 3D microenvironments.

Materials & Methods

The aptamer-functionalized hydrogels were prepared via photo-polymerization of gelatin methacryloyl (GelMA) and acrydite functionalized aptamers having DNA sequence specific for binding to vascular endothelial growth factor ($VEGF_{165}$). Visible light photoinitiator, tris(2,2′ -bipyridyl)dichloro-ruthenium(II) hexahydrate with sodium persulfate was used. For patterning, aptamer-functionalized hydrogels 3D printing technique was employed. The human umbilical vein endothelial cells (HUVECs) and mesenchymal stem cells (MSCs) were used. The construct was 3D bioprinted as lines of aptamer-functionalized bio-ink next to plain GelMA lines (blue beads), making an interface. After 3D printing, the constructs were crosslinked and loaded with VEGF for 1 hr. It was expected that the 3D bioprinted aptamer lines would be able to sequester VEGF from the culture medium, compared to GelMA lines. To study the programmable/triggered growth factor (VEGF) release efficiency, the complementary sequences (CSs) were also added at specific time-points and their effect of microvascular network formation was studied.

Results & Discussion

The results obtained from physicochemical analysis of the aptamer-functionalized hydrogels confirmed the higher aptamer retention capacity of acrydite functionalized aptamers within the hydrogels, in comparison with the control aptamers for as long as 10 days at 37 °C. The VEGF ELISA experiments confirmed triggered release of VEGF from the aptamer functionalized hydrogels in response to CS addition. Without CS addition, these hydrogels could sustain a controlled release for until 10 days. Furthermore, in co-culture experiments, the developed patterned aptamer-functionalized hydrogels showed high cellular viability and ability to guide microvascular network formation (by HUVECs and MSCs) only within the aptamer-functionalized regions of the pattern, and not in GelMA regions, after 10 days of culture (Figure 1). However, differences in the microvascular organization was observed in the samples with triggered VEGF release on on day 5, compared to the samples without the VEGF release. These observations altogether confirmed the ability of patterned aptamer functionalized hydrogels in controlling self-organizing microvascular networks.

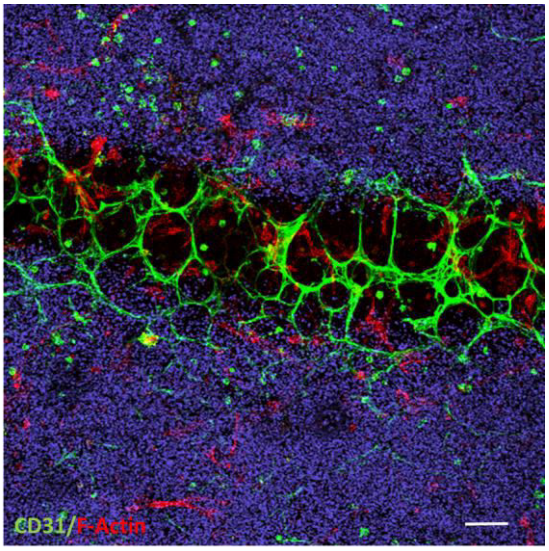

Figure 1: The 3D bioprinted aptamer-functionalized hydrogels guiding the self-organizing microvascular network formation confined within the VEGF–loaded aptamer regions. Blue fluorescent beads indicates GelMA region. Scale bar is 100 microns.

Conclusions

The present study confirms the potential of patterned aptamer-functionalized hydrogels in guiding self-organizing microvascular networks within 3D microenvironment, by spatiotemporally controlling VEGF bioavailability.

Acknowledgements:
This work is supported by an ERC Consolidator Grant under grant agreement no 724469.

References

1. D. Rana, A. Kandar, N. Salehi-Nik, I. Inci, B. Koopman, J. Rouwkema. BioRxiv (2020) doi: https://doi.org/10.1101/2020.09.22.308619.

A new non-invasive technique for measuring the 3D-oxygen gradient in wells during mammalian cell culture

C.J. Peniche Silva[1], G. Liebsch[2], R.J. Meier[2], M. Gutbrod[2], E.R. Balmayor[3], M. van Griensven[1]
[1]Dept. cBITE, MERLN Institute for Technology-Inspired Regenerative Medicine, Maastricht University, Universiteitssingel 40, 6229 ER Maastricht, The Netherlands
[2]PreSens, Precision Sensing GmbH, Am BioPark 11, 93053 Regensburg, Germany
[3]Dept. IBE, MERLN Institute for Technology-Inspired Regenerative Medicine, Maastricht University, Universiteitssingel 40, 6229 ER Maastricht, The Netherlands

Introduction: Oxygen plays an important role in the regulation of the overall cell function and fate during culture. Nevertheless, the accurate monitoring of the oxygen concentration during cell culture remains an underestimated challenge. Oxygen levels at the cell layer in culture are very often assumed to remain equal in value to that of the incubator's atmosphere. However, this assumption does not consider oxygen diffusion properties, cell type, cell density nor the media composition or volume. Consequently, cells in culture are often exposed to significantly lower levels of oxygen concentration than suspected. In the present study, we tested a new non-invasive optical sensor foil-based technique for real-time monitoring of the vertical 3D oxygen gradient that is formed during culture. Furthermore, we compared the obtained 3D oxygen gradient with the oxygen profile measured using a more invasive needle-type oxygen microsensor.

Methods: For the measurement of the 3D oxygen gradient formation during cell culture, we developed a small, 3D-printed ramp with a 25 degrees angle and a maximum height of 3.3 mm to be used with the VisiSens TD camera system (PreSens, Regensburg, Germany). An SF-RPsSu4 oxygen sensor foil (PreSens, Regensburg, Germany) was attached to the surface of the ramp. Thereafter, the ramps containing the sensors were randomly positioned at the bottom of the wells of a 24 well plate (1 ramp per well) prior to cell seeding. Human adenocarcinomic alveolar epithelial cells (A549) were seeded in triplicates at three different initial cell densities (3.5×10^4, 6.8×10^4, and 1.02×10^5 cells/cm^2). The cell culture plate was placed on top of the VisiSens TD camera system inside a cell culture incubator and images were taken every hour for a period of 96 h. Oxygen levels were optically measured using a pixel profiling tool (48 pixels across the sensor). For comparison, the optical fiber-based needle-type sensor PM-PSt7 (PreSens, Regensburg, Germany) was employed for measuring the oxygen concentration profile at different heights inside confluent cell culture wells after 96 h of culture. Cultivation and oxygen concentration measurements were conducted under standard culture conditions in a humidified atmosphere containing 5% CO_2 and 18.6% O_2 at 37˚C. No medium exchange was conducted during the measurements.

Results and discussion: The O_2 gradient obtained after 96 h of culture showed significantly lower O_2 concentrations values closer to the bottom of the well in high cell density cultures (2.53 ± 0.71%) compared to that of lower cell density cultures (11.01 ± 1.21%). Furthermore, it was very interesting to observe that even with low cell density culture, oxygen concentration near the cell layer was lower than that of the incubator atmosphere (Figure 1). The gradient measured with the needle type microsensor was comparable to that obtained with our new, non-invasive technique (Figure 2). Furthermore, the measured oxygen gradients after 96 h were used to calculate the oxygen consumption rate (OCR) of the A549 cells, and the obtained value of ~100 fmol/h/cell matches the OCR value already reported in the literature for this cell line.

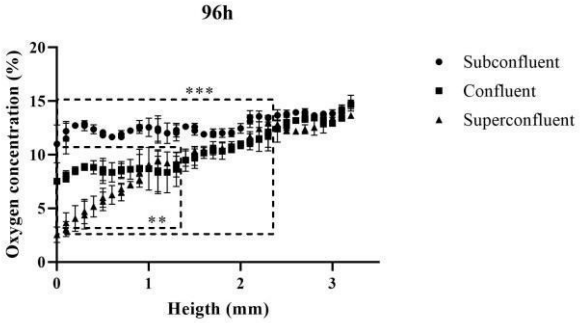

*Figure 1: Oxygen profiles obtained for the three different cell densities at time points 96 h. Significant differences ($p < 0.0001$) between profiles are delimited. ** indicates significant differences between two profiles and *** indicates significant differences between the three profiles.*

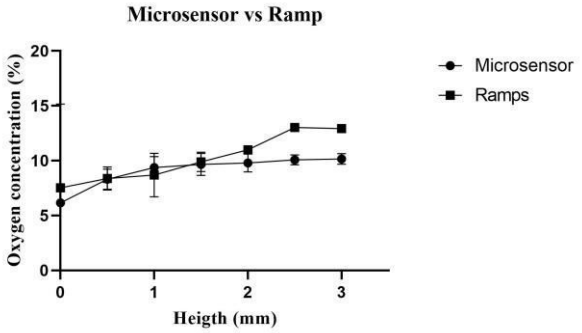

Figure 2: Oxygen profiles after 96 h of culture of confluent wells measured with both techniques.

Conclusions: With our developed sensor foil-based technique, it was possible to measure the oxygen gradient formation during cell culture of A549 cells at different cell densities simultaneously in a non-invasive way. Furthermore, the 3D oxygen gradient measured with the ramps was comparable to that measured with the needle type microsensor. Additionally, our technique was found to be unique in its ability to monitor simultaneously the 3D oxygen gradient formation in several wells of a culture plate.

Acknowledgments: The project was supported by a grant from the Bayerische Forschungsstiftung ("Happihypo" 1163-15).

Generation of Immunoprotective and Enzymatically Crosslinked Polyethylene Glycol-Tyramine Microcapsules for Beta-cell Delivery using Microfluidics

N. Araújo-Gomes[1*], B.M. Liszka-Zoetebier[1*], S.R. van Loo[1], S. Nijhuis[1], T. Kamperman[1], P. de Vos[2], A.M. Smink[2], B. de Haan[2], M. Karperien[1], J. Leijten[1]

[1] Department of Developmental BioEngineering, TechMed Centre, University of Twente, The Netherlands
[2] Section of Immunoendocrinology, Department of Pathology and Medical Biology, University Medical Center Groningen, University of Groningen , Groningen , The Netherlands.

Introduction: Non-autologous beta cell transplantation is currently considered as a therapeutical approach for the treatment of conditions associated with beta-cell loss-of-function and consequent insulin shortage (*e.g.* diabetes type I). Implanted cells can be protected from the host's immune system using immunoprotective biomaterials, such as semi-permeable microcapsules[1] that are capable of preventing the diffusion of molecules larger than 150 kDa (i.e. antibodies), while the diffusion of smaller molecules (i.e. glucose and insulin).
Clinical translation of these immunoprotective microcapsules is currently challenged by the low-throughput production rate of the currently explored platforms. Herein, we describe the development of an immunoprotective and non-degradable microcapsules that are produced in an ultra-high-throughput manner.

Materials and Methods:
20 kDa arm polyethylene glycol–tyramine (PEG-TA) was prepared in a two-step synthesis: 1) ester activation and 2) amidation. PEG-TA conjugates (2,5%, 5%, and 10% w/v) were used to produce enzymatically crosslinked hollow microgels in the presence of horseradish peroxidase (HRP) and non-cytotoxic concentrations of hydrogen peroxide using a delayed outside-in crosslinking strategy[2]. Microcapsule formation was assessed on two production platforms: microfluidic chips and in-air microfluidics (IAMF)[3]. Microcapsule permeability was analyzed via incubation with fluorescently labeled immunoglobulin (IgG) and bovine serum albumin (BSA).
Microgel characterization was performed assessing variables such as cytocompatibility, cyto-immunity, permselectivity, glucose responsiveness *in vitro,* and immune responses formation *in vivo*.

Results and Discussion:
Consistent monodisperse microcapsule with a diameter of ~200 µm and a shell thickness of ~20 µm were successfully produced on both production platforms. FITC-IgG diffusion experiments demonstrated that molecules of >150kDa could not diffuse into the microcapsules (**Fig.1**). Moreover, the microcapsules did allow for the diffusion of smaller molecule like BSA, ensuring transport of nutrients, hormones, waste products, and growth factors through the microcapsule's shell.

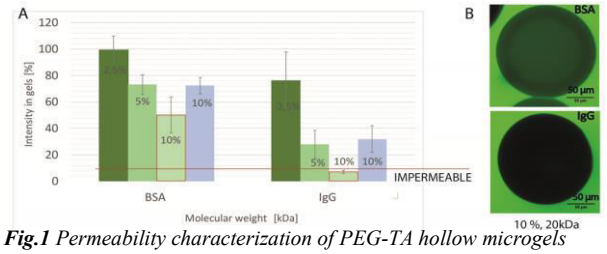

***Fig.1** Permeability characterization of PEG-TA hollow microgels*

Immunological studies revealed that microcapsule contact with THP1 cells did not elicited macrophage activation or allowed for surface attachment. Multiplexed ELISA analysis on live blood immune reactivity was performed, which demonstrated an inverse dose-dependent response (**Fig.2**).

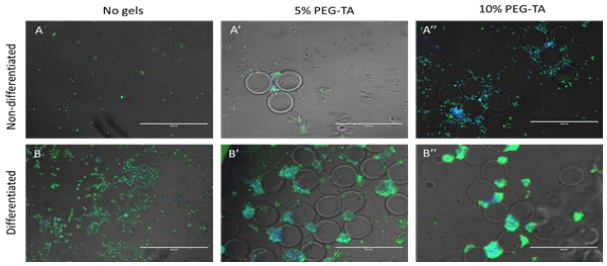

***Fig.2**: Immunostaining of CD68+ THP1 cells exposed to PEG-TA microcapsules.*

Microencapsulated beta-cells remained glucose responsive, capable of releasing insulin without cell death or loss-of-function. Subcutaneous and intra-peritoneal implantation revealed some fibrotic tissue formation and limited macrophage activation, which was related to the microgel geometric profile.

Conclusions:
Ultra-high throughput microfluidic production of immunoprotective PEG-TA microcapsules was achieved. Produced microcapsules showed promising therapeutical potential for the delivery and shielding of non-autologous beta-cells in a living organism.

Acknowledgements:
Financial support was received from the European Research Council (ERC, Starting Grant, #759425) and JDRF award 2-SRA-2018-684-S-B.

Bibliography:
1. Lewińska D, Biomaterials Science, 8, 1536-1574, 2020
2.van Loo SR *et al*., Materials Today Bio, 6:100047,2020
3.Visser CW., Kamperman T *et al.,* Science Advances, Vol. 4, no. 1, 2018

Assessment of the Neutrophil Response to a Panel of Synthetic and Natural derived Biomaterials; a Novel Comprehensive in vitro Approach

Marinus A. Wesdorp[1,2], Andrea Schwab[1], Roberto Narcisi[2], David Eglin[1], Gerjo J.V.M. van Osch[2,3], Matteo D'Este[1]

(1) AO Research Institute, Davos, Switzerland
(2) Erasmus MC, University Medical Center Rotterdam, Rotterdam, the Netherlands
(3) Faculty of Mechanical, Maritime, and Materials Engineering, Delft University of Technology, the Netherlands

INTRODUCTION: Neutrophils play a pivotal role in orchestrating the immune response to biomaterials, the onset and resolution of chronic inflammation, and macrophage polarization. However, their response to biomaterials and consequent impact in tissue engineering approaches has been often overlooked. The neutrophil response can be described by: survival, neutrophil extracellular trap (NET) formation, and release of granules with immunoregulatory factors. Here we aim to investigate these processes in human primary neutrophils exposed to different biomaterial surfaces.

MATERIALS & METHODS: Human primary neutrophils of five healthy donors were seeded at a concentration of $1.0*10^6$/mL in wells coated with a panel of natural and synthetic, and soft and hard biomaterials. The biomaterials used were tyramine substituted hyaluronic acid (THA), tyramine substituted hyaluronic acid functionalized with collagen (THA-collagen), collagen, gelatin methacryloyl (GelMA), polyvinylalcohol (PVA), polycaprolactone (PCL) and tissue culture plastic (TCP). Cell-survival was measured by calcein AM /ethidium homodimer live/dead imaging and lactate dehydrogenase (LDH) secretion. Metabolic activity was measured by the absorbance of CellTiter-Blue. Both cell-survival and metabolic activity were determined after 1,3,5,7, and 24 hours. Formation of reactive oxygen species (ROS) and NET components myeloperoxidase (MPO) and elastase were assessed after 3 hours of exposure of the neutrophils to the different biomaterials. Secretion of a panel of inflammation-related factors was evaluated biochemically.

RESULTS: Neutrophil survival was 90-100% after 24 hours on the soft natural hydrogel surfaces (THA, THA-collagen, collagen and GelMA), 60-70% on PVA and TCP, but was lower than 50% on PCL. Metabolic activity after 1, 3, 5, and 7 hours was 2 to 3-fold higher on TCP and PCL than on soft materials. MPO and elastase levels were 3-10-fold higher on TCP, PCL, and PVA surfaces than on hyaluronan-and collagen-containing hydrogels. In contrast, ROS production was higher on hyaluronan- and collagen containing hydrogels than on PVA, TCP and PCL. MMP9, an important factor in neutrophil regulation and wound healing, secretion was significantly higher on TCP, PVA and PCL surfaces than on hyaluronan-and collagen-containing hydrogels.

DISCUSSION & CONCLUSION: Neutrophils survive better on materials deriving from natural proteins than on synthetic materials. Biomaterials deriving from natural proteins resulted in higher levels of ROS, whereas neutrophils respond with more NET formation on synthetic materials. Stiffness and composition of substrates play a role in neutrophils responses suggesting the ability to be potential characteristics to modulate the inflammatory response. This potential indicates the necessity of further studies elucidating the mechanism triggering this spectrum of responses and its consequences in determining inflammation onset and resolution.

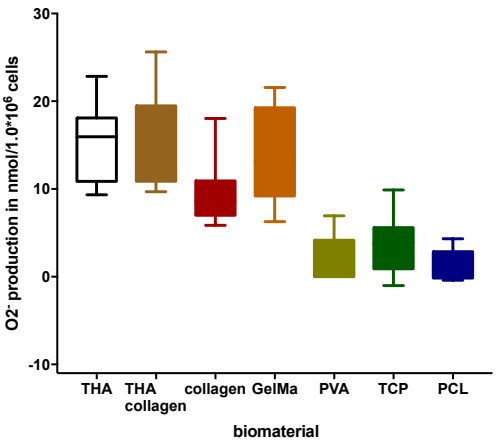

Figure 1. Neutrophils secreted more ROS in response to natural materials than synthetic materials.

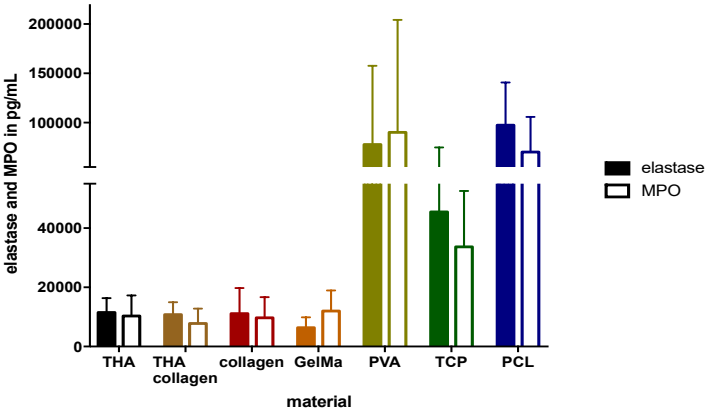

Figure 2. Neutrophils secreted more elastase and MPO in response to synthetic materials than natural materials.

Synovial membrane on chip: studying immune response over inflammation in a multi-cellular system

Carlo Alberto Paggi[1,2], Nuno Araújo-Gomes[1], Mariia Zakharova[3], Luuk van de Schepop[2], Jeroen Leijten[1], Loes Segerink[3], Séverine Le Gac[2], and Marcel Karperien[1]

[1] Department of Developmental BioEngineering, TechMed Center, University of Twente, The Netherlands. [2] Applied Microfluidics for BioEngineering Research, MESA+ Institute for Nanotechnology & TechMed Center, [3] BIOS, MESA+ Institute for Nanotechnology & TechMed Center, The Netherlands

INTRODUCTION

The synovial membrane is a tissue surrounding the articular joints. It comprises a superficial layer presenting a combination of synovial fibroblasts and macrophages and a deeper layer in which nerves, small vessels and other cell types are found. This tissue acts as a key regulator in the homeostasis of the joint, and in rheumatoid disease development and progression. During rheumatoid arthritis, both the synovial fibroblasts and macrophages hyper-proliferate. Moreover, an immune response is triggered as a consequence of the macrophages phenotypic change towards a more pro-inflammatory phenotype. Due to the lack of proper models to mimic this tissue, it remains largely unclear how inflammation influences both these fibroblasts and macrophages.

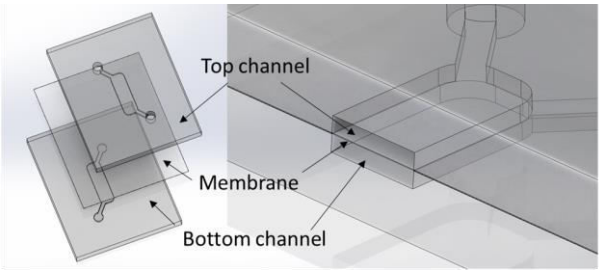

Figure 1: schematic drawing of the system with top and bottom channel separated by a thin transparent PDMS membrane

In this context, we have developed a synovial membrane on chip model, intending to capture the key regulatory pathways that drive the transformation of the synovial membrane in rheumatoid arthritis under the influence of inflammatory stimuli. Our system aims at better understanding how rheumatoid arthritis develops and progresses, and identifying new therapeutic options.

EXPERIMENTAL

The device was fabricated using soft-lithography from polydimethylsiloxane (PDMS). The system comprises a thin horizontal PDMS membrane and two compartments on both sides of the membrane representing the synovial lining (synovial fibroblasts + macrophages) and the sub-intima (endothelial cells). The system was successively coated with polydopamine and collagen I. Both synovial fibroblasts and endothelial cells were seeded in the system and cultured for 5 days. Next, differentiated THP-1 macrophages were seeded in the synovial lining compartment on the synovial fibroblasts. One day after (day 6 of culture in the system) a combination of TNF-α and Il-1β (10 ng/mL) was added to the culture medium in the top channel for two days (from day 6 to day 8) in some devices. Cells in the systems, with and without the inflammatory cocktail were then fixed and stained with CD206, CD80, CD68 (macrophages markers) & cadherin11 and collagen I (synovial lining markers).

RESULTS AND DISCUSSION

Synovial fibroblasts in combination with the endothelial cells and macrophages remained viable in culture for up to 10 days suggesting creation of a favorable environment for the cells (figure not shown). Interestingly, the M0 macrophages nicely integrated in the synovial fibroblasts layer one day after seeding

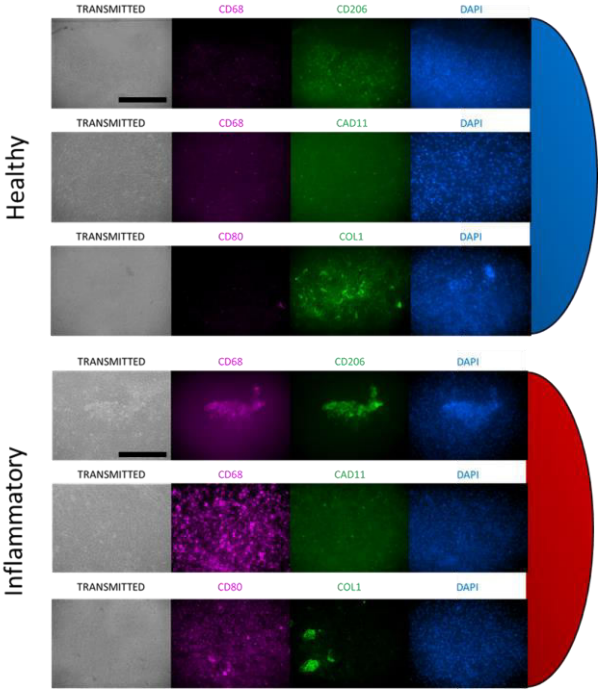

Figure 2: From top to bottom, three examples of healthy and three examples in inflammatory conditions at day 10 (independent devices). Same images are acquired for both conditions: first row; transmitted light, CD68 (v) and CD206 staining (g); second row, transmitted light, CD68 (v) and cadherin 11 staining (g); third row, CD80 (v) and collagen I staining (g). All the samples were counter-stained with DAPI. v=violet & g=green. Scale bar 400 µm.

(figure not shown) suggesting polarization in a macrophage phenotype. Immunofluorescent staining of CD206, CD68 and CD80 revealed that macrophages polarized into the M2 phenotype advocating an anti-inflammatory effect. Co-culture of synoviocytes and the M2 macrophages stimulated the production of collagen type 1indicative for the formation of a native synovial lining. Upon stimulation with pro-inflammatory cytokines the M0 macrophages became CD80 positive, indicative for polarization into the M1pro-inflammatory phenotype.

CONCLUSION

Our synovial membrane on chip enables the culture of 3 cell types simultaneously. It faithfully recreates the synovial lining present in the native articulation. Moreover, it allows mimicking healthy and diseased conditions which is of particular interest to study therapeutic treatments.

CONTACT

C.A. Paggi; +31-53-489-5555; c.a.paggi@utwente.nl

Additional abstracts

Significance of Geometry in Biomimetic Eardrum Scaffolds

S. Anand[1], T. Stoppe[2], M. Neudert[2], S. Danti[3], L. Moroni[1], C. Mota[1]

[1] MERLN Institute for Technology-Inspired Regenerative Medicine, Maastricht University, Maastricht, The Netherlands

[2] Technische Universität Dresden, Carl Gustav Carus Faculty of Medicine, Otorhinolaryngology, Dresden, Germany

[3] Department of Civil and Industrial Engineering, University of Pisa, Research Unit of INSTM, Pisa, Italy

Introduction: The human eardrum (ED) is a thin, concave structure of the middle ear that captures sound waves from the environment and transforms them into mechanical motion [1]. The successful transmission of these acoustic vibrations to the inner ear is attributed to its precise three-dimensional (3D) design comprising of radial and circumferential collagen fibers [2, 3]. However, a limited knowledge is available on the contribution of these discrete micro-anatomical features. Therefore, this work presents a combination of theoretical and experimental approaches toward understanding the significance of geometry in biomimetic eardrum scaffolds (**Figure 1**).

Materials and Methods: A Python script was developed for modelling the anatomical architecture of the human ED. Three test designs (case I, II and III) along with a plain control were chosen to decouple some of its dominant structural attributes. Theoretical comparisons were performed on COMSOL Multiphysics by simulating the appropriate mechanical and acoustical interaction of the selected cases (**Figure 2 (i)**). A dual scale fabrication strategy combining electrospinning and additive manufacturing was implemented for manufacturing the ED scaffolds. The mechano-acoustic response of the fabricated constructs was evaluated by applying the techniques of macroscopic indentation and laser Doppler vibrometry (LDV). Finally, human dermal fibroblasts (hDFs) and human mesenchymal stromal cells (hMSCs) were cultured to assess the influence of 3D hierarchy on cellular alignment and subsequent collagen deposition.

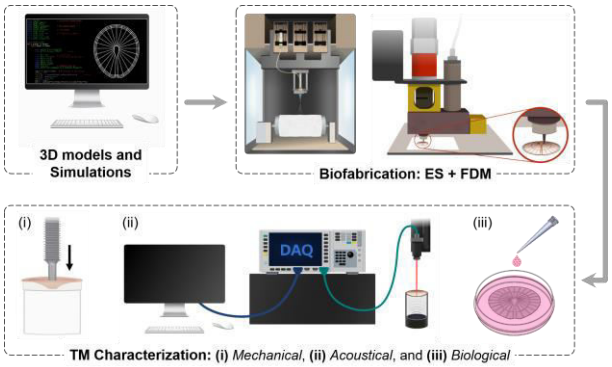

Figure 1. *Schematic diagram illustrating the overall flowchart of this work.*

Results and Discussions: The Python script served as a versatile and robust tool for generating ED models with diverse anatomical features. *In silico* investigation of the chosen designs suggested a geometrical dependency of their mechanical and acoustical responses, where the presence of radially aligned fibers was observed to have a more prominent effect as compared to their circumferential counterparts. The hybrid fabrication strategy was carefully optimized to manufacture biomimetic scaffolds within the dimensions of the native ED. The macro-indentation results corroborated the findings of the theoretical simulations, where radially aligned scaffolds were noted to show a Young's modulus closer to that of the human ED (**Figure 2 (iii)**). The circumferential filaments, on the other hand, were deemed critical for maintaining an optimal resilience and structural integrity. In addition, the LDV measurements demonstrated all the fabricated constructs to be acoustically comparable to the native tissue (**Figure 2 (iv)**). The biological studies performed with hDFs and hMSCs, revealed a favorable influence of 3D hierarchy on cellular alignment and subsequent deposition of extracellular collagen. A higher orientation coherency and collagen production was obtained along the additive manufactured filaments (**Figure 2 (ii)**).

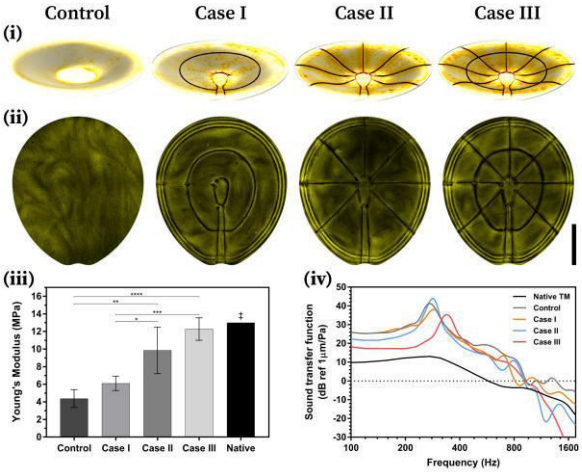

Figure 2. (i) *Computational simulation of the macro-indentation study.* **(ii)** *CNA35-FITC staining at day 14 highlighting the collagen deposition by the cultured hDFs. Scale bar = 3 cm.* **(iii)** *Comparative Young's moduli for the fabricated scaffolds.* **(iv)** *Normalized displacements in response to the applied sound wave.*

Conclusions and Future work: In this study, we investigated the relevance of scaffold geometry in ED tissue engineering. Furthermore, with the optimized biofabrication strategies, a radical improvement has been achieved in the previously reported limits for manufacturing alloplastic TM replacements.

Acknowledgements: This work is a part of the *4NanoEARDRM* project, receiving funding from EuroNanoMed III, the ERA-NET Cofund Action on Nanomedicine under Horizon 2020.

References:

[1] Volandri, G. et al. *J Biomech*. 2011; 44(7):1219-36.
[2] Mota, C et al. *Biofab*. 2015; 7(2):025005.
[3] Danti, S. et al. *Hearing, Balance and Comm*. 2015; 13(4):133-147.

Serum alkaline phosphatase (ALP) activity impacts the osteogenic differentiation process

Sana Ansari, Keita Ito, Sandra Hofmann
Orthopaedic Biomechanics, Department of Biomedical Engineering and Institute for Complex Molecular Systems, Eindhoven University of Technology, P.O. Box 513, 5600 MB Eindhoven, the Netherlands; s.ansari@tue.nl

Introduction

FBS is a widely used supplement in cell culture media which provides cells with vital factors including growth factors, hormones, and vitamins essential for cell survival, growth and division [1]. However, the use of FBS in *in vitro* cell culture is controversial due to a number of reasons most importantly its undefined complex composition and variability which could lead to unexpected and/or unreliable experimental outcomes [2]. For instance, it has been shown that differences in the chemical composition between different FBS suppliers have a significant impact on in vitro mineral formation [3]. The components of FBS which are responsible for these variations are not known yet. The hypothesis of this study is that alkaline phosphatase (ALP) could be one of the compounds in serum which affects the mineralization process.

Materials and methods

The ALP activity of four different types of FBS and the concentration of free phosphate in the osteogenic medium (dexamethasone, 100 nM; ascorbic acid, 50 µg/ml; and β-glycerophosphate, β-GP, 10 mM) were measured. Acellular and cell-seeded silk fibroin scaffolds were cultured in osteogenic differentiation medium supplemented with each type of FBS under static and dynamic conditions for four weeks. µ-CT, calcium and phosphate assay, and Alizarin Red staining were done to measure and visualize the formed minerals. Osteogenic differentiation was investigated through imaging the osteoblast-specific proteins by immunohistochemistry.

Result and discussion

The four different types of FBS used in this study showed significant differences in ALP activity which was able to increase the concentration of free phosphate in the medium in the presence of β-GP (data not shown). This higher serum ALP activity led to more calcium and phosphate precipitation on the scaffolds even when no cells were present (figure 1). When scaffolds were seeded with cells, the FBS type also influenced mineral deposition: higher serum ALP activity resulted in more deposited mineral, measured as deposited calcium and phosphate (figure 2). However, as this was not well correlated to the relative calcium and phosphate deposition between FBS types without cells, the FBS type also had an indirect effect on the cellular ALP activity.

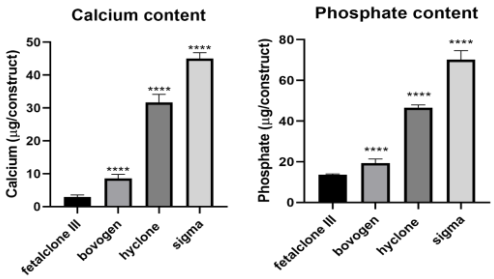

Figure 1 calcium and phosphate content of acellular scaffolds cultured for 4 weeks in osteogenic medium supplemented with different sera.

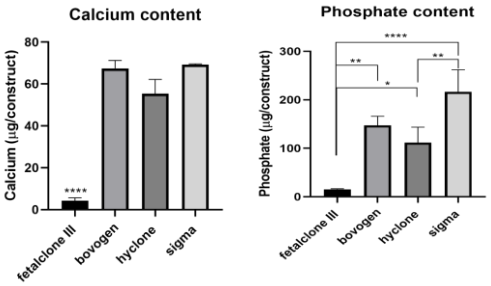

Figure 2 calcium and phosphate content of cell-seeded scaffolds cultured for 4 weeks in osteogenic medium supplemented with different sera.

Summary

The results show that the higher the ALP activity in the serum, the more it enhances the mineralization process on silk fibroin scaffolds. This highlights that the ALP activity inherent to different FBS brands could be one of the driving components having an impact on the mineralization process. We recommend that for mineralization studies, batch testing should include assessing the ALP activity. For future bone tissue engineering studies, conventional FBS should ideally be replaced by defined or serum-free medium where spontaneous or uncontrolled mineralization due to differences in FBS composition could be minimized.

Acknowledgement

We gratefully acknowledge the financial support by the Ministry of Education, Culture and Science (Gravitation Program 024.003.013).

Reference

[1] J. van der Valk *et al.*, "Fetal Bovine Serum (FBS): Past - Present - Future," *ALTEX*, vol. 35, no. 1, pp. 99–118, 2018.

[2] N. Bryan, K. D. Andrews, M. J. Loughran, N. P. Rhodes, and J. A. Hunt, "Elucidating the contribution of the elemental composition of fetal calf serum to antigenic expression of primary human umbilical-vein endothelial cells in vitro," *Biosci. Rep.*, vol. 31, no. 3, 2011.

[3] J. R. Vetsch, S. J. Paulsen, R. Müller, and S. Hofmann, "Effect of fetal bovine serum on mineralization in silk fibroin scaffolds," *Acta Biomater.*, vol. 13, pp. 277–285, 2015.

Ultra-High Throughput Production of Hollow Micromaterials by In-Air Microfluidics for Tissue Engineering Applications

Bas van Loo, Nuno Araújo-Gomes, Vincent de Jong, Tom Kamperman, and Jeroen Leijten

Department of Developmental BioEngineering, Technical Medical Centre, University of Twente, Drienerlolaan 5, 7522NB, The Netherlands, email: Jeroen.leijten@utwente.nl

Introduction: Hollow micromaterials such as hydrogel microcapsules are gaining attention for production of cellular aggregates and drug delivery purposes.[1] Although microfluidic production of microcapsules offers several advantages over conventional micro-aggregate forming techniques, current approaches suffer from low production throughputs and required use of oils and surfactants, which hinders clinical and industrial applications. To address this challenge, we report on the use of a recently developed platform, named In-Air microfluidics[2], enabling ultra-high throughput production of multiple types of hollow micromaterials in an oil-free and surfactant-free manner.

Materials and Methods:
Multiple In-Air microfluidic designs were assessed on their ability to produce hydrogel microcapsules. For the production of the bulk gel composed of hollow compartments the primary fluid was composed of 10% dextran and 50 mM $CaCl_2$ for the core, which was actuated by a piezo-element at 5 kHz for stable droplet production. The secondary fluid was composed of 0.2% alginate and 10% EtOH for the shell. The collection bath was composed of a 0.1 M $CaCl_2$ solution. For the production of compartmentalized fibers the produced droplets were collected in a flowing collection bath with optimized flow speeds. For the production of single hollow microgels a third jet was added (**Figure 1A**) which was composed of 0.2 M $CaCl_2$ and 55% EtOH. Depending on the nozzle sizes different flow rates were used resulting in varying production rates, being 2.2/4.2/6 ml/min for 50/100/200 µm nozzles respectively. 3T3 Fibroblasts were introduced at $1*10^7$ cells/ml in the primary fluid to produce microaggregate forming microcapsules in above described micromaterials. Produced cell-loaded hollow microgels were collected in a collection bath with a surplus of medium, diluting EtOH concentrations to 1.2% within 1 ms and were washed immediately afterwards in fresh culture medium.

Results and Discussion:
Monodisperse microcapsules with diameters between 80 and 300 µm were produced with production flow rates as high as 6 ml/min, resulting in particle production rates of 1.8 kHz. A two nozzle approach effectively produced bulk gels composed of monodisperse hollow compartments (**Figure 1B**). Collecting the flow in a flowing collection bath with optimized flow speed allowed for production of continuous microfibers with regularly spaced hollow compartments (**Figure 1C**). These compartmentalized fibers can form large amounts of consistent and functional 3D microtissues which benefits straightforward retrievability for in vivo applications.

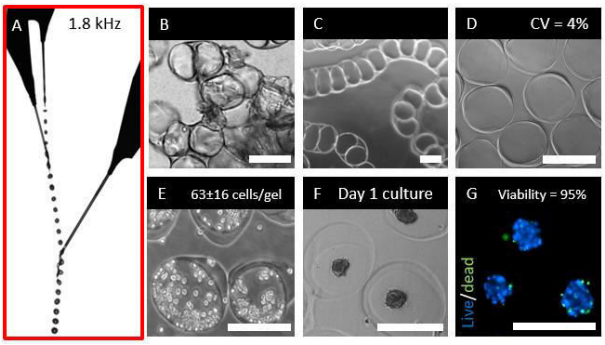

Figure 1: ***(A)*** *Photograph of a functional three nozzle In-Air microfluidic setup, allowing hollow microgel production at 6 ml/min.* ***(B)*** *Two nozzle approach results in bulk gels composed of monodisperse hollow compartments.* ***(C)*** *Collecting in a collection river results in compartmentalized fibers.* ***(D)*** *Addition of a third nozzle results in monodisperse single-compartment hollow microgels.* ***(E)*** *Cell encapsulation with $10*10^6$ cells/ml results in 63±16 cells/gel.* ***(F)*** *Cells form aggregates after 1 day of culture* ***(G)*** *while maintaining high viability of 95% measured by NucBlue Live and NucGreen Dead staining (Thermo). Scalebar is 250 µm.*

Using a three nozzle approach, individual monodisperse (CV =4%) single- (**Figure 1D**), double-, and triple-core hollow microgels could be produced in ultra-high throughput in a single-step manner. By introducing cells at different cell concentrations, the amount of cells per microgel could be tuned from 5±2 till 63±16 cells per hollow microgel (**Figure 1E**). Upon cell culture, microaggregates formed within a single day (**Figure 1F**), reconfirming the high cell viability of 95% upon cell encapsulation (**Figure 1G**).

Conclusions:
Here, we report on how In-Air microfluidics can be used to fabricate distinct hollow-core micromaterials in a clean, single-step and ultra-high throughput manner to facilitate clinical and industrial applications of hollow micromaterials.

Acknowledgements:
The authors acknowledge funding from Dutch Arthritis Foundation (#17-1-405) and European Research Council (ERC, Starting Grant, #759425).

Bibliography:
1.van Loo B *et al*., Materials Today Bio, 6:100047,2020
2.Visser CW., Kamperman T *et al.,* Science Advances, Vol. 4, no. 1, 2018

Regenerative Medicine and Technology – a New Bachelor Program

J. Bauer[1], G. Bendermacher[2], V. LaPointe[1], P. Habibović[1]
[1]MERLN Institute, Maastricht University, Universiteitssingel 40, 6229 ER Maastricht, The Netherlands
[2]Institute for Education, Maastricht University, Universiteitssingel 60, 6200 MD Maastricht, The Netherlands

Regenerative Medicine is a relatively new field at the intersection of science, engineering and medicine. Traditionally, researchers in this field are biologists, chemists, materials scientists, data scientists, engineers or physicians who have acquired skills and knowledge beyond their basic training and stepped into the multidisciplinary world of regenerative medicine. Many of them, however, still find themselves approaching their research questions largely from the perspective of their own discipline and find it difficult to step outside that domain. Having recognized the need for a new multidisciplinary researcher profile that would receive basic training in all the required disciplines to easily enter the aforementioned field, at Maastricht University we have taken the initiative of designing and developing an undergraduate program focusing on Regenerative Medicine and Technology.

Within this program we aim to educate a new generation of researchers that will swiftly adapt to any area of regenerative medicine, and design and develop medical therapies, products and devices for research and clinical use. Applying the principles of problem- and research-based learning, our program will offer a solid scientific and engineering foundation, which will be strongly integrated with the relevant aspects of medicine. An example of this is a real-world, hands-on student research project defined by clinicians within the MUMC+ academic hospital. In addition, special attention will be paid to the development of the translational scientific skills necessary to bring new therapies and products onto the market.

Cartilage-on-chip: a unique tool to study chondrocyte response to mechanical stimulation

Carlo Alberto Paggi[1,2], Jan Hendriks[1], Séverine Le Gac[2], and Marcel Karperien[1]

1 Department of Developmental BioEngineering, TechMed Center and 2 Applied Microfluidics for BioEngineering Research, MESA+ Institute for Nanotechnology & TechMed Center, University of Twente, The Netherlands

INTRODUCTION

During joint movement chondrocytes experience mechanical stimuli from compression and shear strain. Here we present an organ-on-chip platform able to mimic the combination of these two stimuli. The system comprises a 3D cell-hydrogel, a perfusion channel to provide nutrients and an innovative mechanical actuation unit [1] (Fig. 1). The mechanical actuation unit, separated from the rest of the system by a thin elastomeric membrane, consists of 3 individually addressable chambers where positive or negative pressure can be applied. We present here how the different mechanical stimulation patterns can influence the formation by chondrocytes of the pericellular matrix up to 14 days of culture.

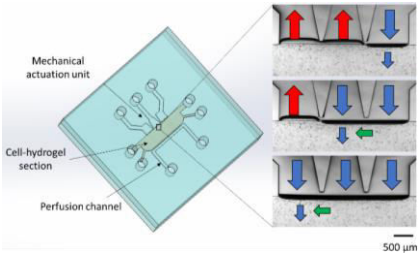

Figure 1: Left: schematic drawing of the cartilage-on-a-chip platform. Right, top view of the mechanical actuation unit with 3 independently addressable chambers. Three different membrane deformation patterns were achieved through application of specific combinations of positive (blue arrow) and negative pressures (red arrow,).

EXPERIMENTAL

The device was fabricated using soft-lithography from polydimethylsiloxane (PDMS). Positive and/or negative pressures were applied using a dedicated set-up to generate different sets of stimulation onto the 3D cell-laden hydrogel (compression or compression & shear strain). Human primary chondrocytes (hCHs) were embedded in low melting temperature agarose (2% w/v) in the platform and cultured for one day with proliferation medium followed by differentiation medium. First, the cell-laden constructs were stimulated for 7 days (1 h x day at 1 Hz) with either compression, or compression and shear strain (wave form). Medium was collected from the device at day 1, 2, 3, 5 and 7 and IL-6 concentration quantified using enhanced SPRi [2]. RNA was extracted and qPCR performed at day 7 for Collagen I and II expression levels. Cell-laden hydrogels were also cultured for 7 days in static condition followed by 7 days with one of the two stimuli or in static conditions for a total of 14 days. All samples were fixed and stained for aggrecan, collagen II and collagen VI expression.

RESULTS AND DISCUSSION

Collagen type 2 mRNA expression was increased from static, to compression and wave compression in which cells are exposed to a combination of stress and strain. Interestingly, collagen type 1 expression was inversely correlated with stress and strain. To determine whether the could be used for the analysis of factors secreted by the cells we measured the pro-inflammatory cytokine IL-6. Chondrocytes release higher level of IL-6 at day 1-2 suggesting a stress induced by the new 3D environment. Furthermore, secretion decreased over time with a nearly not detectable signal at day 7 for the static conditions (Fig. 2) suggesting chondrocyte adaptation to the 3D environment. Moreover, IL-6 was higher in the constructs exposed to mechanical stimuli compared static

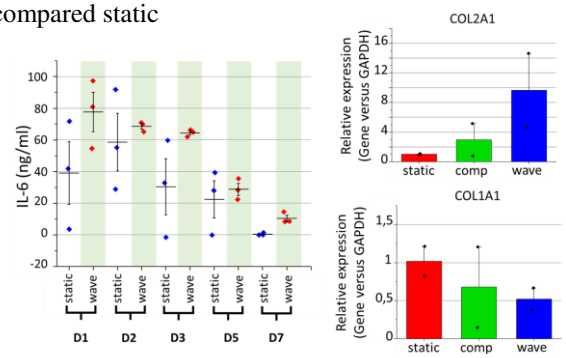

Figure 2: On the left, IL-6 secretion in the cartilage-on-chip device in static (white) and dynamic (wave form, green) conditions at day 1, 2, 3, 5 & 7. On the right: Collagen II and collagen I gene expression levels analyzed for 6 individual devices for the 3 conditions: static (red), compression (green) and wave (compression & shear strain – blue) at day 7.

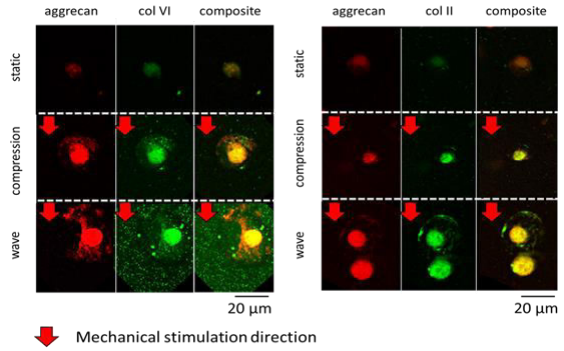

Figure 3: From the right: immunofluorescence images of single cells cultured for 14 days in static or dynamic conditions (7 days static + 7 days with stimulation). The stains show aggrecan in red and Collagen VI (first set of images) or Collagen II (second set of images) in green.

conditions, indicating a role of mechanical stimulation on cytokine production. Aggrecan, collagen II and collagen VI immunostaining revealed enhanced pericellular matrix production in dynamic conditions compared to static culture. The newly produced pericellular matrix was mainly present in the direction of the mechanical stimulation suggesting cell adaptation to the applied stimuli (Fig. 3). Furthermore, combination of compression and shear strain increased both aggrecan and collagen production respect to only compression conditions.

CONCLUSION

Our cartilage-on-a-chip platform can faithfully reproduce multi-modal mechanical stimuli, either physiological or hyper-physiological, and supports long term survival of chondrocytes and supports the creation a quasi-native pericellular matrix. Our model enables the in depth evaluation of the effect of stress and strain on chondrocyte biology.

REFERENCES

[1] C. A. Paggi et al., Sens. Act. B-Chem 315. (2020).
[2] J. Hendriks et al.,Analytical Chemistry. (2018).

A comparison between the response to mechanical stimulation of healthy chondrocytes and primary tumour derived chondrosarcoma cells

Carlo Alberto Paggi[1,2], Isa Porsul[1], Séverine Le Gac[2], and Marcel Karperien[1]

[1]Department of Developmental BioEngineering, TechMed Center and [2] Applied Microfluidics for BioEngineering Research, MESA+ Institute for Nanotechnology & TechMed Center, University of Twente, The Netherlands

INTRODUCTION

Chondrosarcoma is a rare bone tumor characterized by production of abundant cartilaginous matrix. Chondrosarcomas are resistant to chemotherapy and radiation due to their cartilage-like characteristics. Unlike chondrocytes chondrosarcomas do not experience mechanical loading which is one of the key drivers of cartilage matrix production. To study this paradox we developed a chondrosarcoma organ-on-chip model emulating mechanical actuation of a moving joint. Our main objective was to explore the effect of loading on chondrosarcoma cells in comparison with primary chondrocytes in relation to extracellular matrix production.

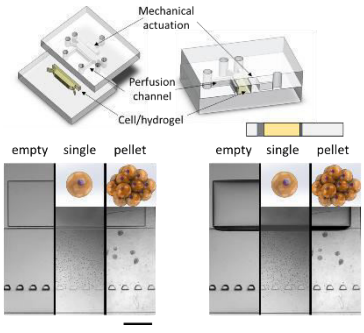

Figure 1: From the top left: schematic overview of the organ-on-chip platform. From bottom left: empty design; design containing single cells; and containing pellets. left: in static, right: at 300 mbar. Scale bar: 500 µm.

EXPERIMENTAL

The organ-on-chip system consisted of a mechanical actuation chamber; a 3D cell-hydrogel chamber; and a perfusion channel, to provide nutrients to the 3D cell construct (figure 1). Agarose 2% (2% w/v) was used to embed human primary chondrocytes (hChs), chondrosarcoma cells, and chondrosarcoma micromasses. An agarose mold containing 3600 wells 200 µm (diameter) was used to create chondrosarcoma micromasses of approximately 50 cells (figure 2). Micromasses were seeded in the system, and in agarose, after 2 days. Culture was performed for 1 day with chondrocyte proliferation medium after which mechanical stimulation was applied, with 100, 200, 300, 500 and 700 mbar compression. Deformation of cells was compared between static (0 mbar) conditions and compression in three sections of cell-laden hydrogel; close to the membrane, in the center and close to the pillars.

RESULTS AND DISCUSSION

One day after cell seeding stable chondrosarcoma micromasses were formed in the agarose microwell array. The average number of cells in the micromasses was 53 (figure 2). We next examined the effect of various cyclic loading regimes on the deformation of micromasses and single cells over time and compared this deformation to primary

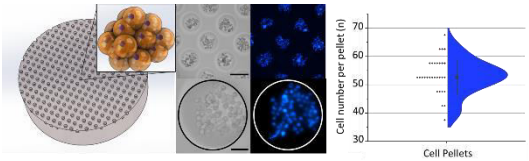

Figure 2: From left to right: schematic representation of the agarose microwells; wells containing chondrosarcoma cells at day 0 with and without nuclear blue staining; violin plot of the cell distribution in the micromasses Scale bar: 50 µm

chondrocytes. As shown in figure 3, for all cell types cell deformation increased with increasing pressure. Cell deformation was highest close to the actuating membrane. In each section of the chip, the hChs presented higher deformation (> 20% at 700 mbar)

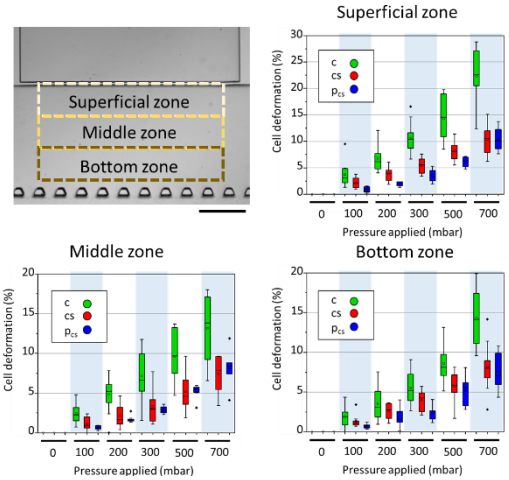

Figure 3: From top left: top view of the device; graph of the cell/pellet deformation at different pressures (100-700 mbar) on the superficial, middle and bottom zone. Scale bar: 500 µm.

compared to chondrosarcoma cells in suspension. Chondrosarcoma cells in the micromasses were most resistant to load induced cell deformation (10% at 700 mbar)

CONCLUSION

Our organ-on-chip system enables study of chondrocytes and chondrosarcoma behavior upon different mechanical stimulation levels. Our data show that chondrosarcoma cells are more resistant to load induced deformation. Whether and how this resistance is linked to cartilage matrix production is subject of further study.

Registration of Microcomputed Tomographic Images to Longitudinally monitor Bone Formation and Resorption in *Ex Vivo* Cultures of Osteochondral Cores

E.E.A. Cramer, N.A.P. van Gestel, K. Ito, S. Hofmann
Orthopaedic Biomechanics, Department of Biomedical Engineering and Institute for Complex Molecular Systems, Eindhoven University of Technology, P.O. Box 513, 5600 MB Eindhoven, the Netherlands

Introduction: Bone remodeling, consisting of bone formation and resorption, is a complex process with interactions between many cell types, including osteocytes, osteoblasts, osteoclasts, and their progenitors MSCs and monocytes. The culture of bone explants provides a unique platform to study bone remodeling because the tissue specific cells are maintained in their native ECM [1]. Effects of for example chemical compounds or mechanical loading on the remodeling process of bone explants are usually analyzed histologically at the end of culture or by the presence of markers in medium. Ideally, bone formation and resorption would be examined in detail over time during culture without destroying the sample. A technique that allows this is microcomputed tomography (µCT), followed by image registration [2]. Image registration uses two subsequent scans to determine and distinguish bone formation and resorption locations within one sample. Voxels appearing only in the first scan (baseline) are considered resorbed bone and voxels present only in the follow-up scan are considered formed bone.
In this study, µCT image registration was integrated and optimized for the bone part of osteochondral cores during *ex vivo* culture, to allow for longitudinal monitoring of bone formation and resorption.
Materials and Methods: Osteochondral cores (Ø=10 mm) were isolated from porcine femoral condyles obtained freshly from the slaughterhouse's left-over material. After creation of a defect (Ø=6 mm) in the bone, the explants (n=5) were cultured in bioreactors comprising two separated media compartments, one for cartilage and one for bone, for 6 weeks [3,4]. Scanning of samples was performed in bioreactors, which were specifically designed to fit in the µCT scanner and to ensure a similar orientation of the sample each time. After segmentation, bone formation and resorption were determined by finding clusters of ≥ 5 voxels that had a difference in attenuation coefficient between both scans ≥ 225 mgHA/cm3. Bone formation and resorption were quantified as percentage of the total bone volume and visualized with color-coded images.
Results: After 6 weeks of culture, 6.48 % ± 0.71 % newly formed bone was detected compared to day 1. Resorption was quantified as 1.47 % ± 0.21 % of the total sample volume compared to the baseline image at day 1. The registered images showed formation (orange) distributed equally around the sample and resorption (purple) only at a few locations (Fig. 1 A+B). Cross-sections showed remodeling occurring mainly at the edges of the sample and inside the created defect (Fig. 1C), while most of the inner trabecular surface was unchanged. Larger clumps of resorbed bone were identified as bone debris from the drilling process present in the baseline image and most likely flushed away during culture.
Discussion: The ability to monitor bone formation and resorption for *ex vivo* cultured osteochondral cores was shown with µCT images from week 6 registered onto the baseline images. Additional analysis, for example with histology or fluorochrome labeling, is needed to validate the µCT results and to optimize image registration. Bone formation was observed, although mainly at the edges, and could probably be further promoted by the integration of mechanical loading. Although resorption was expected due to unloading conditions, osteoclasts were not stimulated through medium components because culture medium was supplemented with factors that are known to promote osteoblasts. Future research could focus on finding optimal culture conditions for osteoclasts in addition to osteoblasts.
Conclusion: This study shows the potential of integrating µCT monitoring and image registration to acquire detailed insights into bone remodeling over time within *ex vivo* culture of osteochondral cores. This is an important step towards the development of a testing platform to study bone remodeling *ex vivo*.

[1] Marino et al., BoneKEy reports, 5: 818, 2016;
[2] Christen and Müller, Curr Osteoporos Rep. 15(4): 311–7, 2017;
[3] De Vries-van Melle et al., Tissue Eng Part C Methods, 18:45-53, 2012;
[4] Schwab et al., ALTEX, 34:267-277, 2017;

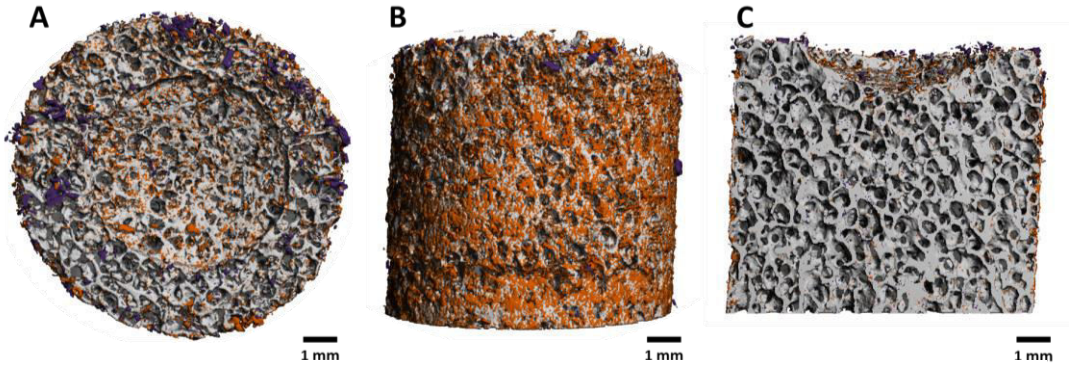

Figure 1 – Registration of week 6 µCT image on day 1 image showing bone formation (orange) and bone resorption (purple) and unchanged mineralized bone (grey). Top view (A), sideview (B) and cross-section (C).

Spatiotemporal analysis of in vivo pathophysiological regenerative processes in bioresorbable synthetic pulmonary valves in sheep using histopathology and Raman spectroscopy

Bente J. de Kort, Arturo M. Lichauco[1], Julia Marzi [3,4,5], Eva Brauchle [3,4,5], Sylvia Dekker[1], Aurelie Serrero[6], Martijn A.J. Cox[6], Katja. Schenke-Layland[3,4,5], Carlijn V.C Bouten[1,2], Anthal I.P.M. Smits[1,2]

[1]Department of Biomedical Engineering, Eindhoven University of Technology, Eindhoven, The Netherlands. [2]Institute for Complex Molecular Systems, Eindhoven University of Technology, Eindhoven, The Netherlands.[3]Department of Women's Health, Research Institute for Women's Health, Eberhard Karls University Tübingen, Tübingen, Germany. [4]Cluster of Excellence iFIT (EXC 2180) "Image-Guided and Functionally Instructed Tumor Therapies", Eberhard Karls University Tübingen, Germany. [5]NMI Natural and Medical Sciences Institute, University of Tübingen, Reutlingen, Germany. [6]Xeltis B.V., Eindhoven, The Netherlands

Introduction

In situ heart valve tissue engineering utilizes the regenerative response of the human body to create a living, functional replacement valve from a resorbable, synthetic and off-she-shelf available graft. Recently, preclinical studies using electrospun supramolecular elastomeric valvular grafts have shown that this principle, also known as Endogenous Tissue Restoration (ETR), enables the regeneration of pulmonary valves with sustained long-term functionality *in vivo*[1,2]. However, in order to prevent unpredicted (adverse) remodeling, more detailed knowledge on the underlying mechanisms of the material-driven endogenous regenerative response is necessary. Therefore, the goal of the present study was to gain a mechanistic understanding of these processes by combining histopathological analysis and Raman spectroscopy to study *in situ* tissue-engineered heart valves.

Methods

In this study, Xeltis Pulmonary Valved Conduits (XPV, Xeltis B.V., Eindhoven, The Netherlands) implanted in the pulmonary position of sheep were analyzed. Explanted valves (follow-up time: 2, 6, 12 (N=5 per timepoint) and 24 months (N=2)) were embedded in paraffin and sectioned longitudinally. Spatiotemporal analysis was performed using Raman spectroscopy and a comprehensive sheep-specific antibody panel[3], focusing on graft degradation, endogenously formed neo-tissue and infiltrating cell phenotypes.

Results and Discussion

Detailed knowledge on graft resorption, neo-tissue formation, as well as the involved cellular influences was obtained. Spectral changes of the graft material 2 months post-implantation indicated starting degradation in the arterial conduit and base region of the leaflet. This correlated with the presence of foreign body giant cells at these iNOS-rich tissue remodeling sites. Interestingly, in the base region multinucleated giant cells were located within the graft, whereas in the conduit material multinucleated giant cells remained on the outer layers with only limited infiltration into the scaffold material. Inflammation resolved upon graft degradation, as was evident for example in the base region of the leaflet after 24 months. Together with the observation that the presence of tissue producing αSMA+ cells decreased with time, this suggests that, over time, synthetic implant remodeling transitions towards homeostatic remodeling and regeneration. Extracellular matrix components, such as collagens and elastin were formed in a highly heterogeneous fashion, suggesting an important role for local hemodynamic loads on the inflammatory and regenerative processes.

Conclusion

Taken together, these findings enhance the understanding of material-driven regeneration and highlight the importance of the micro-environment and hemodynamic loading on the cellular response towards a biomaterial. In order to limit risk of unexpected (adverse) remodeling and to enable a truly safe translation into clinic a better understanding on the mechanism and the cause of variability in tissue-engineered heart valve remodeling is necessary.

Acknowledgements

We gratefully acknowledge the financial support by the Ministry of Education, Culture and Science (Gravitation Program 024.003.013).

1Bennink, G. et al. J. Thorac. Cardiovasc. Surg. 2018;155:2591-2601.
2Kluin, J. et al. Biomaterials 2017;125: 101–117.
3Dekker, S. et al. Front. Cardiovasc. Med. 2018;5:105.

Chemically modified mRNA as an alternative to plasmid DNA for *in situ* production of proteins

C.B. Del Toro Runzer[1], C. Plank[2], E.R. Balmayor[3], M. van Griensven[1]
[1]Dept. cBITE, MERLN Institute for Technology-Inspired Regenerative Medicine, Universiteitssingel 40, 6229 ER Maastricht, the Netherlands.
[2]Ethris GmbH, Semmelweisstraße 3, 82152 Planegg, Germany.
[3]Dept. IBE, MERLN Institute for Technology-Inspired Regenerative Medicine, Universiteitssingel 40, 6229 ER Maastricht, the Netherlands

Introduction: Gene therapy aims to deliver a defined gene into cells to either replace a defective gene or to increase the amount of a specific gene in a targeted cell/tissue in order to produce a higher amount of the desired protein. For the second purpose, gene therapy presents several benefits over direct administration of proteins. It allows the sustained synthesis of one or more proteins with native conformation, true post-translational modifications, and has superior biological effect than recombinant proteins produced industrially.
Plasmid DNA (pDNA) was the first nucleic acid to be pursued as a therapeutic molecule. Later on, *in vitro*-transcribed (IVT) mRNA came into play as it offers several advantages. Unlike pDNA, IVT mRNA is transiently active, does not require transport across the nuclear membrane, is completely degraded and does not hold mutagenesis risks associated to the DNA integrating into the genome. Additionally, mRNA production is simpler and more affordable than pDNA. Nonetheless, using mRNA for protein-replacement therapies also implies certain complications given its unstable nature, tendency to activate an innate immune reaction, and a poor translational efficiency. Therefore, a lot of effort has been directed to tackle these issues by generating chemically modified mRNAs (cmRNAs), where structural elements are removed or replaced to circumvent the above mentioned problems. In this study, we aim to compare the performance of pDNA and cmRNA encoding for the reporter proteins Metridia Luciferase (MetLuc) and enhanced green fluorescent protein (eGFP).

Materials and Methods: For transfection, HEK293 cells were seeded into 48-well plates at a density of $5 \cdot 10^4$ cells/cm^2. After 24 hours, complexes containing 5 pg/cell of eGFP cmRNA (Ethris, Germany) or eGFP pDNA (PlasmidFactory, Germany) were formed with either Lipofectamine 3000 (Invitrogen, USA), or 3D-Fect (OzBiosciences, France) using non-supplemented OptiMEM. Complexes with MetLuc cmRNA (Ethris, Germany) or MetLuc pDNA (PlasmidFactory, Germany) were prepared as described using Lipofectamine 3000. Complexes were incubated for 20 minutes at room temperature. Cells were transfected and incubated at 37°C and 5% CO_2. After 6 hours, the medium was replaced by OptiMEM supplemented with 10% FBS. eGFP samples were imaged using a fluorescence microscope and analysed using flow cytometer quantification after 24 and 48 hours. For MetLuc encoding nucleic acids, supernatants were collected after 24, 48 and 72 hours and stored at -80°C. For quantification of MetLuc expression, 50 µl of coelenterazin (Synchem UG & Co., Germany) were added to 50 µl of the supernatant, and bioluminescence was measured instantly at λ=480 nm.

Results and Discussion: Transfection of HEK293 cells with eGFP pDNA showed a significantly higher percentage of transfected cells when using lipofectamine 3000 when compared to 3DFect after 24 and 48 hours (Fig. 1). For this reason, Lipofectamine was used for the following transfections using eGFP and MetLuc.

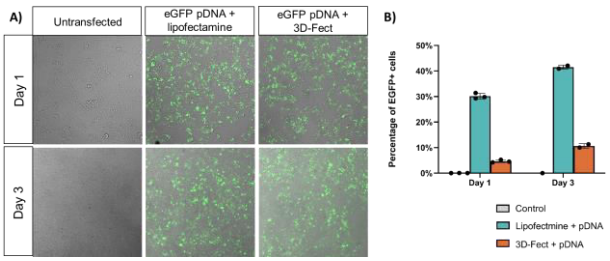

Figure 1. Transfection of HEK293 cells with eGFP pDNA. (A) Representative photomicrographs showing eGFP+ cells. (B) Expression quantification using flow cytometry.

When comparing eGFP cmRNA and eGFP pDNA, cmRNA showed higher expression as depicted in the pseudo-quantification of the microphotographs of Fig. 2A. Contrarily, MetLuc presented higher expression when pDNA was used, with around $1 \cdot 10^7$ relative light units (RLU) at day 3, whereas MetLuc mRNA showed a maximum of $0.5 \cdot 10^7$ RLU at day 2 with no further increase at day 3 (Fig. 2B). mRNA and pDNA seem to have different transfection efficiency also concerning the different proteins. Further characterization of the mean hydrodynamic diameters and zeta potentials of the complexes could provide an insight on this observation.

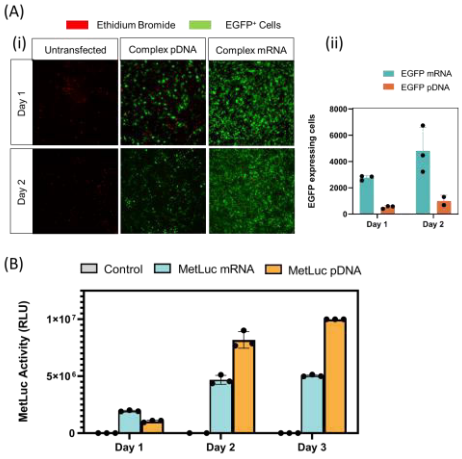

Figure 2. Comparison of pDNA and mRNA transfection efficiency. (A) (ii) Photomicrographs of eGFP expression (ii) Pseudo-quantification of the photomicrograph using FIJI. (B) MetLuc expression of the mRNA or pDNA complexes.

Acknowledgement:
This work has been performed as part of the cmRNAbone project and has received funding from the European Union's Horizon 2020 research and innovation programme under the Grant Agreement No 874790.

In vitro Vascular Regression Near Calcium Phosphate Ceramics

I. Pennings[1,4], L. de Silva[1,4], C. Cheng[3,4], A. J. W. P. Rosenberg[1], D. Gawlitta[1,3,4]
Dept. of [1]Oral and Maxillofacial Surgery & Special Dental Care, [2] Nephrology & Hypertension [3]Orthopaedics, University Medical Center Utrecht, the Netherlands. [4] Regenerative Medicine Utrecht, Utrecht, the Netherlands.

Introduction:

Widely commercialized since the 1980s, calcium phosphate (CaP) ceramics are the most clinically relevant scaffolds for bone tissue engineering due to their resemblance to the mineral phase of bone [1]. Available as cement, paste, scaffold or coating, all forms of CaP ceramics are biocompatible, osteoconductive and demonstrate good osteointegrative behaviour upon implantation [2]. *In vivo*, the components of CaP ceramics (hydroxyapatite [HA] and/or beta-tricalcium phosphate [β-TCP]) gradually dissolve and break down, allowing for new bone to form and remodelling to take place [2]. While bone substitutes have shown favourable results *in vivo*, larger defects tend to exhibit limited vascularization within the material [3]. This lack of vascularization limits the ingrowth of osteoblasts into a large graft resulting in fibrous tissue formation in the core of the graft.

To overcome this, various pre-vascularization strategies have been employed for CaP ceramics. The generation of microvascular structures surrounding the CaP ceramics is expected to accelerate vascularization by inosculating with host capillaries upon *in vivo* implantation. Our research group aimed to use this concept to create a pre-vascularized CaP construct using a co-culture of human mesenchymal stem cells (MSCs) and endothelial colony forming cells (ECFCs). A dedicated cultivation period *in vitro* served to drive osteogenic differentiation of the MSCs and generation of the microvascular structures prior to implantation. However, it was consistently observed that the microvascular structures regressed in the vicinity of the CaP ceramics. Therefore, in this study, we investigated which factor(s) cause(s) vascular regression around the CaP ceramics.

Materials and Methods

CaP bioceramics (35% HA/ 65% β-TCP) were encapsulated within a gelatin-polyethylene glycol (PEG) hydrogel system in combination with human MSCs and ECFCs (1:1 ratio). Constructs were cultured for up to 10 days in osteogenic differentiation medium (ODM) to evaluate their osteogenic and vasculogenic differentiation. The contribution of possible causes to the vascular degradation were assessed: 1) surface topography of the CaPs, 2) CaP combination with the hydrogel, 3) type of culture medium, 4) varying compositions of HA/TCP, 5) dissolution products of the CaPs. Vessel formation was visualized via immunofluorescence staining (αSMA/CD31) on an Evos FL cell imaging system (ThermoFisher) and quantified for the extent of pre-vascular structure formation using Angioquant software. Apoptosis was visualized by Caspase-3 immunohistochemistry analysis on decalcified paraffin sections.

Results and Discussion

The vascular network was found to regress in the vicinity of the CaP ceramics (Fig.1). This occurred regardless of (1) surface topography of the CaPs (micron vs submicron). Also, (2) the type of hydrogel encapsulating the CaPs (gelatin-PEG *vs* Matrigel) did not reduce vascular structure regression. Further, (3) the type of culture medium (osteogenic *vs* endothelial differentiation medium) did not change pre-vascular structure regression. Additionally, (4) varying the ratio of HA/β-TCP of the ceramics did not change the regression of structures. Further investigations (5) of the dissolution products of the CaP granules revealed that the regression of microvascular structures could be attributed to high levels of inorganic phosphate (Pi).

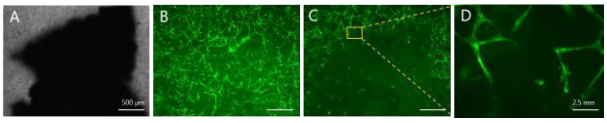

Figure 1. Regression of pre-vascular structures near CaP ceramics *in vitro*. A) Transmitted light images of CaP ceramics (black) embedded within a co-cultured gelatin-PEG hydrogel system. Fluorescence imaging of the ECFCs (+GFP) showing the initially formed microvascular network on B) Day 3 and C) Day 10. A magnification from C) showing regression and apoptosis of the microvascular structures.

Conclusions

The results indicate that the apoptosis of the microvascular structures is a result of the accumulation of the released inorganic phosphate (Pi) from the surface of the CaP ceramics. This accumulation could be attributed to the static conditions in an *in vitro* set up. Typically, this is not of concern in an *in vivo* setting, where conditions are dynamic and rapidly regulated. This observed effect does however pose a significant impediment for groups aiming to pre-vascularize CaP ceramics *in vitro* prior to implantation *in vivo*.

References

[1] Eliaz, N. and N. Metoki, Calcium Phosphate Bioceramics: A Review of Their History, Structure, Properties, Coating Technologies and Biomedical Applications. Materials (Basel), 2017. 10(4): p. 334.
[2] Bansal, S., et al., Evaluation of hydroxyapatite and beta-tricalcium phosphate mixed with bone marrow aspirate as a bone graft substitute for posterolateral spinal fusion. Indian J Orthop, 2009. 43(3): p. 234-9. 19.
[3] de Grado, G. F. Keller, L. Idoux-Gillet, Y. Wagner, Q. Musset, A-M, et al. Bone substitutes: a review of their characteristics, clinical use, and perspectives for large bone defects management. J Tissue Eng . 2018 Jun 4;9:2041731418776819

Adhesives for Fixation of Polycarbonate Urethane Implants to the Bone

P. Farjam, E.E.G. Hekman, J. Rouwkema, G.J. Verkerke
Department of Biomechanical Engineering, University of Twente, Drienerlolaan 5, 7522 NB Enschede, The Netherlands

Introduction The use of polyurethane in medical applications has been reported and evaluated by several authors (1). For use in orthopaedics, there is particularly one member of the polyurethane family, the polycarbonate-urethane (PCU), which has great potential. PCU demonstrated promising characteristics to be used in orthopaedic implants. These include; good biocompatibility and mechanical properties (2) (3), similarities to natural cartilage (4) (5) (3), and good wear properties (5) (4) (6) (7). This makes the use of polycarbonate-urethane in orthopaedic applications compelling. They can be involved in a diverse range of orthopaedic implants including but not limited to joint replacement implants.

Success in the application of an orthopaedic implant depends on multiple factors. Implant design, surface configuration, fixation method and surgical procedure play critical roles to decrease the failure rate of implantation. An insufficient fixation technique may cause serious issues such as movement, delamination, deformation and detachment of an implant which leads to failure of the implant and thus the requirement for additional treatment (8). Utilizing an adhesive as the fixation technique would revolutionize the field of orthopaedic surgery (9). Adhesives form an anchorage based on a chemical and/or physical bonding rather than relying on bulky mechanical interlockings which are currently the golden fixation technique. Therefore, employing adhesives as the anchorage tool brings numerous advantages, such as: preserving the integrity of the tissue and the implant with introducing no invasiveness, possibility to be delivered via minimal-invasive techniques and offering simple and precise applicability. We currently are designing a novel joint replacement prosthesis, build from PCU which adhesives could realise its firm fixation to bone.

Purpose In this study we will evaluate commercial biocompatible adhesives (10) as a candidate fixation technique for PCU based orthopaedic implants.

Method We will analyse adhesion strength of a biocompatible cyanoacrylate-based adhesive in PCU-bone bond by performing mechanical *in vitro* tests. The tests will be conducted according to ASTM standards; F2258 for strength properties of tissue adhesives in tension and F2255 for strength properties of tissue adhesives in lap-shear by tension loading.

References

1. *Using Polyurethanes in Medical Applications.* **Wright, James.** 3, s.l. : Medical Device & Diagnostic Industry, 2006, Vol. 28. 98-109.
2. *Selection of Elastomeric Materials for Complaint-Layered Total Hip Arthroplasty.* **al, F P Quigley et.** 1, s.l. : Proc.Inst. Mech. Eng, 2002, Vol. 216. 77-83.
3. *Poly(carbonate urethane) and Poly(ether urethane) Biodegradation: In Vivo Studies.* **a, Elizabeth M Christenson et.** 3, s.l. : Journal of Biomaterials Research Part A, 2004, Vol. 69A. 407-416.
4. *Analysis and Evaluation of a Biomedical Polycarbonate Urethane Tested in and in vitro Study and an Ovine Arthroplasty Model. Part I: Materials Selection and Evaluation.* **al, Imran Khan et.** s.l. : Biomaterials, 2005, Vol. 26. 621-623.
5. *Analysis and Evaluation of a Biomedical Polycarbonate Urethane Tested in and in vitro Study and an Ovine Arthroplasty Model. Part II: In Vivo Investigation.* **Imran Khan et al.** s.l. : Biomaterials, 2005, Vol. 26. 633-643.
6. *A Biomechanical and Tribological Investigation of a Novel Compliant All Polyurethane Acetabular Resurfacing System.* **Fisher, L M Jennings and J.** s.l. : International Conference: Engineers & Surgeons–Joined at the Hip-IMechE, 2002. 13-15.
7. *A Tribological Study of UHMWPE Acetabular Cups and Polyurethane Compliant Layer Acetabular Cups.* **al, S L Smith et.** 6, s.l. : J Biomater Res Part A, 2000, Vol. 53. 710-716.
8. *Fibrin glue improves osteochondral scaffold fixation: Study on the human cadaveric knee exposed to continuous passive motion.* **G. Filardo, M. Drobnic, F. Perdisa, E. Kon, M. Hribernik, and M. Marcacci.** 4, s.l. : Osteoarthr. Cartil, 2014, Vol. 22. 557-565.
9. *Bone-Adhesive Materials : Clinical Requirements , Mechanisms of Action , and Future Perspective.* **María J. Sánchez-Fernández, Hussein Hammoudeh, Rosa P. Félix Lanao, Machteld van Erk, Jan C. M. van Hest, and Sander C. G. Leeuwenburgh.** s.l. : Adv. Mater. Interfaces, 2019.
10. *Comparison of four chondral repair techniques in the hip joint: A biomechanical study using a physiological human cadaveric model.* **A.J. Cassar-Gheiti, D.P. Byrne, E. Kavanagh, K.J. Mulhall.** 6, s.l. : Osteoarthritis and Cartilage, 2015, Vol. 23. 1018-1025.

Biomaterials-Driven Bone Regeneration on a Microfluidic Chip

M.G. Fois, A. Guttenplan, Z. Tahmasebi Birgani, H. Suk Rho, S. Giselbrecht, P. Habibovic, R. Truckenmüller
Department of Instructive Biomaterials Engineering, MERLN Institute for Technology-Inspired Regenerative Medicine, Maastricht University, Maastricht, The Netherlands

Introduction: Bone loss caused by a disease or a trauma represents a major clinical challenge, requiring efficient regenerative therapies. In this context, autografts (i.e. a patient's own bone) are considered as the optimal treatment. Limited availability and other clinical complications associated with autograft use have led to the development of several synthetic alternatives, including the ones made from calcium phosphate (CaP) ceramics [1]. However, the regenerative potential of synthetic bone graft substitutes has in general been inferior to that of their biological counterparts. Hence, the search for effective and off-the-shelf available synthetic alternatives to replace autografts continues. Traditionally, testing new biomaterials for bone regeneration has relied on simplified in vitro studies followed by testing in animal models [2]. However, advanced cell culture platforms, such as organs-on-chips (OOCs), which recapitulate tissue functions and integrate external physiochemical stimuli, have been described as a potential *in vitro* strategy to sufficiently predict the *in vivo* microenvironment [3].

In this study, we propose an OOC model to mimic the bone regeneration in the presence of biomaterials. To this end, we designed and fabricated an ad-hoc microfluidic chip composed of multiple compartments that represent the bone and the bone defect site. The platform is tested to study homing of human bone marrow-derived mesenchymal stromal cells (MSCs) from the "host bone bed" into the "defect site" in the presence of widely used CaP ceramics.

Materials and methods: Microfluidic chips were fabricated in polydimethylsiloxane (PDMS) using a two-step soft lithography process. Briefly, the device designs were printed on transparent film photomasks. Negative master molds were fabricated in SU-8 photoresist on silicon wafers following the manufacturer's protocol and silanized using trichloro(1H,1H,2H,2H-perfluorooctyl)silane (FOTS). PDMS replicas were made by pouring PDMS mixture onto the SU-8 molds and curing for 1 hour at 80 ˚C, and functionalized by oxygen plasma treatment followed by silanization with FOTS. Fresh PDMS mixture was poured onto the PDMS molds and cured for 1 hour at 65 ˚C. The fluidic connection ports on the PDMS parts were punched and the chip assembly was done by bonding the PDMS parts to a glass slide after oxygen plasma treatment of both surfaces. MSCs were embedded in Matrigel® and seeded into the side channels of the chips. The "defect" chamber contained Matrigel® with or without CaP microparticles with an average size of 20 µm. MSCs homing into the inner chamber was monitored overtime using light microscopy.

Results and discussion: Microfluidic chips were successfully fabricated. The chips were comprised of an inner chamber with independent inlet/outlet, mimicking the bone defect site, and were laterally separated from two host bone bed-mimicking side channels by arrays of pillar (long axes: 160 µm, interpillar distance: 25 µm). The height of the chamber was approximately 100 µm. The pillar geometry and arrangement were optimized to prevent the leakage from side channels to inner chamber upon cell culture, yet to allow cell migration over time. A pair of perfusable side channels were included at each side of the chip for medium supplementation to host bone bed-mimicking channels. MSCs embedded in Matrigel® were contained in the side channels due to the presence of the pillars, as previously observed [4]. Homing of the cells was observed overtime. In addition, CaP microparticles were homogenously dispersed inside the central chamber of the chop. The results further demonstrated the feasibility of monitoring the on-chip cell culture and migration using imaging-based techniques. Next, we plan to study osteogenic differentiation and matrix deposition of migrated MSCs.

Conclusion: We presented a microfluidic chip as the basis of an OOC model designed to mimic the bone defect healing process in the presence of biomaterials. Our results showed the feasibility of the MSC culture and migration in the chip in the presence of biomaterials.

Acknowledgement: This research is supported by the Interreg Vlaanderen-Nederland as part of Biomat-on-Microfluidic Chip project and the Dutch Province of Limburg. We acknowledge the Gravitation Program "Materials Driven Regeneration", funded by the Netherlands Organization for Scientific Research (024.003.013).

References:

1. Habibovic, J Tissue Eng Regen Med, 2007. **1**.
2. Habibovic, J Orthop Res, 2008. **26**(10).
3. Bhatia, Nat Biotechnol, 2014. **32**(8).
4. Carvalho, Sci. Adv., 2019. **5**(eaaw1317).

A 3D-printed bone implant for hip dysplasia treatment

Nasim Golafshan[1,2], Koen Willemsen[1], Harrie Weinans[1], Bart C H van Der Wal[1], Jos Malda1[2,3], Miguel Castilho[1,2,4]
1 Department of Orthopaedics, University Medical Center Utrecht, GA Utrecht, The Netherlands

2 Regenerative Medicine Utrecht, Utrecht, The Netherlands

3 Department of Clinical Sciences, Faculty of Veterinary Medicine, Utrecht University, the Netherlands
4 Orthopaedic Biomechanics, Department of Biomedical Engineering, Eindhoven University of Technology, Eindhoven, The Netherlands

Abstract
Osteoarthritis (OA) is a painful and debilitating condition that affects over 40 million people just in Europe (1). Together with the knee, the hip is one of the joints most frequently involved in OA. One of the two main causes for hip OA is hip dysplasia (HD) (2). HD is characterized by the instability of the hip joint and is caused by incomplete coverage of the femoral hip by the acetabulum. In this study, we have developed a mechanical competent and fully resorbable magnesium phosphate (MgP) - based implant to enlarge the acetabulum. The appropriate design was obtained from CT-scans of eight dog patients and fabricated using a room-temperature extrusion-based process (3). The mechanical compatibility of the implant as well as stability and optimal femoral coverage in the load-bearing quadrant of dog model is being investigated using a custom-built mechanical set-up simulating canine hip joint forces. Our results demonstrate that the 3D-printed implant design adapted well to the acetabulum of canine dysplastic hips, while the the flexibleMgP material composition supported fixation with metallic screws. Implants were able to withstand a maximum shear force of 900Nwithout failure and plastic deformation, which confirmed a proper fixation of the implant to the defect side. . Currently, implant mechanical performance under accelerated in vitro degradation and physiological loading is being performed. Preclinical evaluation in a canine model is planned to demonstrate safety of the proposed implant to treat hip dysplasia.

Refrences:

1. Kingsbury SR, Gross HJ. Osteoarthritis in europe. 2014.
2. Lievense AM, Bierma-Zeinstra SMA,. Influence of hip dysplasia.2004.
3. Golafshan N, Vorndran E.Tough magnesium phosphate-based 3D-printed implants.2020**.**

Mass Spectrometry Imaging for fracture hematoma analysis

R. Groven[1,2], *J. Gruisen*[1], *M. Eveque-Mouroux*[1,3], *S. Nauta*[1,3], *M. Poeze*[1], *M. van Griensven*[2], *T. Porta-Siegel*[3], *B. Cillero-Pastor*[3], *T. Blokhuis*[1]

[1] *Department of Surgery, Maastricht University Medical Center +, Maastricht, The Netherlands*
[2] *MERLN Institute for Technology-Inspired Regenerative Medicine, Department of Cell Biology-Inspired Tissue Engineering, Maastricht University, Maastricht, The Netherlands*
[3] *Maastricht Multimodal Molecular Imaging (M4I) Institute, Division of Imaging Mass Spectrometry, Maastricht University, Maastricht, The Netherlands*

Corresponding author:
R. Groven[1,2]
r.groven@maastrichtuniversity.nl

Background Although fracture treatment improved over the last decades, a substantial part of all fractures shows delayed healing and complications such as non-union[1,2]. Fracture healing is a complex process, involving cell-cell interactions, various cytokines and growth factors[1,3,4,6,8]. Although the fracture hematoma (FH) is known to have a relevant role in this process, the exact mechanisms are poorly understood[1,2,3,5-7]. To improve strategies in fracture treatment, regulatory pathways in fracture healing need to be investigated. Lipids are important structural components of the cell and function as messenger compounds, therefore this study initiates with lipid spectra analysis.
The aim of this translational study is to identify lipid spectra in FH over time with matrix assisted laser desorption/ionization mass spectrometry imaging (MALDI-MSI). MALDI-MSI enables analyses of lipids and their spatial distribution without prior knowledge, biological- or chemical labeling. Therefore, this method is more time-efficient and requires less tissue than conventional methods.
Methods For this study, fourteen FH samples were surgically removed, snap frozen, sectioned, washed and analyzed at different timepoints after fracture injury (1-19 days). The results from MALDI-MSI were subsequently analyzed by means of principal component analysis and discriminant analysis.
Results Principal component analysis and discriminant analyses identified three groups based on distinctive *m/z* values which were associated to FH age; early (1-3 days, n = 4), middle (6-10 days, n = 6) and late group (12-19 days, n = 4). In negative ion mode, the following distinctive *m/z* ratios were identified; 1516.89, 1151.75 and 1029.69. In positive ion mode, the following distinctive *m/z* ratios were identified; 497.37, 524.43, 913.74, 953.73 and 967.75 (figure 1,2).
Discussion This study shows that MALDI-MSI is well capable of making clear distinctions in lipid spectra between the early, middle and late FH groups. The distinctive *m/z* ratios fall within the range of either cardiolipins(*m/z* > 1400) , lyso-phospholipids (*m/z* 300–600) or phospholipids(*m/z* 600–1200). Tandem MS is a crucial next step to identify these specific compounds. Subsequently, a protocol for protein analysis will be developed in order to broaden the application of MALDI-MSI in FH analysis. These findings warrant further research into FH analysis by means of MALDI-MSI and its possible clinical implications in fracture treatment.
Conclusion This translational study revealed the great potential of MALDI-MSI for FH analysis. Protein analysis and further research into lipid spectra detection and identification will aid in both optimizing and personalizing fracture treatment in the future.

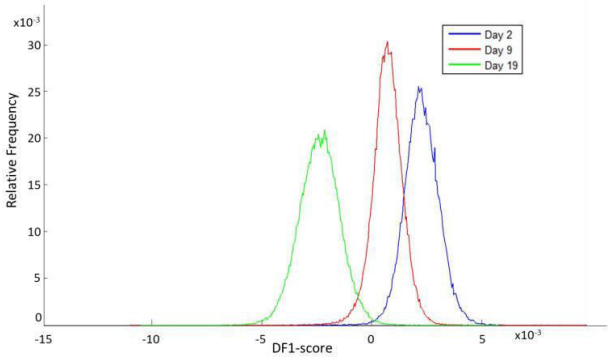

Figure 1: PCA-LDA of the lipid spectra of the three groups (day 2, 9 and 19) in negative ion mode with the highest variance

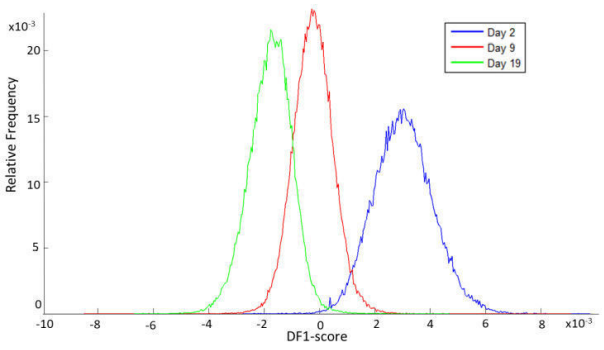

Figure 2: PCA-LDA of the lipid spectra of the three groups (day 2, 9 and 19) in positive ion mode with the highest variance

References

1. Claes L, Recknagel S, Ignatius A. Fracture healing under healthy and inflammatory conditions. Nat Rev Rheumatol. 8, 133, 2012;
2. Bastian OW, Kuijer A, Koenderman L, et al. Impaired bone healing in multitrauma patients is associated with altered leukocyte kinetics after major trauma. J Inflamm Res. 18, 69, 2016;
3. Kolar P, Schmidt-Bleek K, Schell H, et al. The Early Fracture Hematoma and Its Potential Role in Fracture Healing. Tissue Eng Part B Rev. 16, 427, 2010;
4. Marsell R, Einhorn TA. The biology of fracture healing. Injury. 42, 551, 2011;
5. Grundnes O, Reikerås O. The importance of the hematoma for fracture healing in rats. Acta Orthop. 64, 340, 1993;
6. Schell H, Duda GN, Peters A, Tsitsilonis S, Johnson KA, Schmidt-Bleek K. The haematoma and its role in bone healing. J Exp Orthop. 4, 2017;
7. Park SH, Silva M, Bahk WJ, McKellop H, Lieberman JR. Effect of repeated irrigation and debridement on fracture healing in an animal model. J Orthop Res. 20, 1197, 2002;
8. Schindeler A, McDonald MM, Bokko P, Little DG. Bone remodeling during fracture repair: The cellular picture. Semin Cell Dev Biol. 19, 459, 2008.

Can we control lumen growth in epithelial cells by modulating the physical microenvironment?

M.J. Hagelaars, L.W. Kuntz, C.V.C. Bouten and S. Loerakker

Soft Tissue Engineering and Mechanobiology, Eindhoven University of Technology, Eindhoven, the Netherlands

Introduction: Epithelial cells organize into cellular aggregates containing a central lumen according to a universal mechanism. Lumen inflation can be imposed by the secretion of ions in the opening aperture as water then passively follows the created osmotic pressure[1,2]. Cell proliferation is implied to maintain lumen growth as cellular tension by the cytoskeleton could restrict the expansion[3]. The extracellular microenvironment could also act as a resistance to the growing lumen. To reach a lumen with a certain diameter, the interplay of these several morphogenetic processes in lumen growth and stabilization has to be first fully understood before control can be exerted. Here, we focused on the role of the extracellular environment in the formation as well as the further growth of a central lumen in MDCK cysts.

Material and Methods: Madin Darby Canine Kidney (MDCK) cells were seeded in 3D collagen-I gels of variable collagen concentrations (1, 2 and 3 mg/ml). Cells were fixed at either a general time point (10 days) or were followed over time with standard fixation times at 2, 4, 7, 10, 14 and 21 days. Samples were analyzed using IF staining to characterize the formed cellular aggregate. Cell-free gels were characterized with SEM and microindentation to obtain fiber density and initial gel stiffness respectively. Cell-laden gels were characterized using only microindentation.

Results and Discussion: All gels formed dense collagen fiber networks. Fiber density increased with increasing collagen concentration (*Fig 1 – SEM images)*. Cysts were formed in the 1 mg/ml and 2 mg/ml collagen gels (*Fig 1*). These cysts were very heterogeneous with a high variety in size and cell number. Interestingly the stiffness of the surrounding gel seemed to stiffen in the 1 mg/ml collagen gels after 10 days, while the 2 mg/ml showed no change in comparison to the initial stiffness. The 3 mg/ml concentration collagen gel contained essentially no cysts after 10 days of culture and were excluded from further analysis.

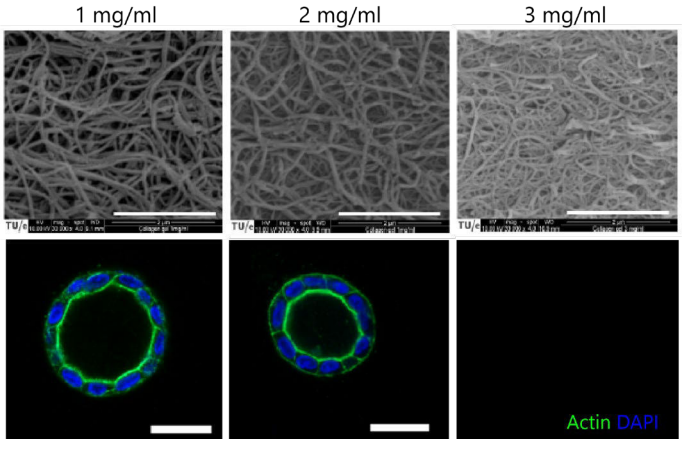

Figure 2: MDCKs grown in different concentration collagen gels (1,2 and 3 mg/ml). Cells were stained for DAPI and actin to image the cyst formation in the different conditions. Scale bar represents 25 um.

Cyst growth did not stabilize in 21 days, when cultured in a 2 mg/ml collagen gel (*Fig 2a*). The cyst growth was accompanied by both lumen growth (*Fig 2a*) as well as cell proliferation (*Fig 2b*). Both were still highly variable in different samples.

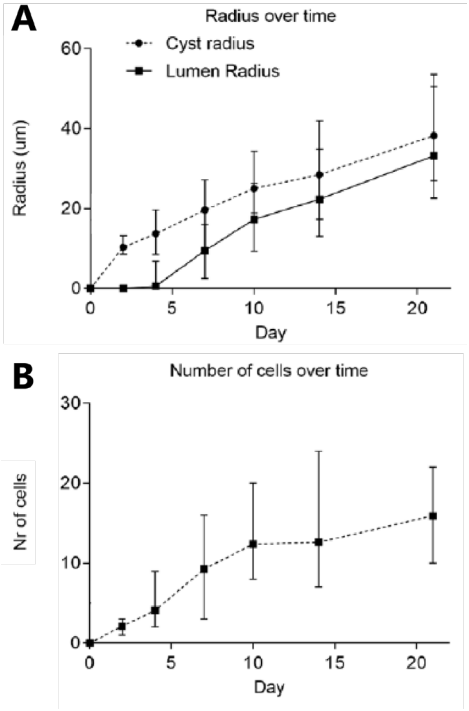

Figure 1: Characterization of MDCK cysts grown in a 2 mg/ml collagen gel concentration over time. A) Quantification of the cyst and lumen radius over time and (B) the number of cells per cyst over time.

Conclusion and Outlook: Our results imply that the environment can influence the lumen and cyst formation in the early stages. However, if an aggregate is able to form the resistance posed by the environments used in these experiments were not able to restrict lumen growth and create a stabilization. The found heterogeneity could possibly be explained by local differences in matrix composition. In the future, the influence of the other morphogenetic processes should be investigated to obtain a full understanding of the interplay that could possibly stabilize lumen growth. Furthermore, implementation of these processes in a computational model could further help explain the individual as well as the combined mechanical effect the processes have on lumen growth.

Acknowledgements: This study is supported by the partners of RegMed XB and powered by Health~Holland, Top Sector Life Sciences & Health.

References

1. Sigurbjörnsdóttir, S. *et al. Nat. Rev. Mol. Cell Biol* **15**, 665–676 (2014).
2. Bryant, D. M. & Mostov, K. E. *Nat. Rev. Mol. Cell Biol.* **9**, 887–901 (2008).
3. Gupta, K. *et al. J. Hepatol.* **66**, 1231–1240 (2017).

Harnessing Circulating Monocytes for *in situ* Endothelialization of Blood Contacting Supramolecular Surfaces

D.M. Ibrahim[1], M.G.J. Schmitz[1], P.A.A. Bartels[1], A.I.P.M. Smits[1], P.Y.W. Dankers[1], and C.V.C. Bouten[1]

[1] Department of Biomedical Engineering and Institute for Complex Molecular Systems, Eindhoven University of Technology, Eindhoven, the Netherlands

Introduction. The lack of a hemocompatible blood-material interface represents a major challenge for implanted synthetic biomaterials that are in direct contact with blood [1]. The optimal way to meet such a pivotal hemocompatibility requirement is to create an endothelial lining at the implanted blood-material interface [2], ideally through *in situ* endothelialization. This requires i) implanting a biomaterial with specific characteristics to recruit and interact with circulating cells that can form a functional endothelium directly in the body [3], and ii) targeting the most favorable cell source for *in situ* endothelialization. The source of cells recruited in such a process has been under investigation, with the main focus on circulating endothelial progenitor cells (EPCs) [4,5]. However, EPCs represent a very small fraction of the peripheral blood (0.002%-0.01%) [6]. Growing evidence suggests that the more abundantly present monocytes (CD14+) have a strong potential to differentiate into endothelial-like cells, thereby contributing to endothelium formation on implanted artificial surfaces [7].

Approach. Here, we focus on designing and testing novel material surfaces to recruit and differentiate circulating monocytes for implant endothelialization. To this end, a supramolecular biomaterial based on hydrogen bonding units is functionalized via a modular approach [8,9] with a heparin binding peptide, to subsequently bind heparin and VEGF to the material. Current testing of the material will tell the efficiency to recruit angiogenic monocytes and their ability to differentiate into endothelial like cells to form a protective monolayer against thromboembolic events on blood- contacting supramolecular implants.

Preliminary Results. Preliminary results showed the ability of monocytes cultured statistically on the functionalized supramolecular biomaterial to display endothelial markers after 14 days in culture.

Future outlook. Further experiments to confirm the previous finding through exploring more endothelial markers. Additionally, the functionalized supramolecular biomaterials' ability to capture immune cells in a dynamic environment will be tested as well.

References

[1] L. Weidenbacher, E. Müller, A.G. Guex, M. Zündel, P. Schweizer, V. Marina, C. Adlhart, L. Vejsadová, R. Pauer, E. Spiecker, K. Maniura-Weber, S.J. Ferguson, R.M. Rossi, M. Rottmar, G. Fortunato, In Vitro Endothelialization of Surface-Integrated Nanofiber Networks for Stretchable Blood Interfaces, ACS Applied Materials and Interfaces. (2019).

[2] B.D. Ippel, P.Y.W. Dankers, Introduction of Nature's Complexity in Engineered Blood-compatible Biomaterials, Advanced Healthcare Materials. 7 (2018) 1700505.

[3] A. de Mel, G. Jell, M.M. Stevens, A.M. Seifalian, Biofunctionalization of Biomaterials for Accelerated in Situ Endothelialization: A Review, Biomacromolecules. 9 (2008) 2969–2979.

[4] N.H. Anthony J. Melchiorri, J.P. Fisher, Strategies and Techniques to Enhance the In Situ Endothelialization of Small-Diameter Biodegradable Polymeric Vascular Grafts, TISSUE ENGINEERING: Part B. 19 (2013).

[5] R.J. Smith, T. Yi, B. Nasiri, C.K. Breuer, S.T. Andreadis, Implantation of VEGF-functionalized cell-free vascular grafts: Regenerative and immunological response, FASEB Journal. 33 (2019) 5089–5100.

[6] Y.M.& Y.J. Meng Qin, Xin Guan, Huihui Wang, Yu Zhang, Bin Shen, Qingyu Zhang, Wei Dai, An effective ex-vivo approach for inducing endothelial progenitor cells from umbilical cord blood CD34+ cells, Stem Cell Research and Therapy. (2017) 8–25.

[7] R.J. Smith, B. Nasiri, J. Kann, D. Yergeau, J.E. Bard, D.D. Swartz, S.T. Andreadis, Endothelialization of arterial vascular grafts by circulating monocytes, Nature Communications. 11 (2020).

[8] V. Bonito, A.I.P.M. Smits, O.J.G.M. Goor, B.D. Ippel, A. Driessen-Mol, T.J.A.G. Münker, A.W. Bosman, T. Mes, P.Y.W. Dankers, C.V.C. Bouten, Modulation of macrophage phenotype and protein secretion via heparin-IL-4 functionalized supramolecular elastomers, Acta Biomaterialia. 71 (2018) 247–260.

[9] P.Y.W. Dankers, M.C. Harmsen, L.A. Brouwer, M.J.A. Van Luyn, E.W. Meijer, A modular and supramolecular approach to bioactive scaffolds for tissue engineering, Nature Materials. 4 (2005) 568–574.

Repair of Chondral Defects using Cartilage Organoids, an ex vivo study in Human Explants

M.W.A. Kleuskens[1], J.F. Crispim[1], C.C. van Donkelaar[1], R.P.A. Janssen[1,2] and K. Ito[1]

[1]Orthopaedic Biomechanics, Department of Biomedical Engineering, Eindhoven University of Technology, PO Box 513, 5600 MB Eindhoven, The Netherlands, [2] Orthopaedic Center Máxima, Máxima Medical Center Eindhoven/Veldhoven, The Netherlands

Introduction:

Autologous chondrocyte implantation is a clinically used technique to regenerate articular cartilage (AC) in focal defects. One of the persisting challenges in AC regeneration is the inferior quality of repair tissue and lack of integration with the surrounding cartilage. Previous research has shown that adding porcine notochordal cell-derived matrix (NCM) to the culture medium induces proliferation and matrix production of bovine chondrocytes in alginate beads.[1] Besides, NCM is rich in proteoglycans and collagen type II, important cartilage matrix components. Adding NCM to a 3D spinner flask culture of chondrocytes provides the chondrocytes with a cartilage-like matrix to attach to, while also inducing proliferation, leading to their self-assembly into organoids with a pericellular and territorial matrix and maintenance of chondrogenic phenotype. The present study hypothesizes that these organoids might improve cartilage tissue formation and integration in short-term cartilage repair. Here, this novel approach will be compared to an autologous chondrocyte implantation-like procedure using 2D expanded chondrocytes.

Methods: Fresh chondrocytes were isolated from human tissue (n=5) of patients undergoing total knee replacement (TKR) surgery at the Máxima Medical Centre, Eindhoven under IRB approval. Chondrocytes were cultured for 12 days in traditional 2D culture flasks (10^6 cells in a T175 flask) without NCM and in spinner flasks (50000 cells/ml), supplemented with NCM (D0: 0.25 mg/ml; D4: 0.5 mg/ml; D12: 1 mg/ml), forming cartilage organoids. During culture, cell count and cell viability were monitored. Osteochondral explants (Ø 10mm, 5 per donor) were isolated from tissue of six different TKR subjects and a Ø 6mm chondral defect was created in the center of each explant. Organoids and 2D cultured chondrocytes were implanted into the defects (10^6 cells/80µl) using Tisseel fibrin sealant (figure 1). The constructs were cultured for 28 days in a double-chamber culture platform, in which cartilage and bone compartments are separated to allow for supplementation of tissue-specific medium. Biochemical content and histological appearance of the implants was analyzed after 1 and 28 days of culture.

Results and discussion: Adding NCM resulted in increased proliferation of the chondrocytes (3.9-fold) compared to the control group without NCM, though proliferation was slightly less than in 2D expansion. Cell viability of >90% was maintained throughout the culture period and it was observed that cells attached to the NCM as well as to each other. Immunofluorescent images of NCM cultured organoids before implanting them into the defects showed the presence of proteoglycans, collagen type II and cartilage-marker Sox-9, confirming the chondrogenic phenotype of the cells within the organoids (figure 2). Analysis of the biochemical content and histological appearance of the cultured constructs after 28 days is pending.

References: [1]de Vries et al., *Sci Rep*, 2018

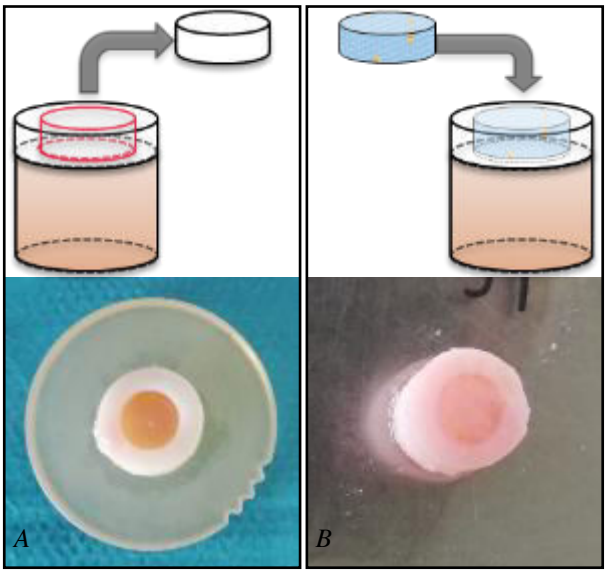

Figure 1: A) Human osteochondral plugs were harvested and a Ø 6mm chondral defect was created in the center of each explant. B) Defects were filled by embedding organoids or single cells in Tisseel fibrin glue.

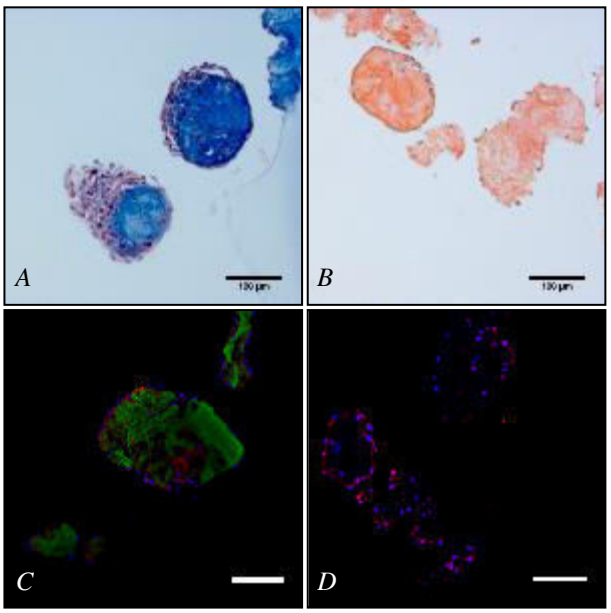

Figure 2: Histological analysis of organoids before implantation into the defects. A) Alcian blue (proteoglycans); B) Picrosirius red (collagen); C) immunofluorescent localization of collagen type I (red) and collagen type II (green). Nuclei in blue; D) immunofluorescent localization of SOX9 (red). Nuclei in blue. Scalebar = 100 µm.

Repair of Chondral Defects using Cartilage Organoids, an ex vivo study in Human Explants

M.W.A. Kleuskens[1], J.F. Crispim[1], C.C. van Donkelaar[1], R.P.A. Janssen[1,2] and K. Ito[1]

[1]Orthopaedic Biomechanics, Department of Biomedical Engineering, Eindhoven University of Technology, PO Box 513, 5600 MB Eindhoven, The Netherlands, [2] Orthopaedic Center Máxima, Máxima Medical Center Eindhoven/Veldhoven, The Netherlands

Introduction:

Autologous chondrocyte implantation is a clinically used technique to regenerate articular cartilage (AC) in focal defects. One of the persisting challenges in AC regeneration is the inferior quality of repair tissue and lack of integration with the surrounding cartilage. Previous research has shown that adding porcine notochordal cell-derived matrix (NCM) to the culture medium induces proliferation and matrix production of bovine chondrocytes in alginate beads.[1] Besides, NCM is rich in proteoglycans and collagen type II, important cartilage matrix components. Adding NCM to a 3D spinner flask culture of chondrocytes provides the chondrocytes with a cartilage-like matrix to attach to, while also inducing proliferation, leading to their self-assembly into organoids with a pericellular and territorial matrix and maintenance of chondrogenic phenotype. The present study hypothesizes that these organoids might improve cartilage tissue formation and integration in short-term cartilage repair. Here, this novel approach will be compared to an autologous chondrocyte implantation-like procedure using 2D expanded chondrocytes.

Methods: Fresh chondrocytes were isolated from human tissue (n=5) of patients undergoing total knee replacement (TKR) surgery at the Máxima Medical Centre, Eindhoven under IRB approval. Chondrocytes were cultured for 12 days in traditional 2D culture flasks (10^6 cells in a T175 flask) without NCM and in spinner flasks (50000 cells/ml), supplemented with NCM (D0: 0.25 mg/ml; D4: 0.5 mg/ml; D12: 1 mg/ml), forming cartilage organoids. During culture, cell count and cell viability were monitored. Osteochondral explants (Ø 10mm, 5 per donor) were isolated from tissue of six different TKR subjects and a Ø 6mm chondral defect was created in the center of each explant. Organoids and 2D cultured chondrocytes were implanted into the defects (10^6 cells/80µl) using Tisseel fibrin sealant (figure 1). The constructs were cultured for 28 days in a double-chamber culture platform, in which cartilage and bone compartments are separated to allow for supplementation of tissue-specific medium. Biochemical content and histological appearance of the implants was analyzed after 1 and 28 days of culture.

Results and discussion: Adding NCM resulted in increased proliferation of the chondrocytes (3.9-fold) compared to the control group without NCM, though proliferation was slightly less than in 2D expansion. Cell viability of >90% was maintained throughout the culture period and it was observed that cells attached to the NCM as well as to each other. Immunofluorescent images of NCM cultured organoids before implanting them into the defects showed the presence of proteoglycans, collagen type II and cartilage-marker Sox-9, confirming the chondrogenic phenotype of the cells within the organoids (figure 2). Analysis of the biochemical content and histological appearance of the cultured constructs after 28 days is pending.

References: [1]de Vries et al., *Sci Rep*, 2018

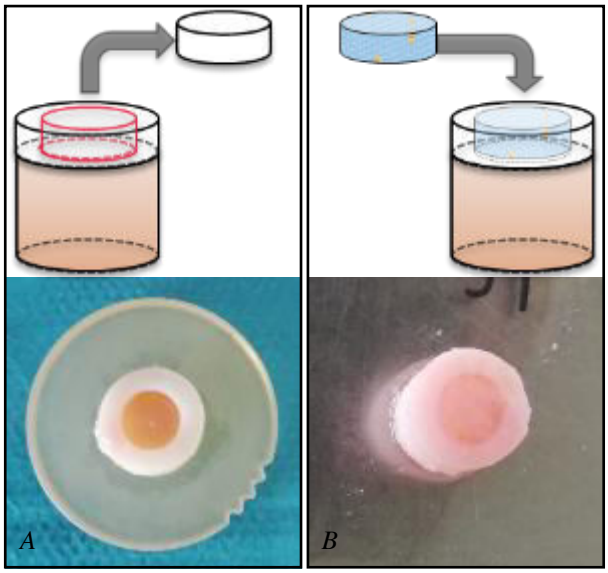

Figure 1: A) Human osteochondral plugs were harvested and a Ø 6mm chondral defect was created in the center of each explant. B) Defects were filled by embedding organoids or single cells in Tisseel fibrin

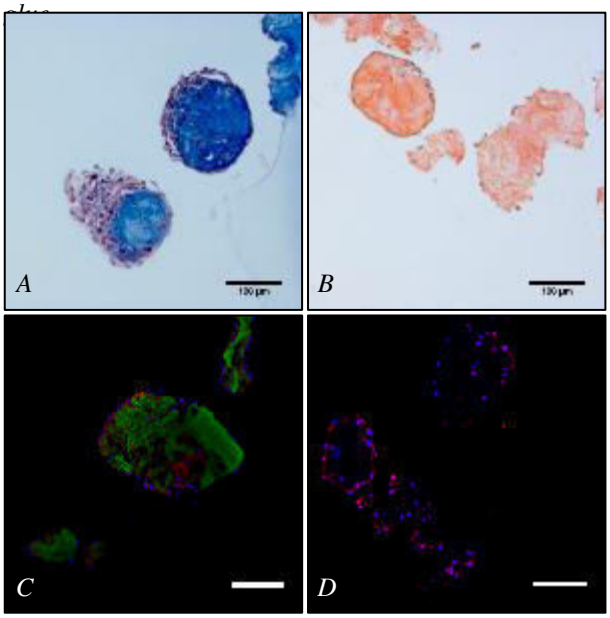

Figure 2: Histological analysis of organoids before implantation into the defects. A) Alcian blue (proteoglycans); B) Picrosirius red (collagen); C) immunofluorescent localization of collagen type I (red) and collagen type II (green). Nuclei in blue; D) immunofluorescent localization of SOX9 (red). Nuclei in blue. Scalebar = 100 µm.

Macrophage-Driven *in situ* Vascular Tissue Engineering in a Hyperglycemic Context – an *in vitro* study

S.E. Koch[1,2], F.L.P. Verhaegh[1,2], S. Smink[1,2], C.V.C. Bouten[1,2], A.I.P.M. Smits[1,2]

[1] Department of Biomedical Engineering, Eindhoven University of Technology, The Netherlands
[2] Institute for Complex Molecular Systems, Eindhoven University of Technology, The Netherlands

Introduction

Macrophages have a commanding role in biomaterial-driven in situ tissue regeneration. Depending on their polarization state, macrophages mediate the formation and remodeling of new tissue by secreting essential growth factors and cytokines that either promote or inhibit tissue formation[1]. Therefore, successful integration of *in situ* tissue engineered vascular grafts (TEVG) depends largely on the regenerative potential of the recipient [2]. A large cohort of the patients requiring vascular replacements, suffer from systemic co-morbidities like diabetes, which gives rise to an aggressive oxidative inflammatory environment. These hyperglycemic conditions hamper a well-balanced regenerative process.[3] This is also reflected in animal experiments in which promising TEVG results found in healthy animals, could not be replicated in diabetic animals [4]. Furthermore, hyperglycemic conditions seem to polarize the macrophages into a more pro-inflammatory M1 state. Which is also reflected in the macrophage metabolism, in which the M1 macrophages mainly use glucose as a quick energy source, whilst the more regenerative M2 macrophages rely on fatty acid metabolism[5]. To gain a more fundamental understanding of the underlying biological processes, we study the macrophage-driven vascular tissue regeneration in hyperglycemic conditions via an *in vitro* approach.

Material and Methods

To simulate various phases of the *in situ* regenerative cascade, human macrophages and myofibroblasts in mono- or coculture were seeded in 2D and 3D in resorbable polycaprolactone bisurea (PCL-BU) scaffold in normoglycemic (5 mM glucose), hyperglycemic (25 mM glucose) and osmotic control conditions (5 mM glucose, 20 mM mannitol) for 7 days. Macrophages derived from human peripheral blood mononuclear cells were isolated from buffy coats and myofibroblasts were obtained from the saphenous vein. For 2D studies, macrophages were polarized in by a cytokine stimulus into different phenotypes. For 3D studies, unpolarized macrophages were seeded onto the scaffolds, for a biomaterial-induced phenotype. Emphasis was given to the analysis of polarization state, cytokine excretion and tissue production.

Results and Discussion

High glucose concentration or high osmotic pressure did not affect macrophage cell morphology compared to normoglycemic conditions in when seeded in 2D set-up. Also, cytokine-induced macrophage polarization was not affected by a hyperglycemic of hyperosmotic environment in 2D monocultures. Proceeding with the PCL-BU scaffold 3D mono-cultures, the macrophages showed a slight preference towards the M1 phenotype in both hyperglycemic and high osmotic pressure conditions, suggesting that this polarization did not solely occur due to high glucose concentrations. Myofibroblasts cultured in the 3D PCL-BU scaffolds tended to become more contractile and had a higher collagen gene expression under hyperglycemic conditions compared to the normoglycemic and hyperosmotic conditions. Co-culturing of macrophages and myofibroblasts resulted in a more inflammatory macrophage phenotype, combined with decreased tissue production. The obtained results showed a relatively large donor-to-donor variation, which is not unexpected as monocytes and macrophages represent a heterogenous cell type which immune responsiveness is determined by genetic, epigenetic and environmental influences[7].

Conclusion and future outlook

The relatively large donor-to-donor variation stresses the importance of taking scaffold-independent patient-specific factors into account when studying *in situ* biomaterial driven tissue engineering[2]. Currently, we aim to shed light on the main metabolic pathways involved in these tissue regeneration processes within the same *in vitro* static set up. Furthermore, as it is known that the hemodynamic milieu (e.g. flow and stretch) greatly influences macrophage behavior[6], and the paracrine signaling to myofibroblasts and subsequent tissue production, *in vitro* experiments with co-cultures of macrophages and myofibroblasts subjected to hemodynamic loads in normoglycemic and hyperglycemic conditions are conducted. The overall aim is to gain understanding of the immunological processes underlying regeneration in a clinically relevant context.

Acknowledgements

This research is part of the InSiTeVx project (436001003); financially supported by ZonMw within the LSH 2Treat Programme and the Dutch Kidney Foundation.

References

[1] Wissing&Bonito et al, 2017, *NPJ Regen Med,* 2(1), p18
[2] Smits&Bouten, 2018, *Curr Opin Biomed Eng*, 6, p17-26
[3] Dhulekar&Simionescu, 2018, *Acta Biomater*, 70, p25-34
[4] Wang et al, 2016, *Biomater Sci*, 4(10), 1485-1492
[5] Viola et al, 2019, *Front Immunol*, 10, 1-16
[6] Wissing&van Haaften et al, 2020, *Biomater Sci,* 8(1), 132-147
[7] Huang&Wells (2014), *J. Immunol*, 193, 13-19

Contact: s.e.koch@tue.nl

Osteoconductivity of Amorphous and Crystalline Calcium Phosphate Coatings in the Presence and Absence of Incorporated Bovine Serum Albumin

M.Li, G.Wu, Y.Liu
Department of Oral Implantology and Prosthetic Dentistry, Academic Centre for Dentistry Amsterdam (ACTA), University of Amsterdam and Vrije Universiteit Amsterdam, Amsterdam, The Netherlands E-mail:m.li@acta.nl

Introduction: Dental implants represents a break-through in dentistry and has been considered as the best replacement of missing teeth. Surface modification is one of the easiest ways to improve osseointegration[1]. Rapid osteointegration could not only permit early loading but also contribute to long term implant usage. Biomimetic calcium phosphate (CaP) coatings have been developed for coating medical device as a slow and local drug delivery system[2]. The aim of this study was to compare the osteoconductivity of the amorphous and crystalline CaP coatings in the presence and absence of incorporated bovine serum albumin (BSA) in vitro and in vivo, using specially designed titanium pins.

Materials and Methods: Amorphous and crystalline coatings in the absence and presence of BSA were prepared.

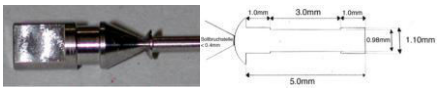

Characterization of coatings were evaluated by Scanning Electron Microscopy (SEM) and Fourier Transform Infrared Spectrometer(FTIR). Deposition of BSA of the types was examined by Confocal Laser-Scanning Dual-Channel-Fluorescence Microscopy(CLSM). Loading and release of BSA was evaluated by Enzyme Linked Immunosorbent Assay(ELISA). Activity of Alkaline Phosphatase(ALP) of different coatings was evaluated in vitro.

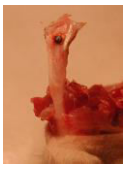

Six different groups participating. Rats orthotopic model was used (n=6 rats per group). Time points are 3 days, 1, 2 and 4 weeks. Histological and histomorphor-mitrical ananlysis were done in order to determine bone to implant contact(BIC).

Results:

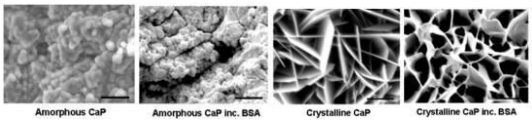

Fig.1. SEM of biomimetic coatings. Scale bar=5 μm.

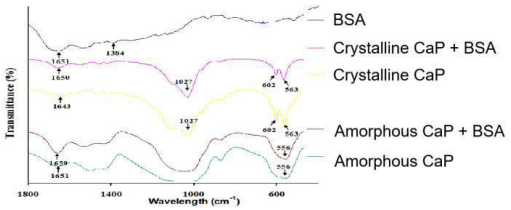

Fig.2. FTIR of amorphous and crystalline coatings

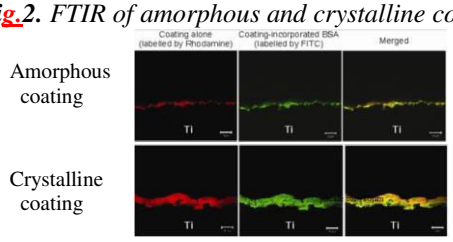

Fig.3. Distribution of the coating materials by CLSM

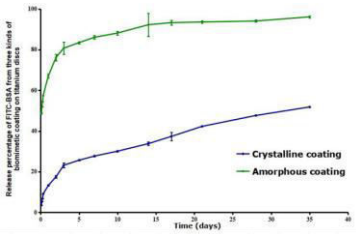

Fig.4. Release profiles of incorporated BSA.

The mean loading of FITC-BSA incorporated into the amorphous and crystalline CaP on each titanium pin is 8.37 μ g and 88.15 μ g respectively(n=6).

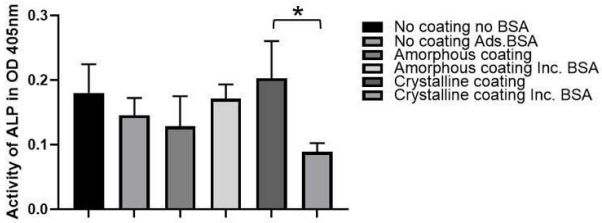

Fig.5. Activity of ALP in primary osteoblasts after an 8-day culture in different groups

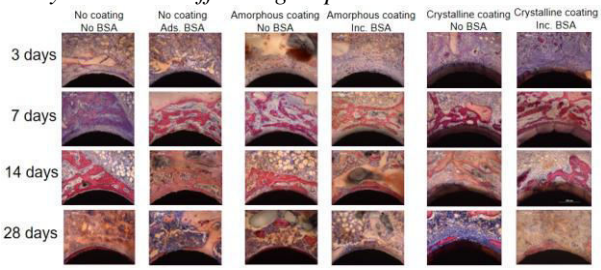

Fig.6. Histological observations of each group

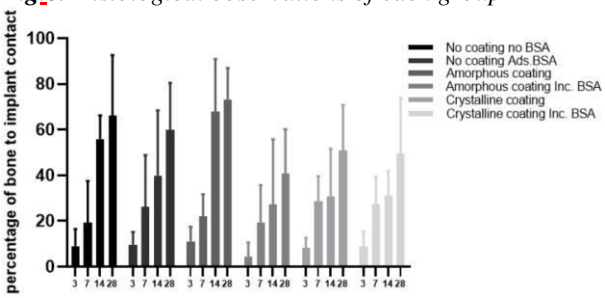

Fig.7. BIC obtained on the surface of titanium pins.

Conclusion: Biomimetic crystalline CaP coating can be an ideal carrier for protein or drugs; the amorphous biomimetic CaP coating promoted osteoconductivity and incorporation of BSA did not improve osteogenesis.

References:

[1] C. BR, K. J, L. C, Analysis of technical complications and risk factors for failure of combined tooth-implant-supported fixed dental prostheses, Clinical implant dentistry and related research (2020).

[2] J. WR, B. KA, J. F, H. M, G. K, A. I, L. D, H. R, R. B, Optimizing Manufacturing and Osseointegration of Ti6Al4V Implants through Precision Casting and Calcium and Phosphorus Ion Implantation? In Vivo Results of a Large-Scale Animal Trial, Materials (Basel, Switzerland) 13(7) (2020).

TWIST1 controls cellular senescence and energy metabolism in mesenchymal stem cells

C Voskamp[1], LA Anderson[1], WJLM Koevoet[2], S Barnhoorn[3], PG Mastroberardino[3], GJVM van Osch[1,2], R Narcisi[1]

[1]Department of Orthopaedics; [2]Department of Otorhinolaryngology, [3]Departments of Molecular Genetics. All authors from the Erasmus MC, University Medical Center Rotterdam, 3015 CN Rotterdam, the Netherlands

INTRODUCTION: Mesenchymal stem cells (MSCs) are promising cells for regenerative medicine applications. One of the limitations that reduces the therapeutic use of MSCs is cellular senescence. Cellular senescence is a state of the cell in which cells stop proliferating, while still be metabolically active. By acquiring a specific senescence-associated secretory phenotype (SASP), senescent MSCs can contribute to tissue degeneration and chronic inflammation. The molecular mechanism behind cellular senescence in MSCs remains largely unknown. The transcription factor TWIST1 is suggested to play a role in cellular senescence, since its expression is reduced in slow proliferating MSCs. The aim of this research was therefore to determine the role of TWIST1 in regulating cellular senescence in MSCs.

MATERIALS & METHODS: To determine the effect of the silencing of *TWIST1* on senescence, human MSCs from 3 different donors were treated with 15 nM TWIST1 siRNA (siTWIST1). Scramble siRNA and untreated cells were used as controls. To overexpress *TWIST1*, human MSCs from 3 different donors were transduced with a third generation TWIST1 overexpression lentiviral construct. Untreated MSCs, MSCs transduced with a GFP or with an empty vector were used as control. Moreover, as additional reference, irradiation was used in to induce senescence in MSC (gamma irradiation - 20 Gy) in order to compare the effect of TWIST1 with another classical method to induce senescence. After irradiation and TWIST1 manipulation, MSCs were analyzed for cellular senescence markers by qPCR (IL-6, IL8, P16, P21) and senescence-associated beta-galactosidase (SA-β-gal) activity staining. The expansion capacity of the MSCs was determined by cell count. A metabolic evaluation of the cells was performed using the Seahorse XF apparatus, in order to evaluate changes in cellular bioenergetics.

RESULTS: *TWIST1* overexpressing MSCs had a reduced percentage of SA-β-gal positive cells (71% reduction), a decreased expression of the SASP related genes *IL-6* (1.8-fold reduction) and *IL-8* (2.4-fold reduction) and an increased expansion rate (1.7-fold), indicating that high *TWIST1* expression delays cellular senescence in MSCs. On the other hand, silencing of *TWIST1* resulted in an increased percentage SA-β-gal positive cells (9.5 fold), a reduced expansion rate (20-fold reduction) compared to control conditions and an increase expression of the senescence markers *P21* (2.1-fold) and *P16* (5.9-fold). These results were comparable with the data collected from irradiation-induced MSCs, condition in which we also detected down-regulation of *TWIST1 (*1.7-fold reduction compared to non-irradiated MSCs). Surprisingly, the expression of SASP related genes *IL-6* and *IL-8* was reduced in siTWIST cells compared to controls (1.6-fold and 7.2-fold reduction, respectively). This was different from what we and others observed in irradiation-induced MSCs, where *IL-6* and *IL-8* are upregulated compared to untreated MSC.
In addition, metabolic evaluation performed by the Seahorse XF apparatus showed that both *TWIST1* silencing-induced and irradiation-induced senescent MSCs had a higher oxygen consumption and mitochondrial respiration compared to control MSCs while, differently from the irradiated MSCs, *TWIST1* silencing-induced senescent MSCs have an unaltered extracellular acidification rate (ECAR) compared to the controls. These data suggest that the glycolytic capacity (linked to ECAR) is unaltered in siTWIST1-MSCs, in contrast to irradiation-induced senescent MSCs where this parameters increases.

CONCLUSION: Overall, our data indicate that TWIST1 is implicated in the regulation of cellular senescence in human MSCs. Interestingly, we also demonstrated that *TWIST1* silencing-induced senescence is characterized by a specific SASP gene profile (low *IL-6* and *IL-8*) and a peculiar metabolic state (low extracellular acidification rate), differently compared to irradiation-induced senescence. Our findings highlight how senescent MSCs can be phenotypically heterogeneous, suggest that reduction of *TWIST1* expression might drive aging in MSCs, and makes TWIST1 an interesting target for MSC-based tissue engineering approaches.

Bifurcation angles vs Tortuosity: what controls mechanical signals of vascular networks? (a computational study)

P. Padmanaban[1], M. Z. Sultan[1] and J. Rouwkema[1]

[1]Department of Biomechanical Engineering, Technical Medical Center, Faculty of Engineering Technology, University of Twente, 7500 AE Enschede, The Netherlands

Motivation

To make functional engineered tissues, hierarchical multiscale complexity, efficient perfusion with controlled mass transfer and easy fabrication strategy is necessary. Besides vessel diameter, bifurcation angles, and tortuosity features are vital geometric components of vascular networks that directly influences the blood flow circulation. In reaction to the fluid flow and wall shear stresses (WSS), *in vivo*[1] and *in vitro*[2,3] studies have shown the variety of vascular responses to mechanical signals developed within the vascular networks. Examples include that veins can transform into arteries when subjected to high stresses by flow manipulation; patterned lattice structures and spiral channels, improve tissue perfusion and alters endothelial cell morphology under flow. However, the effect of bifurcation angles and tortuosity on the mechanical signals developed within vascular networks are not much explored.

Methods

Bifurcation geometries represented in **Figure 1B** were extracted from the *in vivo* experimental imaging data of developing chicken vascular networks and are designed using the SolidWorks software (2019 SP5). The diameter of the parent vessel and the corresponding daughter vessels is kept constant at 100µm for all the models. Furthermore, the length of the vessels is 3mm till the bifurcation and each bifurcation is 1,5mm long. This offers uniformity with the designs and makes them computationally cost-effective. Fluid flow shear stress were computed using COMSOL Multiphysics software (version 5.5) by solving Navier-stokes equation. Three different viscosities ($1e^{-3}$, $1e^{-4}$, $1e^{-5}$ Pa.s) and five different velocities (1,2,3,5,10,15µm/s) were tested on 3 designs, of increasing bifurcation angles and tortuosity. Both continuous and pulsatile flow types were studied.

Results and Discussion

An idealized model-based approach were applied, by varying a single feature at a time, geometrical or flow property, while others are kept constant to figure out how WSS is affected by each parameter. To summarize, the viscosity and input velocity has a proportional influence on WSS. Tortuosity free model (design 1) shows uniform shear stress and partial tortuosity model (design2) shows higher shear stress at bifurcations. Interestingly design3 exhibits higher stress at bends. Furthermore, the simulation outcomes were compared between the designs and principal component analysis (PCA) were plotted.

Conclusions and Future directions

In conclusion, using CFD simulations we have shown that by increasing bifurcation angles and tortuosity, the WSS developed due to the blood flow can be controlled. Future work will focus on fabricating the perfusable vascular networks with complex bifurcations and tortuous designs. Additionally, these structures will be embedded into the hydrogel system along with multiple cell types. By employing these complex structures, this system has the potential to regulate the vascular organization within engineered hydrogels, by tuning the local shear stress and blood flow velocity.

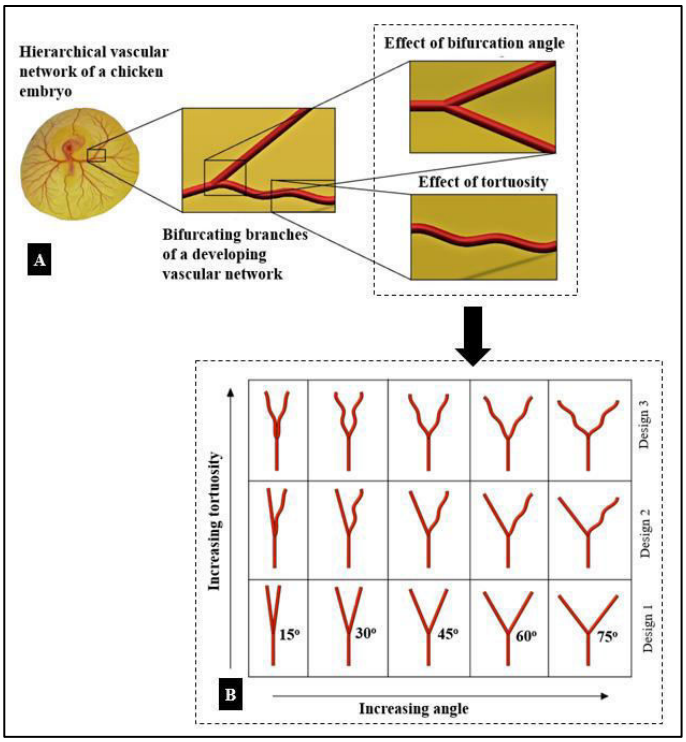

Figure 1. Overview of this study: ***Panel A*** *represents the chicken embryo exhibiting hierarchical multiscale vascular network of embryonic development day 4 and SolidWorks designs of bifurcating branches and tortuous vessel.* ***Panel B*** *shows the SolidWorks 3D bifurcation geometries that mimic the vascular structures in a chicken embryo with varying complexity.*

References

[1] le Noble F et al. **2004** *Development* 131 361-75
[2] Miller SJ et al. **2012** *Nat. Mater.* 11 768-774
[3] Mandrycky C et al. **2020** *Sci. Adv.* 6 eabb3629

Acknowledgements

This work is supported by an ERC Consolidator Grant under grant agreement no 724469.

Optimization of transcript therapy with chemically modified mRNA with the final goal of overcoming osteoporosis

C.S.J. Polain[1], C. Plank[2], E. Bonvin[3], M. van Griensven[1], E.R. Balmayor[4]
[1]Department cBITE, MERLN Institute, Maastricht University, Universiteitssingel 40, 6229 ER Maastricht, The Netherlands
[2]Ethris GmbH, Semmelweisstraße 3, 82152 Planegg, Germany
[3]OZ Biosciences SAS, 163 Av. de Luminy, zone entreprise, case 922, 13288 Marseille cedex 09, France
[4]Department IBE, MERLN Institute, Maastricht University, Universiteitssingel 40, 6229 ER Maastricht, The Netherlands

Introduction

Osteoporosis is a metabolic bone disease caused by the over-activity of osteoclasts, bone degrading cells, which leads to an imbalance between bone formation and resorption. This results in brittle bones that are prone to fragility fractures. Osteoporosis affects more than 75 million people in Europe, the United States and Japan combined, leading to at least 8.9 million fractures annually.

The ultimate goal of our study is to develop an efficient therapy to treat osteoporotic fractures. This novel therapy comprises combining growth factors or other small molecules, (stem) cells and biomaterials. Bioactive growth factors are difficult and expensive to produce. Moreover, they need to be administered in supraphysiological amounts. Therefore, gene therapy approaches are considered that make use of the translation machinery of local cells. To make the gene therapy more efficient and less dangerous concerning mutagenesis, messenger RNA (mRNA) can be used. However, mRNA is instable and immunogenic. Chemical modifications can overcome these disadvantages. The chemically modified mRNA (cmRNA) must be delivered to the cells. Typically, lipid vectors as non-viral entities are used for that. In the current study, we tested five different vectors to deliver cmRNA to a cell line with the aim of finding the best transfection set-up. The first is to optimize the cmRNA concentration and the ratio of cmRNA-to-lipid.

Materials and Methods

A lipid titration was performed in order to find the optimal cmRNA concentration and cmRNA-to-lipid ratio by transfecting 2 $x10^4$ A549 cells in a 96-wells plate with Metridia Luciferase (MetLuc) cmRNA, a reporter luciferase that is excreted by cells. Both cmRNA:lipid ratios as well as total cmRNA amount was tested with 12 ratios ranging from 0.5:1 to 1:11 cmRNA:lipid w/v and cmRNA at doses starting from 50 pg/cell up to 0.78 pg/cell following a 1:2 dilution. cmRNA-lipid complexes (lipoplexes) were prepared by mixing selected lipid transfection enhancers, designated for simplicity as OzB1, OzB2, OzB3, OzB4, OzB5 (OzBiosciences), and Xfect (Takara) with MetLuc cmRNA.

A Coelenterazine assay was performed to assess functional translation of the cmRNA, by detecting MetLuc expression after 24 hours, 48 hours, and 72 hours. This was measured using a Clariostar plate reader, and was expressed in Relative Light Units (RLU). PrestoBlue, a cell viability assay, was performed to assess cytotoxicity at the same observation times.

Results and Discussion

Overall, high concentrations of cmRNA and high concentrations of lipid lead to increased cytotoxicity and decreased functionality. Generally, the best concentrations of cmRNA ranged between 12.5 and 6.25 pg per cell, and optimal cmRNA-to-lipid ratios ranged between 1:4 and 1:6.

In terms of transfection vector performance, lipid vector OzB3 was the best performing, resulting in overall highest expression of MetLuc, reaching up to $10x10^6$ RLUs, and lowest toxicity, reaching up to 100% cell viability.

Conclusions / Summary

From these results, we can conclude that the best concentrations of MetLuc cmRNA ranged between 12.5 and 6.25 pg per cell, and optimal cmRNA-to-lipid ratios ranged between 1:4 and 1:6. The best performing lipid was OzB3. Based on these results, the next step is to apply this knowledge in the transfection of cmRNA encoding for therapeutic genes in bone or stem cells from osteoporotic patients.

Acknowledgements

This work has been performed as part of the cmRNAbone project and has received funding from the European Union's Horizon 2020 research and innovation programme under the Grant Agreement No 874790.

Platelet-Rich Plasma Does Not Inhibit Inflammation or Promote Regeneration in Human Osteoarthritic Chondrocytes Despite Increased Proliferation

M. Rikkers[1], K. Dijkstra[1], B.F. Terhaard[1], J. Admiraal[1], R. Levato[1,2], J. Malda[1,2], L.A. Vonk[1,3]
[1]Department of Orthopaedics, University Medical Center Utrecht, Utrecht, The Netherlands
[2]Department of Equine Sciences, Faculty of Veterinary Sciences, Utrecht University, Utrecht, The Netherlands
[3]CO.DON AG, Berlin, Germany

Introduction

Platelet-rich plasma (PRP) is a concentrated blood product, rich in growth factors and anti-inflammatory components. Through activation of PRP by thrombin and calcium, a growth factor-loaded gel forms which can be used as a 3D substrate to culture cells. We hypothesize that PRP gel stimulates cartilage regeneration, superior to commercially available fibrin gel. The aim of the study was to assess the anti-inflammatory properties of PRP and investigate the regenerative potential of PRP gel on cartilage extracellular matrix (ECM) production by primary chondrocytes.

Methods

PRP was prepared from blood derived from healthy volunteers by double-spin centrifugation. Primary human chondrocytes (passage 2) derived from osteoarthritic knees were cultured in monolayers, after which inflammation was mimicked by stimulation with TNF-α. Next, the cells were treated for 48 h with 0-, 2-, 5-, 10-, or 20% (v/v) PRP. Expression of genes involved in inflammation and chondrogenesis was measured by real-time PCR. In addition, chondrocytes were cultured in PRP gels and fibrin gels consisting of increasing concentrations of PRP. After 28 days of culture without any additional growth factors, production of cartilage extracellular matrix (ECM) was assessed. Deposition and release of glycosaminoglycans (GAG) and collagen was quantitatively determined and visualized by (immuno)histochemistry. Proliferation of chondrocytes was assessed by quantitative measurement of DNA.

Results

The inflammatory response of TNF-α-stimulated chondrocytes could not be suppressed by PRP, as determined by gene expression of inflammatory markers COX2 and IL1B. Expression of chondrogenic markers COL2A1 and ACAN was downregulated by PRP, independent of PRP concentration. Chondrocytes cultured in PRP gel for 28 days proliferated significantly more when compared to chondrocytes cultured in fibrin gels. This effect was dose-dependent. Significantly less GAGs and collagen was produced by chondrocytes cultured in PRP gels when compared to fibrin gels. This was qualitatively confirmed by histology.

Discussion & Conclusions

Platelet-rich plasma stimulated chondrocyte proliferation in a dose-dependent manner. However, production of cartilage ECM was strongly downregulated by PRP. Furthermore, PRP did not act anti-inflammatory on chondrocytes in an in vitro inflammation model.

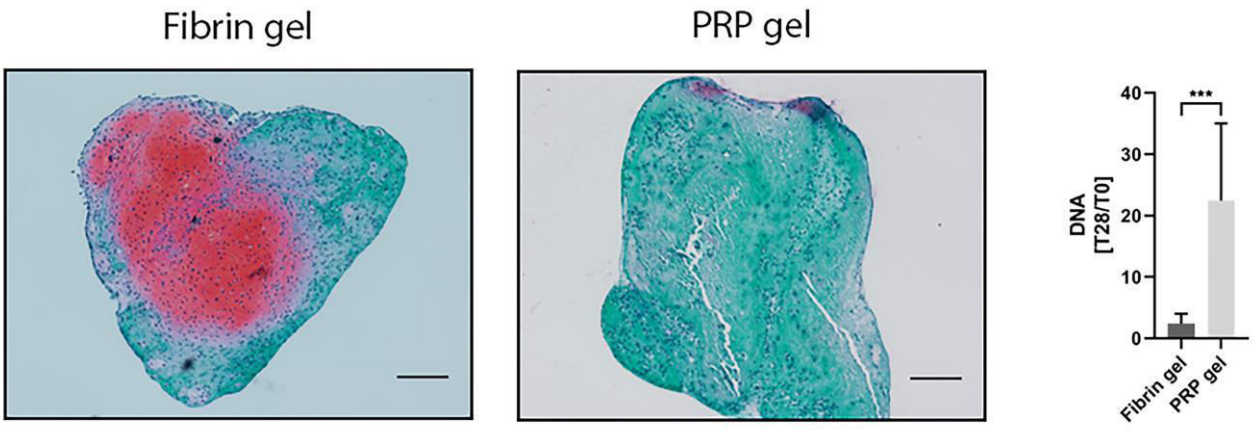

Figure 1. Proteoglycan production and proliferation in fibrin and platelet-rich plasma gels. *Formation of proteoglycans by osteoarthritic chondrocytes cultured for 28 days in fibrin gel (left panel). Production of proteoglycans in platelet-rich plasma gel was absent (middle panel). Scale bar = 200 µm. Amount of DNA increased significantly more in platelet-rich plasma gels compared to fibrin gels (right panel).*

Merging Modular Molecular Design with High Through-Put Screening of Supramolecular Biomaterials

Moniek G.J. Schmitz[1,2], Laurence Burroughs[3], Xuan Xue[3], Martijn Riool[4], Leonie de Boer[4], Annika F. Vrehen[1,2], Phani K. Sudarsanam[1,2], Jan de Boer[1,2], Sebastian A.J. Zaat[4], Morgan R. Alexander[3], Patricia Y.W. Dankers[1,2]

In *in-situ* tissue engineering applications there is a threat of the development of biomaterial-associated infections (BAI). The fiber-like, porous morphologies of the biomaterials serve as an ideal niche not only for eukaryotic cells but for bacteria as well. Upon implantation, bacteria and tissue cells compete for the biomaterial surface[1]. Colonization of biofilm-forming bacteria in the biomaterials results in failure of regeneration and therefore must be prevented. There are many different strategies to tackle this problem but most promising are multifunctional approaches in which biomaterials actively promote eukaryotic cell attachment and hinder bacterial colonization at the same time. Current treatments, for example based on the release of antibiotics, will not provide long-term protection against BAI due to the increase of multidrug-resistant bacterial strains[2]. Therefore, new strategies to prevent BAI should be developed.

In our research, supramolecular biomaterials based on fourfold hydrogen bonding 2-ureido-4[1H]-pyrimidinone (UPy) moieties are used. These UPy-materials can be functionalized with bioactive compounds via a modular approach in which the UPy-base material is mixed with UPy-modified additives[3]. Different supramolecular peptide additives are developed to either promote eukaryotic cell attachment or induce bacterial cell death via antimicrobial peptides (AMPs).

Here, we develop a high-throughput screening method to determine the best combination of peptides to create a biomaterial with both regenerative and antimicrobial activity against multi-drug resistant bacteria.

In this study an UPy end-functionalization polycaprolactone with a Mn of 2 kDa (*i.e.* PCLdiUPy) is used as base polymer. In total 6 different UPy-additives are investigated; 1) UPy-COOH, 2) UPy-cRGD, 3) UPy-heparin binding peptide[4] (UPy-HBP) and three UPy-functionalized AMPs 4) UPy-LASIO-III[5], 5) UPy-SAAP-148[6] and 6) UPy-TC-84[7].

It is the first time that SAAP-148 and TC-84 were coupled to the UPy-moiety. Therefore the antimicrobial activity of these peptides was assessed both in solution and as solid dropcast material against *S. aureus* JAR 060131, *E. coli* ESBL, *S. aureus* LUH14616 and *A. baumannii* RUH875. Besides this, the cytotoxicity of these peptides was tested against human dermal fibroblasts (HDF).

To facilitate screening of the best combination of peptides a high through-put library was designed with 195 unique combinations of the 6 additives. In each combination there is a maximum of 3 additives present and all additives are present in either 1 or 5 mol%. The library was printed as a microarray on poly-HEMA dipcoated slides using a XYZ3200 dispensing station (Biodot) using 3 quilled silicon pins maintaining 60-65% relative humidity. Three replicates of the library were printed on each slide. The library will be assessed by ToF-SIMS, HDF cell attachment and bacterial cell death.

Coupling of the UPy-linker to the SAAP-148 peptide does not influence its antimicrobial activity in solution. For the solid dropcasted materials incorporation of 5 mol% UPy-SAAP-148 is enough to kill all 4 bacterial strains. This indicates the peptide remains active after immobilization in the materials. Unfortunately, the TC-84 peptide loses its antimicrobial activity upon UPy-coupling both in solution and as solid. Cytotoxicity experiments show a slight reduction in HDF metabolic activity upon incorporation of 5 mol% UPy-SAAP-148.

All 195 unique combinations were printed successfully. The library sticks to the poly-HEMA slide upon immersion in culture medium and cells can be successfully cultured and visualized on the micro-arrays. ToF-SIMS results show the presence of an additive can be correlated to the presence of certain ions representing that additive. In the next step the biological response of every component will be correlated to the presence these ToF-SIMS ions to determine the best combination of peptides for a multifunctional biomaterial.

In conclusion, a new screening platform is developed which enables screening of different material compositions for desired biological responses.

1. Gristina, A. G. *et al*., Science (1987)
2. Boucher, H. W. *et al*., Clin. Infect. Dis. (2009)
3. Dankers, P. Y. W. *et al*., Nat. Mater. (2005)
4. Bonito, V. et al., Acta Biomater. (2018)
5. Zaccaria, S. *et al*., J. Polym. Sc. Part A Polym. Chem. (2018)
6. de Breij, A. *et al.*, Sci. Transl. Med. (2018)
7. Omardien, S. *et al.*, Biochim. Biophys. Acta – Biomembr. (2018)

Acknowledgements: This research was financially supported by the research program of DPI, project 731.015.505 and the Gravitation Program “Materials

1 Institute for Complex Molecular Systems, 2 Department of Biomedical Engineering, Eindhoven University of Technology, P.O. Box 513, 5600 MB Eindhoven, The Netherlands. 3 Laboratory of Biophysics and Surface Analysis, School of Pharmacy, University of Nottingham, Nottingham NG7 2RD, UK. 4 Department of Medical Microbiology and Infection Prevention, Amsterdam institute for Infection and Immunity, Amsterdam UMC, University of Amsterdam, 1105 AZ Amsterdam, The Netherlands.

Material driven liver fibrosis - a microfluidic approach

F. Stein,[†1] M. Sacchi,[†1,2] D. Rana,[1] A. Kandar,[1] D. Feitosa-Afonsso,[1] R. Bansal,[2] and J.Rouwkema[1*]
[1]*Department of Biomechanical Engineering, Technical Medical Centre, University of Twente,*
[2]*Faculty of Science and Technology, University of Twente*

Introduction:
Liver fibrosis is characterized by a progressive tissue stiffening which can result in complete organ failure. Initiated by chronic tissue injury followed by inflammation and ECM deposition instigating the recruitment and activation of immune cells in the damaged tissue such as myofibroblasts (MF)[2]. Several approaches have been reported to induce liver fibrosis either by genetic manipulation, adding of chemicals or by usage of certain diets[3].

Aim:
The aim of this study is to induce different liver fibrotic conditions by varying the mechanical environment of encapsulated single cells and cell spheroids. Synthesized Gelatin-Methacryloyl (GelMA)[1] of different stiffnesses will be used to mimic the mechanical ECM environment reported in different states of liver fibrosis to investigate the effect on cells represented in liver tissue. Therefore, liver mimicking spheroids will be cultivated made of Hepatocytes (HepG2), Endothelial cells (HUVEC) and Stellate cells (LX2) and their morphological changes and orientation before hydrogel encapsulation will be analyzed. Furthermore, a microfluidic chip will be designed allowing to perfuse liver mimicking spheroids encapsulated in GelMA of different mechanical properties and co-cultivated with HUVECs and Monocytes (TH1).

Material and Methods:
Manufactured SU8/Si wafer are used as a positive mold to create microfluidic chips of poly(dimethylsiloxane) (PDMS). Microwell array platforms made of 4 % agarose are used to cultivate non-adherent liver-spheroids made of HepG2, HUVEC and LX2 (8:2:1). Cell spheroids, consisting each of approximately 267 cells, were cultivated for 7 days to analyze the spheroid formation, spheroid compaction and the eventual change of the initial cellular composition over time using a custom developed MATLAB based program for automate data analysis, cytometry and Live/Dead staining at each day.

Results and Conclusion:
By synthesizing GelMA and using rheological measurements we proved to mimic the reported mechanical environment of healthy liver tissue and different states of liver fibrosis. Furthermore, we designed a hexagonal microfluidic system, mimicking the *in vivo* like structure of liver lobules, allowing us to simultaneously perfuse 3 separated hydrogels chambers (Fig.1) with a physiological relevant wall shear stress and interstitial flow velocity.

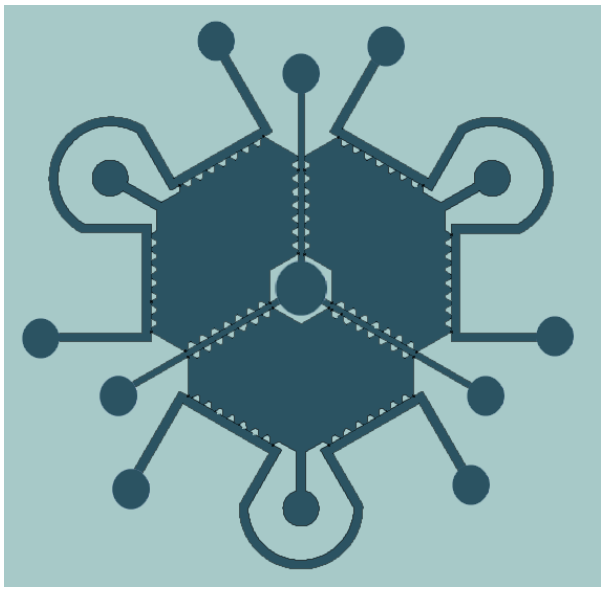

Figure 1. *Schematic overview of a liver-lobule-like designed microfluidic system allowing the simultaneous controlled perfusion of 3 separated hydrogel pockets through the central channel*

References:
1. Yue K, Santiago G, Alvarez M, Tamayol A, Annabi N, Khademhosseini A. Synthesis, properties, and biomedical applications of gelatin methacryloyl (GelMA) hydrogels. Biomaterials 2015, 73:254-71
2. Seki E, Minicis S, Osawa Y, Österreicher C, Brenner D, Schwabe R. TLR4 enhances TGFßbeta signalling and hepatic fibrosis. Nature Medicine 2007, ,1324-1332
3. Yanguas S., Cogliati B., Wilebroards J., Vinken M. Experimental models of liver fibrosis. Arch Toxicol. 2016, 90(5):1025-1048

Acknowledgements
This work is supported by an ERC Consolidator Grant under grant agreement no 724469.